CHAPTER 1

ELECTROCHEMICAL GAS SENSORS

FUNDAMENTALS, FABRICATION, AND PARAMETERS

J. R. Stetter
G. Korotcenkov
X. Zeng
Y. Tang
Y. Liu

1. INTRODUCTION

Sensor technologies are increasingly being used for sophisticated analytical applications in gases and liquids. Chemical sensors can be based on thermoelectric effects, thermal conductivity, catalytic combustion (combustible gas sensors), surface plasmon resonance, and both aqueous and solid-state electrochemistry; heated metal oxide (HMOX) electronic devices, surface acoustic wave or cantilever mechanical devices, optical and fiber optical effects, and magnetic effects have been reported for various applications (Christofides and Mandelis 1990; Brajnikov 1992; Ishihara and Matsubara 1998; Janata et al. 1998; Wilson et al. 2001; Stetter et al. 2003b; Ando 2006; Aroutiounian 2007; Lundstrom et al. 2007). However in this chapter, we will consider the subclass identified as electrochemical gas sensors and discuss the fundamentals of their construction, operation, performance, and application.

Electrochemical approaches to sensing different gas molecules can provide one of the lowest-power approaches combined with analytical performance that includes sensitivity, selectivity, and relatively low

cost. For many widespread applications such as personal monitoring, a sensor with simplicity and low cost as well as small size and minimal power consumption is highly desired. Electrochemical sensors, in fact, are very versatile, as they are sensitive to a wide range of toxic gases such as CO, NH_3, SO_2, NO, NO_2, as well as oxygen and are often amenable to miniaturization (Stetter et al. 1988; Madou and Joseph 1991). The possibility to work at room temperatures (RT) is an important advantage of liquid and polymer electrolyte electrochemical gas sensors, since a power-consuming heater is not needed and the gas sample and sensing environment are unperturbed by the measuring device (Limoges et al. 1996; Shi and Anson 1996). RT operation is also an important criterion to achieve intrinsically safe performance in potentially hazardous situations (Stetter 1984).

Liquid and polymer electrolyte gas sensors are not yet as thermally robust as those devices that can be made with solid-state materials such as the HMOX sensors or high-temperature zirconia electrolyte sensors. However, ambient amperometric and potentiometric devices typically offer higher selectivity than the chemiresistor semiconductor sensors. In general, electrochemical sensors are reported to last for years; as is typical for all sensors, the actual lifetime will depend on the conditions of use, but 5 years or more is not an unusual sensor lifetime (www.transducertech.com).

The overall electrochemical sensing approach, including that of potentiometric, amperometric, and conductimetric sensors, offers an attractive package of combined analytical and logistical characteristics that result in being able to provide relatively high analytical performance at modest cost for many applications (Stetter and Blurton 1976, 1977; Janata 1989; Vaihinger et al. 1991; Mari et al. 1992; Chang et al. 1993; Stetter and Li 2008) Therefore, a variety of electrochemical sensors are found in real-world gas-detection processes, both in stationary and in portable applications. Operation at low temperature typically utilizes liquid or polymer electrolytes, while high temperature requires solid-state materials for sensor component parts.

Due to the large number of related publications, in the present chapter we will consider selected results that are important for understanding the principles of operation of electrochemical gas sensors; more detailed discussions of general principles of a broad range of electrochemical sensors can be found elsewhere (Stetter and Blurton 1976, 1977; Janata 1989; Vaihinger et al. 1991; Chang et al. 1993; Mari et al. 1992; Cao et al. 1992; Bontempelli et al. 1997; Alber et al. 1997; Bakker et al. 1997; Holzinger et al. 1997; Buhlmann et al. 1998; Yamazoe and Miura 1998; Kulesza and Cox 1998; Hodgson et al. 1999; Opekar and Stulık 1999, 2002; Brett 2001; Reinhardt et al. 2002; Knake et al. 2005; Bobacka et al. 2008; Stetter and Li 2008). We apologize in advance to any of our colleagues whose work may not be adequately represented here and acknowledge their many important contributions.

2. FUNDAMENTALS OF ELECTROCHEMISTRY FOR GAS SENSORS

Electrochemical sensors are based on the measurement of the properties of the electrode and/or electrolyte as they interact with the analyte. The characteristics of an electrochemical sensor depend on the entire electrochemical detection system, including sampling, transport to and in the electrolyte, electron-transfer reactions, and diffusion of products. In this part, we will discuss the electrochemical properties and the electrochemical systems in detail. This part is not intended to replace any books or chapters

about fundamental electrochemistry; rather, it is more like an introduction to the concepts that are related to electrochemical sensors and that are needed to understand and appreciate their operation.

We need to note that understanding the electrochemistry is only the first step in understanding an electrochemical sensor. After the principles are understood, performance must be linked to the operating environment, the device design, the specific electrode materials and structures used, as well as the conditions of the sensing process. Trying to link the fundamental electrochemical behavior to the observed analytical performance is a challenge that is often met only by a careful synthesis of empirical and theoretical understanding.

2.1. POTENTIAL AND POTENTIOMETRY

Potentiometry is a method in which the potential of an electrochemical cell is measured at zero (near-zero) current. In a potentiometric gas sensor, the steady-state potential (sometimes this is also an equilibrium potential for a specific chemical reaction) of an electrode changes with the partial pressure of the analyte in the gas phase. For example, consider a partial or half-cell with the following construction:

$$\mathrm{A}_{(\text{gaseous analyte, } g)} \mid \mathrm{M}_{(\text{solid electrode, } s)} \mid \mathrm{A}^{+}_{(\text{electrolyte, } l)} \tag{1.1}$$

In practice, the solid electrode can be a conductor with or without surface modification, and the electrolyte can be liquid or solid-state. The half-reaction of the above electrode is

$$A^{+}_{(l)} + e^{-}_{s} \rightarrow A_{(g)} \tag{1.2}$$

At equilibrium, the electrochemical potentials are also at equilibrium.

$$\bar{\mu}^{l}_{A^+} + \bar{\mu}^{s}_{e} = \bar{\mu}^{g}_{A} \tag{1.3}$$

Here $\bar{\mu}^{\alpha}_{i}$ represents the electrochemical potential of species i in phase α, which equals its chemical potential μ^{α}_{i} plus an electronic term $zF\phi^{\alpha}$ in which z is the charge of species i, F is Faraday's constant, and ϕ^{α} is the internal potential of phase α. Therefore, Eq. (1.3) can be written as

$$(\mu^{l}_{A^+} + F\phi^{l}) + (\mu^{s}_{e} - F\phi^{s}) = \mu^{g}_{A} \tag{1.3a}$$

or

$$F(\phi^{l} - \phi^{s}) + \mu^{l}_{A^+} + \mu^{s}_{e} = \mu^{g}_{A} \tag{1.3b}$$

$$F(\phi^{l} - \phi^{s}) + (\mu^{0l}_{A^+} + RT\ln[A^{+}]) + \mu^{0s}_{e} = \left(\mu^{0g}_{A} + RT\ln\frac{p_A}{p_0}\right) \tag{1.3c}$$

$$F(\phi^{l} - \phi^{s}) + RT \ln \frac{[A^{+}]}{(p_A / p_0)} = \mu_A^{0g} - (\mu_{A^{+}}^{0l} + \mu_e^{0s}) \tag{1.4}$$

The activity effect of electrons is neglected because the electron concentration in the solid electrode is a constant. p_A is the partial pressure of A and p_0 is 1 atm.

Considering

$$F(\phi^{l} - \phi^{s}) = -FE \tag{1.4a}$$

and

$$\mu_A^{0g} - (\mu_{A^{+}}^{0l} + \mu_e^{0s}) = -FE^0 \tag{1.4b}$$

Eq. (1.4) is transformed as

$$-FE + RT \ln \frac{[A^{+}]}{(p_A / p_0)} = -FE^0 \tag{1.5}$$

or

$$-FE + RT \ln \frac{a_{A^{+}}}{(p_A / p_0)} = -FE^0 \tag{1.5a}$$

Equation (1.5a) is for a one-electron transfer reaction and will vary depending on the number of electrons involved; the sign of the potential will depend on whether the analyte is oxidized or reduced on the electrode surface. Potentiometry is most frequently explained based on this equation, a Nernst-type equation which relates the partial pressure of the analyte and the electrode potential.

In our discussion above, the potential is measured with respect to a reference electrode. In the case of mixed potential gas sensors, the reference electrode is replaced with an electrode where a gas is oxidized or reduced. For example, a CO sensor contains two dissimilar electrodes. The oxygen in the air is reduced on one electrode and the CO is oxidized on the other electrode. When the pressure of oxygen in the air is a constant, the potential difference of the two electrodes is logarithmically related to the pressure of CO according to an equation similar to Eq. (1.5a) (Garzon et al. 2000). The two half-reactions on the two electrodes are

$$\begin{aligned} O_2 + 4e^{-} &\rightarrow 2O^{2-} \\ 2CO + 2O^{2-} - 4e^{-} &\rightarrow 2CO_2 \end{aligned} \tag{1.6}$$

In the potentiometric gas sensors, a wide dynamic range of analyte concentration can be measured. The sensing principle is thermodynamic or competitive thermodynamic in nature, thus the chemical and diffusion processes must reach equilibrium or steady-state conditions. The time to establish an equilibrium situation at the electrode often limits the response time of the gas sensors.

2.2. CURRENT, CHARGE, AND AMPEROMETRY

Both current and charge can be the signal measured in an amperometric method. Current reflects the rate of electron transfer and the charge is the integral of current with respect to time. Therefore, we can say that the amperometry is a method in which the current is monitored.

2.2.1. Voltammetry

Voltammetry is one type of amperometry, in which the potential applied to the electrode is controlled and programmed. Among the most popular voltammetric methods are linear sweep voltammetry (LSV) and its variation, cyclic voltammetry (CV). In CV, the potential sweeps linearly forward and backward between two potentials for several cycles. Cyclic voltammetry is especially powerful in the study of electrode reaction mechanisms. In LSV, the potential sweeps linearly in one direction for one time. This continuous potential change causes dynamic response in current, the size and direction of which is determined by many physical/chemical processes occurring at the electrode surface (see Figure 1.1).

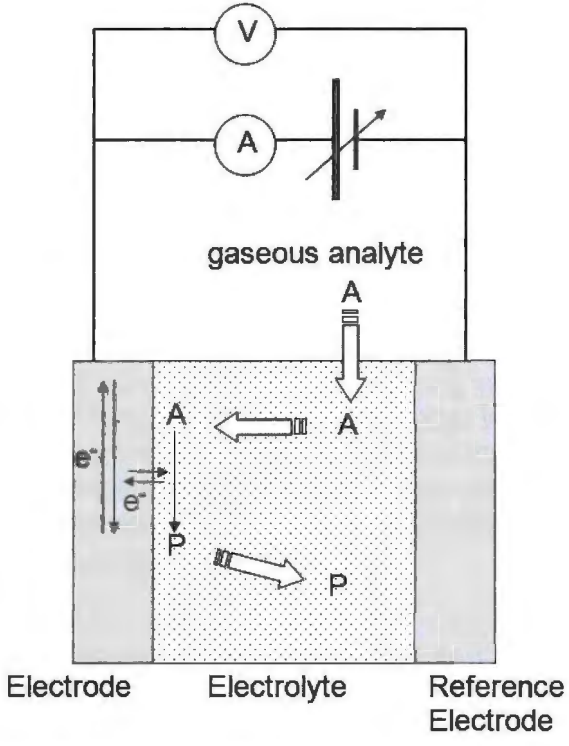

Figure 1.1. Amperometry. Electrons cross the electrode–electrolyte interface with the help of a faradaic process (electrochemical reaction involving the analyte, electrolyte, and/or electrode). The electrons then flow (observed as a current) in the external circuit.

Square-wave voltammetry (SWV) and differential pulse voltammetry (DPV) also belong to the widely used voltammetry techniques. They originated from DC polarography using mercury as working electrode. In the absence of an electroactive species of interest, there will be a residual current between the anodic and cathodic background. It is composed of a current due to double-layer charging and a current caused by low-level oxidation or reduction of the components in the system. In LSV, the current at a *working electrode* is measured while the potential between the working electrode and a *reference electrode* is swept linearly in time. In pulse voltammetry (DPV and SWV), the potential sweep is a series of stair steps. The current is measured at the end of each potential change, right before the next, so that the contribution to the current signal from the capacitive charging current is minimized. Generally speaking, SWV is most sensitive and LSW is least sensitive. However, the sensitivity gain is balanced by the increase complexity of the instrumentation and software. So, depending on whether sensitivity is more important or the cost is more important for a certain application, the user can select among these various voltammetry techniques.

In Figure 1.1, the processes are classified with arrows according to the location:

- Gas–electrolyte interface: analyte dissolving in electrolyte
- Electrolyte: analyte diffusion, before chemical reaction of the analyte
- Electrolyte–electrode interface: analyte adsorption, analyte oxidation or reduction, heterogeneous electron transfer, product desorption, product diffusion, after chemical reaction of the product
- Electrode: electron flow

With careful design of the system, the characteristic current, i.e., the limiting current in LSV or the peak current in CV, DPV, and SWV, is quantitatively related to the concentration of analyte in the electrolyte. And the potential at which the peak currents are observed is related to the thermodynamic potential of the reaction from which the electron flows.

2.2.2. Galvanometry

Galvanometry is another type of amperometry, in which no extra potential is applied to the electrodes and the spontaneous external current between two electrodes is monitored (see Figure 1.2). The sensor is designed so that the presenting current results from an interfacial reaction of the analyte. The amplitude of the current reflects the rate of the reaction and therefore the concentration of the analyte.

2.2.3. Coulometry

Coulometry is an electrochemical method wherein the total charge or the total number of transferred electrons rather than the rate of electron transfer (i.e., the current) is measured. This is an advantage when the magnitude of current is small and difficult to distinguish from the background. Since the charge is the integral of current with respect to time, the signal in coulometry is indeed the current, and this means that coulometric methods belong to the family of amperometric techniques.

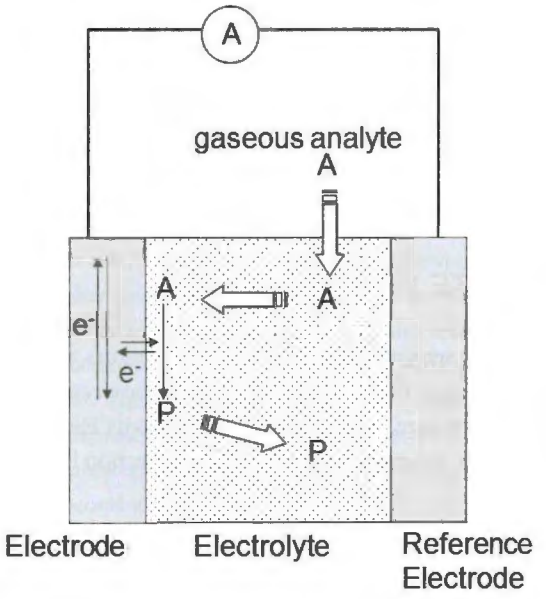

Figure 1.2. Galvanometric sensor. The reference electrode and working electrode are chosen so that the reaction of the analyte is spontaneous (e.g., the galvanometric oxygen sensor).

2.3. CONDUCTIVITY/RESISTANCE AND CONDUCTOMETRY

Conductometry is one of the most commonly used sensing methods for gases. In the conductometric gas sensor, the electrical properties, i.e., the conductivity of the active materials, in the presence and absence of analyte(s), are used to determine the components and concentrations. Therefore, the target analytes for a conductometric gas sensor will cause changes of charge carrier density or mobility in the active materials, leading to significant alterations in their conductivity. This process can be related to the surface reactions (Stetter 1978). By selecting suitable active materials and structures, conductometric sensors offer sensitivity to a wide range of analyte types and concentrations. Because the resistance is proportional to the reciprocal of the conductance, the signal in conductometry can also be reported as the resistance or the relative resistance change. Many reviews have been written about the conductometric types of gas sensors (Potje-Kamloth 2008).

3. TYPES OF GASEOUS INTERACTIONS IN SENSING

In this section, we will survey the electrochemical gas sensors from a new point of view: the specific interaction between the analyte gases and the sensors. As we are going to talking about specific interactions, we will not cover electronic noses or gas sensor arrays, where each single interaction might be more or less specific. The gas/sensor interactions in electrochemical sensors fall into two categories, depending on

the location of interaction. In one category, the interaction takes place between the analyte gases and the electrolyte; in the other, it takes place between the analyte and the electrode. The electrode in the latter category may be a bare conductor material or it may be modified with a coating. The following discussion is not intended to be comprehensive, but we have tried to include various types of interactions with some examples. A given material may also be used in several sensors that are selective to different gases by varying the fabrication methods and/or the additives.

3.1. GAS/ELECTROLYTE INTERACTIONS

The electrolyte can be the active sensing material when it undergoes an analyte-specific reaction. The gas/electrolyte interaction can change the ionic conductivity of the electrolyte or affect the (ion or semi-) conducting properties of the electrolyte. The change in conductivity is used as the signal to quantify the concentration of the analyte gas. Consequently, this type of interaction is often found in conductometric gas sensors.

3.1.1. Physical Sorption

Analyte gas molecules are absorbed or adsorbed by the electrolyte, changing the conductivity or mobility of the ions in the electrolyte. The changes in the electrolyte conductivity, electrode potential, or the current in the circuit have a relationship to the partial pressure of the gas.

For example, a sensor for propane (C_3H_8) uses the zeolite ZSM-5 doped with a certain concentration of Na^+ as a two-phase electrolyte (Dubbe et al. 2006). ZSM-5 is a highly porous zeolite. Throughout its structure it has an intersecting two-dimensional pore structure that allows a species to move from one point to anywhere else in the ZSM5. The electrochemical cell is represented as follows:

$$\text{Au (reference)} \mid (Na_2CO_3, BaCO_3) \mid \text{zeolite } (Na^+) \mid \text{Au (sensing)} \tag{1.7}$$

The potential of the sensing electrode is determined by the activity of Na^+ in zeolite, as the activity of solid sodium is generally taken as unity

$$E_S = E_S^0 + \frac{RT}{F} \ln \left[\frac{a(Na^+)}{a(Na)} \right] \tag{1.8}$$

The proper cage size of the zeolite (0.51–0.56 nm diameter) provides the electrolyte with a higher selectivity to C_3H_8 (Wu et al. 1986). Larger molecules are prevented from adsorption in the cage and smaller molecules may not change the Na^+ activity efficiently. Upon being occupied by the C_3H_8, the Na^+ activity in the zeolite is reduced, lowering the potential of the sensing electrode.

In general, adsorption is the name given to solid/gas interfacial bonds with the special case of chemisorptions for high-energy interactions, while physisorption refers to low-energy dispersive forces between the sorbate and sorbent, typically 5 kcal/mole or less. Absorption generally describes the

phenomenon by which the sorbate is incorporated into the sorbent (not restricted to the surface), such as the interaction of hydrocarbons and polymers. This process is often described as partitioning (e.g., in the literature on gas–liquid chromatography).

3.1.2. Gas Oxidation and Reduction

Gases with electron-accepting or electron-donating abilities can be oxidized or reduced on a contacting electrolyte, generating ions or changing the electronic status of the electrolyte. This type of interaction is often used in semiconducting electrolytes such as metal oxides and conductive polymers. The main chemical reaction in the metal oxide gas sensor is the ionization of oxygen adsorbed on the surface of the oxides (Barsan et al. 2001, 1999). The sensors operate through a shift in the equilibrium of the surface oxygen reaction by target gas. The resulting alteration in chemisorbed oxygen leads to a change in resistance of the metal oxide sensing materials. Reducing gases such as H_2, CO, and CH_4 lead to an increase of conductance for *n*-type semiconductors (such as SnO_2, TiO_2, ZnO, Fe_2O_3, etc.) and a decrease for *p*-type semiconductors (such as NiO, Co_2O_3, etc.), whereas oxidizing gases such as O_3, NO_x, and Cl_2 behave conversely. The electrical conduction is controlled by potential barriers associated with grain boundaries. Moreover, the electric conductivity of the metal oxide is extremely sensitive to the composition of the surface, which also varies reversibly to the surface reaction involving chemisorbed oxygen and the gas mixture component. Since performance, such as sensitivity, selectivity, and response time, is dependent on the surface reaction between the metal oxide and gas molecules in the ambient, the particle size, microstructure, and doping level will have a large influence on the response of the metal oxide sensors.

Conducting polymers usually are organic compounds with an extended π-orbital system, through which the electrons can move in the polymer. Typically, conducting polymers show poor conductivity in the neutral state. They will present high conductivity when the neutral polymers are doped. Moreover, when gas molecules are absorbed on the conducting polymers, their conductivity alters sharply. These unique properties make conducting polymers promising in electrochemical impedance gas sensors. For example, the conductivity of polyaniline (PAN) is based on its degree of oxidation and doping. It has been reported that fabrication methods, film thickness, and the type of copolymers can makes PAN useful in sensing some gases (Xie et al. 2002). With pure PAN films prepared by a Langmuir-Blodgett technique, NO_2 could be selectively analyzed as NO_2 because the analyte obtained electrons from the π-electron network of PAN. The resulting positively charged PAN became more conductive with more charge carriers.

$$NO_2 + PAN \rightarrow NO_2^- + PAN^+ \tag{1.9}$$

Similarly, electron-donating or reducing gases can also be analyzed with conductive polymer electrolytes, as, for example, BF_4^--doped polythiophene (PTh), a *p*-type polymer (see Figure 1.3). The conductance of this *p*-type conductive polymer relies on the mobility of the "holes" (Mohammad 1998). Electrochemical gas sensors with *p*-type PTh experienced decreased conductivity with electron-donating NH_3 gas. On the contrary, *n*-type semiconductors may experience conductivity increase with reducing gases. A similar observation can be made for carbon nanotube sensors (Stetter and Maclay 2004). A H_2S analyte was reported to pump electrons into the semiconducting In_2O_3 nanowires (Zeng et al.

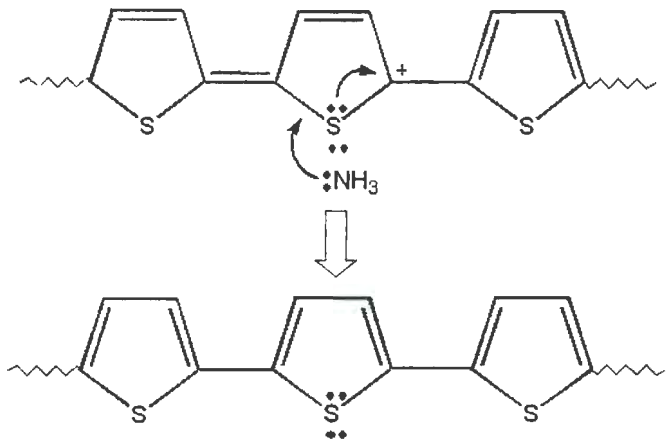

Figure 1.3. BF_4^--doped polythiophene (PTh). (Reprinted with permission from Mohammad 1998. Copyright 1998 IOP.)

2009), and some other reducing gases (H_2, NH_3, liquefied petroleum gases or LPG) can be oxidized by surface-bound oxygen ions (O^-, O^{2-}, O_2^-) on the sensor surface, increasing the charge of the conduction band of an *n*-type semiconductor. Some gas sensors have been used to study this phenomenon (Biswas et al. 2008).

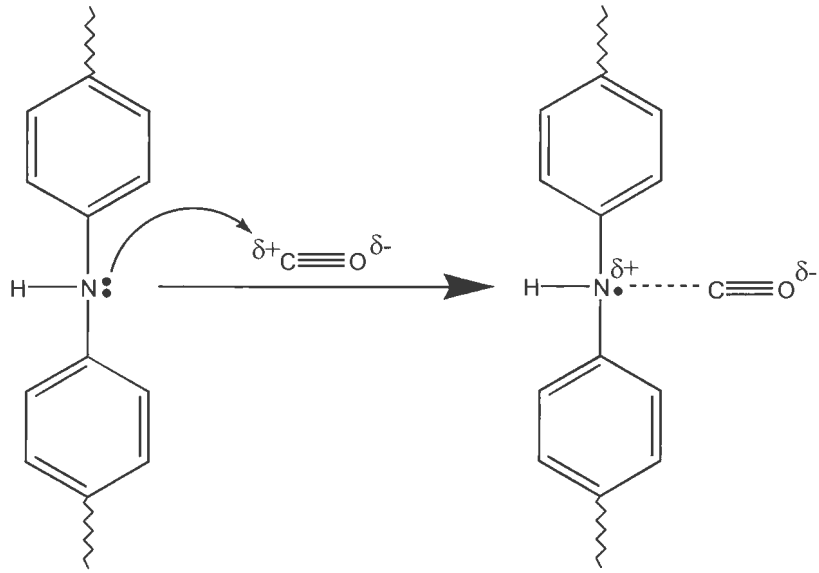

Figure 1.4. Partial redox CO sensor in which the conductivity of the PNA electrolyte increased with CO concentration as the CO/PAN interaction produced more charge carriers.

$$2NH_3 + 3O^- \rightarrow N_2 + 3H_2O + 3e^- \tag{1.10}$$

3.1.3. Partial Redox

In some cases, the gas/electrolyte interaction results in partial electron transfer rather than a total reduction or oxidation. The electrons distribute unevenly among the carbon atom and the oxygen atom within a carbon monoxide molecule. The carbon atom bears positive charge to some degree, which attracts the lone-pair electrons from the amine group of PAN (see Figure 1.4). The result is an increase in the number of charge carriers. A carbon monoxide sensor has been reported based on such an interaction (Watcharaphalakorn et al. 2005).

3.1.4. Hydrogen Bonding

Hydrogen bonding refers to the particularly tight bond formed between hydrogen in one molecule and a heteroatom [O, F, N] in another molecule without forming a covalent bond (see Figure 1.5). The energy of the hydrogen bond is stronger than that of simple dispersive forces and yet weaker than covalent bonds. Gases such as methanol, with both hydrogen bonding basicity and acidity, can form hydrogen bonds to solid electrolytes such as conductive polymers such as PAN (Tan and Blackwood 2000).

The hydrogen bonds form partial positive charges with the lone pair of electrons in the amine nitrogen in the PAN backbone, making them more localized and decreasing the number of polarons in PAN. In addition, hydrogen bonding effectively increases the degree of PAN cross-linking, further decreasing the mobility of electrons. Therefore, decreasing electrolyte conductivity in the PAN is an indicator of the presence of methanol.

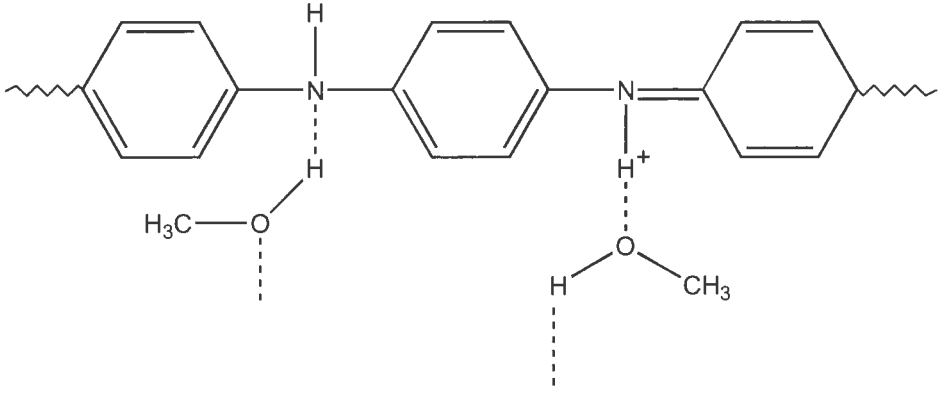

Figure 1.5. Dashed lines indicate hydrogen bonds. (Reprinted with permission from Tan and Blackwood 2000. Copyright 2000 Elsevier.)

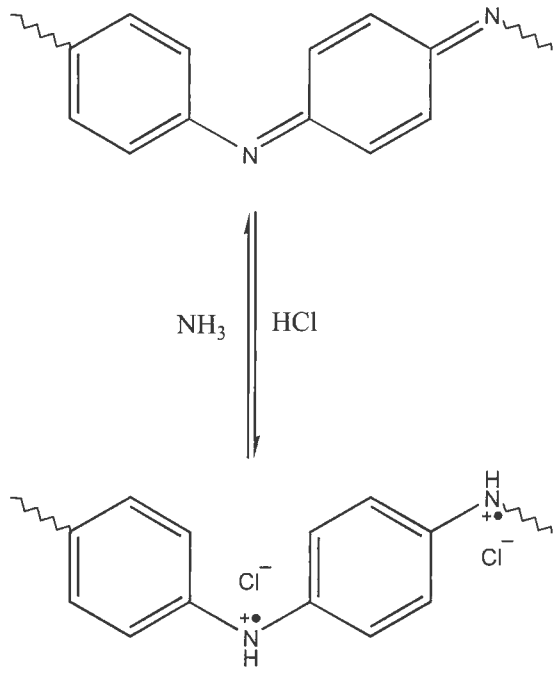

Figure 1.6. HCl can form a covalent or ionic bond, while ammonia will reduce PAN, illustrating acid/base reactions that can be used for sensing in PAN films. (Reprinted with permission from Virji et al. 2004. Copyright 2004 American Chemical Society.)

3.1.5. Acid–Base Reaction

Certain analyte gases with strong acidity or basicity may result in total protonation or deprotonation instead of forming hydrogen bonds with the electrolyte. It has been reported that HCl and NH_3 gases interact with PAN according to the reactions shown in Figure 1.6, increasing or decreasing, respectively, the conductivity of polymer on nanofibers (Virji et al. 2004).

3.2. GAS/ELECTRODE INTERACTIONS

The electrode is a conductor of electrons and is typically a metal. Interfacial electron transfer takes place at the electrode surface, resulting in oxidation or reduction; therefore, redox reactions are typically gas/electrode interactions. However, it is not necessary that the analyte gas be reduced or oxidized; it could be the electrode that is reacted electrochemically.

Several strategies can be applied to obtain selectivity for an analyte. One is to apply a coating to the electrode that alters reactivity. If only the analyte gas is able to be adsorbed by the coating and penetrate to the sensing electrode surface, selectivity is obtained. Another strategy is to select an electrolyte which specifically supports the redox reaction of the analyte gas.

3.2.1. Physical Sorption

Physical adsorption does not reduce or oxidize but rather increases the concentration of reacting adsorbates at the reaction interface sites. In this type of interaction, the analyte gas molecules can facilitate the reduction or oxidation of other gases, which are used as a reference or probe. A CO_2 gas sensor took advantage of the reduction of oxygen in the air (Satyanarayana et al. 2008) and the reduction of the oxygen took place at the electrode surface and the solid electrolyte conducted CO_3^{2-} ions.

$$2Li^+ + CO_2 + \frac{1}{2}O_2 + 2e^- \rightarrow Li_2CO_3 \tag{1.11}$$

CO_2 molecules helped with the removal of the adsorbed O_2, and since the O_2 was present in the ambient air and its partial pressure was the same at the sensing and the reference electrodes, the potential of the sensing electrode was determined by the CO_2 partial pressure. This resulted in a potentiometric atmospheric CO_2 sensor that follows the relationship:

$$E = A - \frac{RT}{2F} \ln P_{CO_2} \tag{1.12}$$

3.2.2. Gas Oxidation and Reduction

In a typical amperometric CO gas sensor, the molecules of CO are directly oxidized at the anode surface to produce CO_2. The current generated on the sensing electrode is related to the rate of CO reaction, which can be limited by reaction rate or diffusion (Stetter and Li 2008).

$$CO + H_2O \rightarrow CO_2 + 2H^+ + 2e^- \tag{1.13}$$

In cases when the analyte gas is difficult to reduce or oxidize, a catalyst may be included in the surface as an integral composite material or as a modifying coating. For example, in an amperometric CH_4 sensor with a carbon nanotube electrode loaded with palladium, the Pd catalyst facilitates CH_4 to gain electrons from the nanotube. The reduction current showed correlation with the CH_4 partial pressure (Lu et al. 2004).

Potentiometry has been equally utilized with redox reactions. An oxygen sensor based on reduction of oxygen monitored the potential of the sensing electrode (Pasierb and Rekas 2009).

$$O_2 + 4e \rightarrow 2O^{2-}$$
$$E = \frac{RT}{4F} \ln \frac{p}{p_0} \tag{1.14}$$

Potentiometric oxygen sensors are very often used with high-temperature electrolytes.

3.2.3. Biological Reaction

A direct analysis is illustrated by the following enzymatic reaction, which is indeed one type of redox reaction catalyzed or mediated by enzymes. This type of reaction has great potential to be engineered into a sensor with very high selectivity. In an enzymatic gas sensor, formaldehyde could be analyzed as it was oxidized to produce reduced nicotinamide adenine dinucleotide (NADH) in the presence of formaldehyde dehydrogenase (FALDH). The oxidation current of NADH was measured as the signal of the sensor (Mitsubayashi et al. 2008).

$$\begin{aligned} &CH_2O + NAD^+ + H_2O \xrightarrow{\text{FALDH}} CHOOH + NADH + H^+ \\ &NADH \xrightarrow{\text{Pt electrode}} NAD^+ \end{aligned} \tag{1.15}$$

A similar enzymatic formaldehyde gas sensor has also been reported but with a little more complicated sensing mechanism (Achmann et al. 2008). The selectivity and control offered by the enzymatic reaction allows the sensor to be quite selective.

In an indirect analysis of gas using biological reactions, the analyte gas was consumed by another species, and the latter species was monitored to indicate the concentration of the analyte gas. Specifically, in a CH_4 sensor, methanotrophic bacteria were used to simultaneously consume oxygen through CH_4 oxidation; therefore, the concentration of CH_4 was reflected by the concentration change in oxygen in a closed sensor compartment (Damgaard et al. 1998).

3.2.4. Catalysis and Other Gas Interactions in Sensing

Unlike the redox reactions and the enzymatic reactions discussed above, in the catalysis reaction, the sensor is monitoring a process that is catalyzed or mediated by the analyte gas. The resulting gas sensors are selective to the gases which have catalytic activity. Catalytic reactions occur wherever there is a material that influences the rate of a chemical reaction but itself is unchanged, as occurs in most amperometric sensors when we compare the reactivity of two noble-metal electrodes (Blurton and Stetter 1977). An example is the selective oxidation of NO on gold electrodes in the presence of CO. While both oxidation of CO and NO are thermodynamically favored, only the NO rection is observed because the rate of the CO oxidation is many orders of magnitude lower (Zaromb et al. 1983). Catalytic additives also influence sensing in most semiconductor (HMOX) sensors.

In a study of ionic liquids as electrolytes, it was found that the SO_2 content in gas environment reduced the activation energy for diffusion. This occurred because the ionic liquid viscosity decreased with increasing SO_2 content. Cyclic voltammetry of some redox species such as ferrocene and *N,N,N′,N′*-tetramethyl-*p*-phenylenediamine (TMPD) in this ionic liquid showed that the limiting current was linearly proportional to the SO_2 content in the whole range from 0 to 100%, suggesting a promising method of SO_2 sensing (Barrosse-Antlle et al. 2009). This latter example illustrates the number of ways chemical bonding phenomena are involved in production of an analytical signal in electrochemical sensors.

4. FUNDAMENTALS OF ELECTROCHEMICAL GAS SENSORS

Electrochemical gas sensors can be divided into three main classes according to the operating principle: amperometric, potentiometric, and conductometric sensors (Stetter and Blurton 1976, 1977; Janata 1989; Weppner 1987; Vaihinger et al. 1991; Mari et al. 1992; Chang et al. 1993; Brett 2001; Stetter and Li 2008). Potentiometric sensors can be fabricated in very small sizes because the generated voltage can be easily measured with very high precision and the potentials generated are independent of the dimensions of the sensor. In contrast, the amperometric sensor's signal (current) is proportional to the electrode area and will become smaller as the size is reduced. However, miniaturized amperometric sensors with improved signal-to-noise ratio are becoming available through the use of nanostructured electrodes and high-precision electronics (Stetter and Maclay 2004). The goal for any type of electrochemical gas sensor is always to achieve high signal-to-noise ratio of a sensor via innovation and improvement in electrode/electrolyte interface, electrochemical cell design, and electronics.

4.1. AMPEROMETRIC GAS SENSORS

The amperometric gas sensor, or AGS (Stetter and Blurton 1976, 1977; Vaihinger et al. 1991; Cao et al. 1992; Chang et al. 1993; Kulesza and Cox 1998; Hodgson et al. 1999; Ishihara et al. 2003; Stetter and Li 2008;), combines versatility, sensitivity, and ease of use in common gas-detection situations with relatively low cost and, recently, with the possibility for miniaturization (Buttner et al. 1990; Cao and Stetter 1991; Stetter and Maclay 2004). The simplest amperometric cell consists of two electrodes (see Figure 1.7a), i.e., a working electrode and a counter electrode, and the electrolyte solution in which the two electrodes are immersed. The amperometric gas sensor is operated under an externally applied voltage, which drives the electrode reaction in one direction (no external voltage is required in the galvanic sensor design). This two-electrode detection principle presupposes that the potential of the counter/reference electrode remains constant. A potentiostat is usually used to measure the working electrode potential. In reality, the surface reactions at each electrode cause them to polarize, and significantly limits the concentrations of reactant gas they can be used to measure. Therefore, in practice, many amperometric sensors have a more complicated configuration. In particular, many AGSs are built using a three-electrode scheme, given in Figure 1.7b. In the three-electrode designs, the current at the sensing electrode can be measured at constant potential and, since the reference electrode is shielded from any reaction, it maintains a constant potential to provide a true thermodynamic potential for the reactions.

The mass transport of analyte gases in the electrochemical cell shown in the inset in Figure 1.7 can be simple diffusion due to concentration gradient or convection aided by a small air pump, which transports the sample to the gas-porous membrane through which the analyte diffuses/permeates to the sensing electrode. Figure 1.8 illustrates an AGS in a thin-film "fuel cell" configuration.

In the AGS, the current generated by reaction of target gas at the sensing or working electrode is measured as the sensor signal; it can be measured at a fixed or variable electrode potential. Electroactive analyte, participating in electrochemical reaction, diffuses from the surrounding gas to the electrochemical cell, through the porous layers, and dissolves in the electrolyte, through which it proceeds to diffuse to the working electrode surface. The reaction rate, reflected by the current at the sensing electrode, can

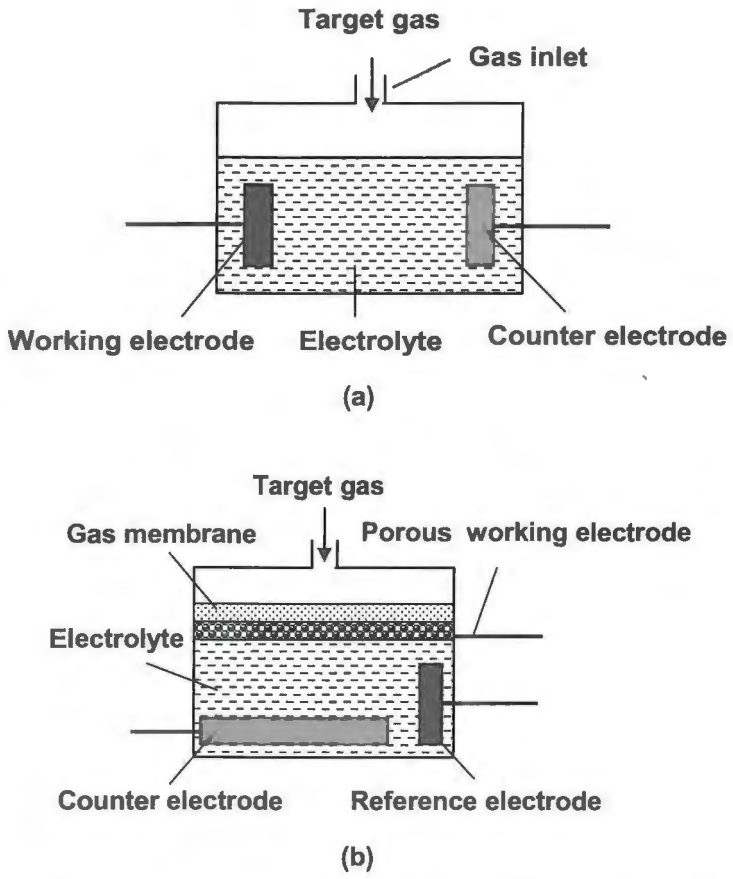

Figure 1.7. Schematic diagram of electrochemical gas sensors with (a) two- and (b) three-electrode configurations. (Reprinted with permission from Korotcenkov 2009. Copyright 2009 American Chemical Society.)

be limited by the rate of reaction at the surface or the rate of gas diffusion to the electrode surface. If the device is operated under diffusion-limited conditions, the current is proportional to the concentration of the analyte in the surrounding gas (Stetter and Blurton 1976, 1977; Vaihinger et al. 1991; Chang et al. 1993; Stetter and Li 2008). Application of Faraday's law relates the observed current (sensor signal) to the number of reacting molecules [concentration] by

$$I = nFQC \tag{1.16}$$

where I is current (C/s), Q is the rate of gas consumption (m^3/s), C is the concentration of the analyte (mol/m^3), F is Faraday's constant (9.648×10^4 C/mol), and n is the number of electrons per molecule participating in the reaction.

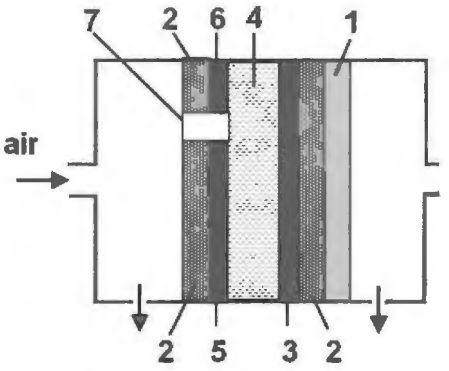

Figure 1.8. Schematic diagram of the hydrogen AGS thin-film structure, operated in a fuel cell mode: 1, PTFE membrane; 2, Pt/Ru mesh (embedded into the catalyst layer); 3, working electrode (Pt/C catalyst thin layer); 4, Nafion-117 membrane; 5, counter electrode; 6, reference electrode; 7, insulator. (Adapted with permission from Lu et al. 2005. Copyright 2005 Elsevier.)

Table 1.1 lists possible electrochemical reactions for gas analysis. One can see that during H_2, CO, NO_2, and SO_2 detection we have $n = 2$, while for reaction with participation of H_2S we have $n = 8$.

Of course, the reactions shown in Table 1.1 reflect only a general view of the processes taking place in electrochemical sensors. In practice, these processes are more complicated. For example, the reaction of H_2 detection consists of two stages. In general, the electrode processes in a H_2 sensor with a Nafion (DuPont) electrolyte electrode include the anode reaction

Table 1.1. Example electrode reactions for aqueous electrolyte amperometric gas sensors

Target gas	Electrode reaction
H_2	$H_2 + 2OH^- = 2H_2O + 2e^-$
CO	$CO + H_2O = CO_2 + 2H^+ + 2e^-$
O_2	$O_2 + 4H^+ + 4e^- = 2H_2O$
NO_2	$NO_2 + 2H^+ + 2e^- = NO + H_2O$
NO	$NO + 2H_2O = NO_3^{2-} + 4H^+ + 3e^-$
H_2S	$H_2S + 4H_2O = SO_4^{2-} + 10H^+ + 8e^-$
SO_2	$SO_2 + 2H_2O = SO_4^{2-} + 4H^+ + 2e^-$
CO_2	$CO_2 + H_2O + 2e^- = HCOO^- + OH^-$
MMH	$(CH_3)N_2H_3 + 4OH^- = CH_3OH + N_2 + 3H_2O + 4e^-$
CH_3CH_2OH	$CH_3CH_2OH + H_2O = CH_3COOH + 4H^+ + 4e^-$
CH_3CHO	$CH_3CHO + H_2O = CH_3COOH + 2H^+ + 2e^-$

Source: Data from Chang et al. 1993; Hodgson et al. 1999; Stetter and Li 2008.

$$H_2(g) \rightarrow 2H^+ + 2e^- \tag{1.17}$$

and the cathode reduction

$$½O_2 + 2H^+ + 2e^- \rightarrow H_2O(l) \tag{1.18}$$

Under short-circuit condition, reaction (1.17) occurs at the sensing or working electrode, WE, whereas reaction (1.18) occurs at the counter, or CE, electrode. Simultaneously, the protons move toward the counter electrode through the proton-conducting electrolyte Nafion. This process results in a flow of an equivalent number of electrons in an external electrical current. The anodic oxidation reaction of hydrogen is often limited by the diffusion process to the sensing electrode by the sensor design. The number of protons produced is proportional to the hydrogen concentration. Since the number of H_2 molecules reaching the WE is limited by the diffusion of H_2 from the bulk air sample to the WE surface, the external current is proportional to the hydrogen concentration in the gas phase (Nikolova et al. 2000), which can be derived from combining Fick's law and Faraday's law, correlating the flux/number, J_{H2}, of hydrogen molecules being pumped per second to the current I:

$$J_{H_2} = \frac{I}{2q} \tag{1.19}$$

where I is current C/s and q is the electric charge of an electron (1.6×10^{-19} C).

The flux of hydrogen diffusing through the aperture of an amperometric sensor is given by Fick's first law:

$$J_{H_2} = A \cdot D_{H_2} \frac{\partial P_{H_2}}{\partial x} \tag{1.20}$$

where A is the area of the diffusion barrier (m^2), D is the diffusion coefficient (m^2/s), P_{H_2} is the hydrogen concentration (mol/m^3), and x is the thickness of the barrier (m). Thus, Eqs. (1.19) and (1.20) can be rearranged to give the current:

$$I = 2qAD_{H_2} \frac{\partial P_{H_2}}{\partial x} \tag{1.21}$$

It is necessary to note that in "fuel cell" mode, the same Eqs. (1.17) and (1.18) reactions take place on the electrodes with one distinction: The reaction (1.18) takes place with participation of oxygen from the gas phase. As derived from Eq. (1.21), the properly designed diffusion-limited amperometric gas sensor has a linear relationship between the H_2 partial pressure and the generated electrical current, which can be easily measured with very high precision (see Figure 1.9). Similar equations can be written for other gases and sensor systems as well.

Linear response is often an advantage in a sensor, since sensitivity is constant over a broad range of concentrations and the electronics and compensation are simplified. However, a sensor with exponential

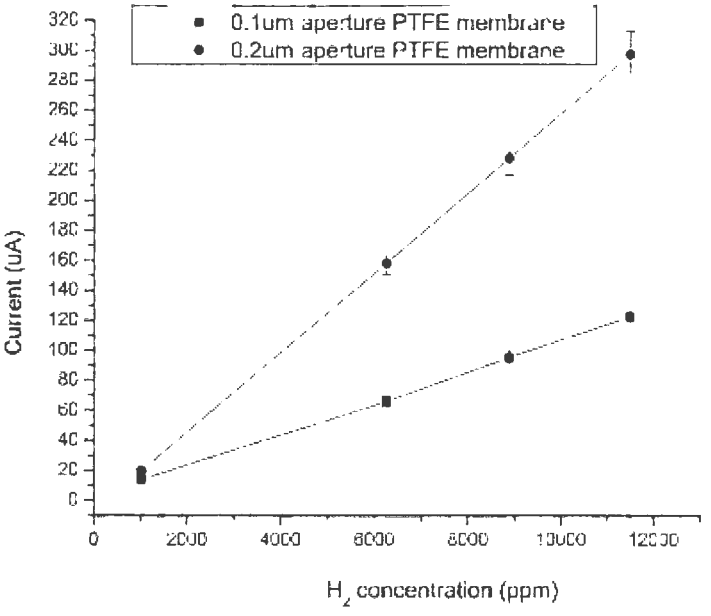

Figure 1.9. Calibration curves for Pt/Nafion-based H_2 sensors with different aperture PTFE diffusion membranes. (Reprinted with permission from Lu et al. 2005. Copyright 2005 Elsevier.)

response can sometimes provide advantages such as sensitivity at the lowest levels (Barsan et al. 1999). However, as has been established for many gases, the AGS also can detect low levels when it is optimized (Ramesh et al. 2003), and the AGS with Nafion and liquid electrolytes have been demonstrated for ppm- and sub-ppm-level detection sensitivity in various applications (Stetter et al. 1977; Blurton and Stetter 1978; Ollison et al. 1995; Sakthivel and Weppner 2007).

For example, the specific configuration of a hydrogen sensor having a very low limit of detection is shown in Figure 1.10 (Ramesh et al. 2003). This sensor uses PVA–H_3PO_4 electrolyte and functions like an H_2/air fuel cell. The reference electrode in this AGS can be Pt/air, i.e., the hydrogen activity (or combined water and oxygen activities) in air are used as a reference. While this is not the most reversible system, the thermodynamic potential of the Pt in this case remains stable over long periods of time and enables the electrochemical cell to have a long lifetime. Under potentiostatic control, the sensor response/current is controlled by the rate of bulk hydrogen diffusion to the WE surface, where the oxidation rate of hydrogen at the WE surface is much higher than the diffusion rate. This diffusion-limited process is the condition that often provides the most stability for sensing hydrogen in the gas ambient environment (Sakthivel and Weppner 2006).

4.2. POTENTIOMETRIC GAS SENSORS

In the ideal condition, potentiometric sensors are sensors based on thermodynamic equilibrium for specific electrochemical reactions involving a redox reaction. Examples include ion sensors or ion-selective

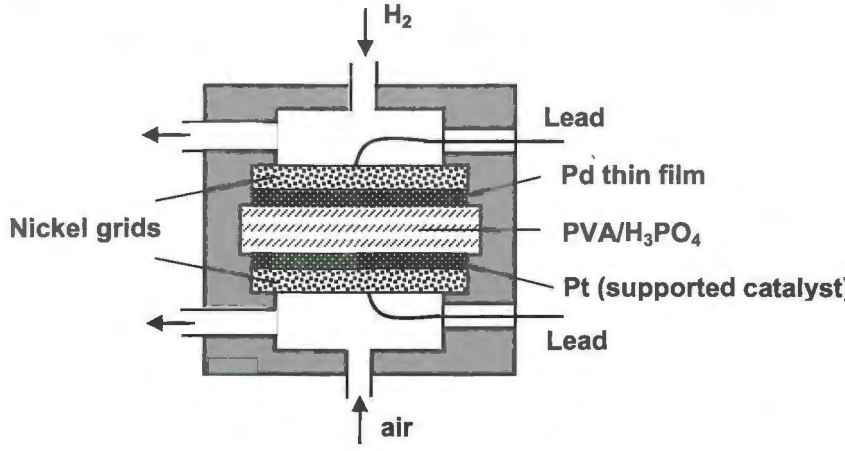

Figure 1.10. Schematic diagram of the polymer/acid electrolyte AGS for hydrogen. (Reprinted with permission from Korotcenkov 2009. Copyright 2009 American Chemical Society.)

electrodes (ISEs) that are based on redox or ion-exchange reactions (Holzinger et al. 1997; Yamazoe and Miura 1998; Bobacka et al. 2008) and are typically used in detection of analytes in liquids, such as the gas sensors described here. The simplest configuration for the potentiometric gas sensor consists of two electrodes in contact with an electrolyte, similar in arrangement to the two-electrode version of an amperometric sensor except that the measurement is taken at zero current (or as near to zero as possible) and all reactions must be in equilibrium to observe the themodynamic potential. In the simplest concept, the operation of a potentiometric gas sensor is based on the concentration dependence of a potential (E) of a sensing electrode compared to a reference electrode (RE). The chemical concentration effect on the potential of an electrode is given by the Nernst equation as

$$E = A \pm \frac{RT}{nF} \ln a \tag{1.22}$$

where A is a constant, R is the universal gas constant (8.314472 J/K mol), T is absolute temperature (K), F is Faraday's constant (9.648×10^4 C/mol), n is the number of electrons participating in the electrochemical reaction, and a is the chemical activity of analytes, $a_X = \gamma_X[X]$, where γ_X is the activity coefficient of species X. (Since activity coefficient tends to be unity at low concentrations, activities in the Nernst equation are frequently replaced by simple concentrations.) The Nernst equation expresses the chemical concentration effect on the observed electrical potential; e.g., for a reaction involving one electron, a change in potential of 59.1 mV is observed for each order-of-magnitude change in the activity of analyte a. The "ln a" term is derived by writing the Nernst equation for the chemical reaction at the sensing electrode. Since activity is often approximated by concentration, the measured value of E is a measure of the concentration of target analyte a. In the more general Nernst equation, ln a is expressed as ln Q, where Q is the reaction quotient for the reaction under consideration.

In most cases, modern potentiometric sensors function as concentration cells. For H_2 sensors, such a cell is shown in Figure 1.11. The potential observed between the two electrodes is given by the Nernst equation summed for the two reactions, i.e.,

Sum of

$$E_a = E^0 + RT/F \ln[H^+]/[H_{2a}]^{1/2} \tag{1.23}$$

and

$$E_b = E^0 + RT/F \ln[H^+]/[H_{2b}]^{1/2} \tag{1.24}$$

where *a* and *b* represent each side of the membrane with a different concentration of H_2 as above, such that the concentration-cell Nernst equation is written as

$$E_a = E^0 + RT/F \ln[H_{2b}]/[H_{2a}]^{1/2} \tag{1.25}$$

and the potential depends on the difference in the pressure of the H_2 on each side of the membrane.

A potentiometric sensor can measure analyte concentrations over a very wide range, often more than 10 decades. In potentiometry, the chemical and diffusion processes must be at equilibrium conditions in the sensor for a thermodynamically accurate signal to be observed. Comparatively, the amperometric sensors rely on Faraday's law and a dynamic reaction achieving a steady-state condition in the sensor.

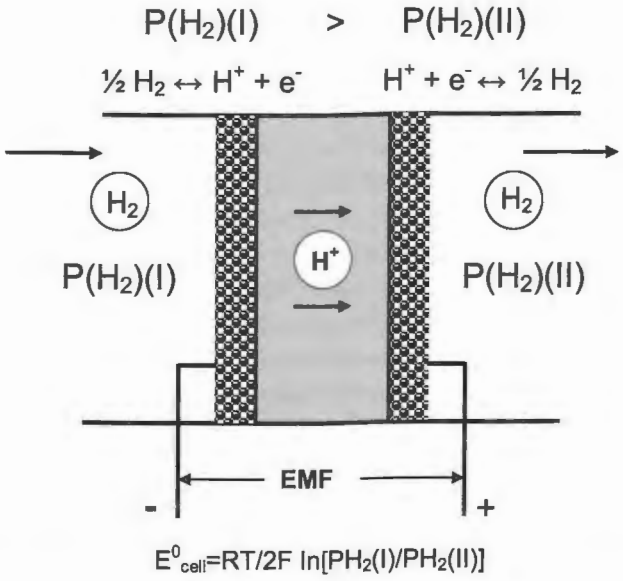

Figure 1.11. Working principle of hydrogen concentration cell using a proton-conducting membrane. (Reprinted with permission from Elsevier. Adapted with permission from Sundmacher et al. 2005. Copyright 2005 Elsevier.)

In potentiometric sensors where equilibrium is not obtained or several reactions are involved simultaneously, deviations from Nernstian behavior are observed; these systems are often called "mixed" potential sensors. The sensors are often able to be calibrated and provide useful sensing performance, but understanding the molecular and chemical reaction basis for the signal is more difficult.

Interestingly, the amperometric sensor signal will get smaller with the size of the electrode because of the decreasing rate of analyte reaction at the electrode surface, while the potentiometric sensor has no such dependence on geometry. This situation becomes most interesting in nanostructures, in which the thermodynamic potential can be characteristic of aggregates of atoms and different from a bulk system of components. The amperometric sensor reaction rate is typically enhanced by the high surface areas afforded by nanostructured electrode materials, while the thermodynamic potential of aggregate systems has a different meaning.

It is necessary to note that during the past decade, the chemical sensing abilities of ion-selective electrodes have been improved to such an extent that it has resulted in a "new wave of ion-selective electrodes" (Bakker and Pretsch 2005; Pretsch 2007). This can be attributed to the considerable improvement in the lower detection limit of ISEs, new membrane materials, new sensing concepts, and a deeper theoretical understanding and modeling of the potentiometric response of ISEs (Bobacka et al. 2008). The response of potentiometric ion sensors, i.e., ion-selective electrodes and/or ion-sensitive sensors (ISSs) and sensors with solid-state contact made of conducting polymer films, is a complex, time-dependent phenomenon that depends on the electroactive material (membrane/film) and the electrolyte solution as well as the specific membrane/solution interface's composition and the thermodynamics and kinetics of reactions (Bobacka et al. 2008). Potentiometric gas sensors should evolve to use this knowledge.

4.3. CONDUCTOMETRIC GAS SENSORS

In conductometric sensors the measurement of solution resistance is not inherently species-selective. Therefore this approach to design of gas sensors, based on liquid electrolytes, would observe conductivity changes that are larger for hydrogen, since there is a large conductivity of the proton compared to other ions. This results in a similar selectivity as is observed in the gas-phase thermal conductivity measurement, in which hydrogen has thermal conductivity many times that of other gases. The conductometric detectors can be useful in situations where it is necessary to ascertain, for example, whether the total ion concentration is below a certain permissible maximum level or for use as an online detector after separation of a mixture of ions by ion chromatography (Brett 2001). Such situations arise in electro-remediation technologies. Some people consider all resistance measurements and heated metal oxide sensors as electrochemical, since the resistance changes as the surface charge is altered or as the bulk stoichiometry is changed. However, HMOX devices rely primarily on electronic changes as opposed to electrochemical changes, i.e., electronic versus electrolytic conductivity. In any case, we will not consider the HMOX hydrogen sensor here and also will not consider the limited applicability of liquid conductometric sensors further. It is sufficient to say that electrolytic conductivity can be used for sensing and is an important aspect/property of many electrolytes, including those used in gas sensors.

5. ANALYTES

Experiments have demonstrated that many gases, such as H_2, O_2, CO, NO_2, NO, O_3, SO_2, H_2S, and organic vapors with electroactive functional groups such as alcohols or aldehydes, can be measured with an appropriately designed electrochemical gas sensors. In principle, any electroactive gas or one that can generate an electroactive species can be measured with an electrochemical approach. Classes of gaseous compounds which have been detected by electrochemical sensors are given in Table 1.2.

Reactions for NO_2, N_2O, CO_2, and O_2 analyses are electrochemical reductions, while the other analytes utilize electro-oxidation to produce the analytical signal (Chang et al. 1993). We have to note that each sensor can have a unique design and a different set of materials and geometries for membranes, electrolytes, and electrodes in order to take advantage of chemical properties of a specific target analyte and survive under various operating conditions. The next section presents several examples of such designs. There are many chemical and biological materials that can be measured with electrochemical sensors that are not included here.

Table 1.2. Classes of gaseous compounds analyzed amperometrically

1	Hydrocarbons and carbon/oxygen compounds	CO, CO_2, C_2H_4, C_2H_5OH, EtO
2	Oxides of nitrogen	NO, NO_2, N_2O
3	Sulfur compounds	H_2S, CH_3SH, C_2H_5SH, SO_2
4	Reduced nitrogen	NH_3, N_2H_4, $(CH_3)N_2H_3$, $(CH_3)_2 N_2H_2$
5	Other	O_2, H_2, Cl_2; O_3, PH_3, As_3, HCN, $CHClBrCF_3$

Source: Reprinted with permission from Chang et al. 1993. Copyright 1993 Elsevier.

6. ELECTROCHEMICAL GAS SENSOR DESIGNS AND MATERIALS

Electrochemical sensors may consist of six major parts (see Figure 1.7): filter, membrane (or capillary), working or sensing electrode, electrolyte, counter electrode, and reference electrode. Each part of the sensor influences the overall performance and analytical characteristics of the sensor. Therefore, it is often the major goal of research efforts to find the link between the analytical performance of the electrochemical sensor and the construction/design and materials from which the sensor is made, as well as the many factors included in the testing of the sensor, such as mass transfer of the analyte to the electrode. Choosing appropriate materials for sensor construction and selecting an efficient sensor geometry is critical to obtaining optimal sensor operation and performance. The materials that participate in specific chemical interactions and their fundamental electronic and electrochemical properties, and their stability, will control sensory reaction thermodynamics and kinetics. The geometry and dimensions of the sensor device have a profound effect on a gas sensor's analytical performance, including the observed sensitivity, selectivity, response time, and signal stability. The "minor" details of sensor design can have a profound influence on the accuracy, precision, background current, noise, stability, lifetime, and

selectivity of the resulting sensor. Note that often the choice of optimum sensor materials and geometry for a given application are not obvious.

6.1. ELECTROLYTES

As shown in Figure 1.12, the electrolyte is part of the electric circuit of an electrochemical sensor system. The role of the electrolyte is to transport charge within the sensor, contact all electrodes effectively, solubilize the reactants and products for efficient transport, and be stable chemically and physically under all conditions of sensor operation.

On the other hand, the modifying coating is not a part of the electric circuit, although ion transport and electron transport sometimes take place within the coating or at the coating/electrode interface. The difference between the electrolyte and the electrode modifying coating is not always obvious, and sometimes the classification in a structure is a bit arbitrary

An electrolyte can be either/both ion-conducting and/or electron-conducting. Examples of commonly used electrolytes include aqueous electrolytes, nonaqueous electrolytes, polymers, ionic liquids, and solid electrolytes. In conductometry, the electrolyte is designed and fabricated to change conductivity only when it interacts with the analyte gas molecules. In potentiometry and amperometry, the electrolyte can contribute to the sensitivity and selectivity by having special solubility and reactivity toward the analyte, its reaction rate on the electrode surface, or the product of the reactions in the sensor.

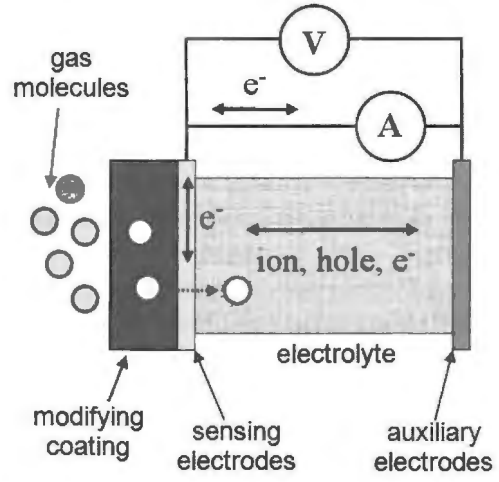

Figure 1.12. Schematic diagram of electrochemical sensor operation.

6.1.1. Liquid Electrolytes

The role of the liquid electrolyte in electrochemical sensors is to transport charge within the sensor, contact all electrodes effectively, solubilize the reactants and products for efficient transport, and be

stable chemically and physically under all conditions of sensor operation. For electrochemical gas sensor applications, the electrolyte solution needs to support both counter electrode and sensing electrode reactions, form a stable reference potential with the reference electrode, be compatible with the materials of construction, and be stable over long periods of time under various operating conditions.

Prior to 1970, electrolyte solutions for amperometric sensors were mainly aqueous in nature. Even nowadays, aqueous solutions are still used as the electrolytes for gas sensing, e.g., acid or halide electrolytic solutions are used for acidic gas (Imaya et al. 2005) and for other gas-detection applications (Ho and Hung 2001). As illustrated in the preceding examples, aqueous electrolytes are effective in many electrochemical gas sensors. Examples of commonly used electrolytes in H_2 sensors are presented in Table 1.3. Electrolytes used for designing other electrochemical sensors are listed in Table 1.4. One can observe that most electrochemical gas sensors utilize H_2SO_4 and NaOH electrolytes.

Table 1.3. Examples of electrochemical H_2 sensors based on liquid and polymer electrolytes

Gas	Electrolyte	Membrane	Electrode material	Sensor type	LOD $[H_2]$	Upper range
H_2-air	6 N KOH or 5 N H_2SO_4	Teflon	Pt			
H_2	5 M H_2SO_4	Teflon	Pt/C			4,000 ppm
H_2	9 M H_2SO_4	PTFE	Au			
H_2	1 M H_2SO_4	Nafion	Pt-Ag/AgCl	A	<1%	16% ppm
H_2-N_2	1.0 M NaOH	PTFE	Pt/C	A	<0.1%	2%
H_2-air	H_2SO_4	Teflon	Pt-Ag/AgCl	A	<0.2%	0.2–4%
H_2-N_2	H_2SO_4	Teflon	Pt-Ag/AgCl	A	<0.4%	1–100%
H_2-air	Nafion	PTFE	Pt/C	A	<50 ppm	12,000 ppm
H_2-N_2(CO_2)	Nafion	Ionic polymer	Pt			10%
H_2-N_2	Nafion		Pt	A	10 ppm	10%
H_2-N_2	0.5 M H_2SO_4	PTFE	Pt/C	A	<0.1%	2%
H_2-argon	Nafion	Teflon	Pt/C	A	<10 ppm	4%
H_2-argon	PVA/H_3PO_4	Teflon	Pd and Pt	A	<10 ppm	
H_2	Nafion/ 0.1 M H_2SO_4		Pt			5,000 ppm
H_2-air	Nafion		Pt	A, P	20 ppm	4,000 ppm
H_2-air	Nafion		Pt	P	30 ppm	1,000 ppm
H_2	Nafion	Teflon	Pt	A	<10 ppm	1,000 ppm
H_2-air	PBI/H_3PO_4		Pt/C-Ag/AgCl	P	$<10^{-4}$ Pa	1 Pa

PTFE, polytetrafluoroethylene; PVA, polyvinylalcohol; PBI, polybenzimidazole; A, amperometric; P, potentiometric; LOD, limit of detection.

Source: Reprinted with permission from Korotcenkov et al. 2009. Copyright 2009 American Chemical Society.

Table 1.4. Amperometric sensors for electroactive gases

Analyte	Type	Arrangement	Detection limit (ppm)	Upper limit of dynamic range (ppm)
H_2	SPE[a]	Pt/Nafion/0.1M H_2SO_4	n/a	5,000
	GDE[a]	Teflon-bonded WC/5M H_2SO_4	n/a	40,000
CH_4	SPE	Pt/Nafion/10 M H_2SO_4	1,300	80%
	GDE	Teflon-bonded Pt/2 M $NaClO_4$ in γ-butyrolactone	60,000	100%
C_2H_4	SPE	Au/Nafion/0.5 M H_2SO_4	0.001	500
C_2H_2	SPE	Au/Nafion/0.5 M H_2SO_4	0.02[b]	10
CH_2CH_2O	SPE	Pt/Nafion/10 M H_2SO_4	0.015	100
CH_2O	SPE	Au/Nafion/0.5 M H_2SO_4	0.013	1
C_2H_5OH	SPE	Au/Nafion/1 M NaOH	0.002	0.5
	SPE	Au/Nafion/1 M NaOH	1	476
CO	SPE	Pt/Nafion/1 M H_2SO_4	1.7	33,000
CO_2	GDE	GoreTex/Pt/0.5 M H_2SO_4	<5%[b]	50%
	GDE	Teflon/Pt/DMSO	40,000	100%
	Clark	Nonporous Teflon/Au/DMSO	n/a	15
O_2	SPE	Pt/Nafion/1 M H_2SO_4	n/a	5%
	GDE	Silicon-sieve/Pt/Nafion/H^+	n/a	80%
	Clark	Nonporous Teflon/Au/DMSO	n/a	90%
O_3	SPE[c]	Au/Nafion/H_2SO_4	0.2	350
	SPE	Au/Nafion/1 M $HClO_4$	0.22	44,800
	SPE	Au/Nafion/0.5 M H_2SO_4	0.0006	n/a
N_2O	Clark	Nonporous Teflon/Au/DMSO	n/a	90%
NO	SPE	Au, Pt/Nafion/10 M H_2SO_4	0.0010	1
	SPE[c]	Au/*a*-$ZrPO_4$/TiH_x	0.2	20
	GDE	Silicon-sieve/Au/Nafion/H^+	5	100
	SPE[d]	Au/NASICON-$NaNO_2$	n/a	1
NO_2	SPE	Au, Pt/Nafion/10 M H_2SO_4	0.004; 0.017	1
	SPE[d]	Au/NASICON-$NaNO_2$	0.01	1
	SPE	C, Au/*a*-$ZrPO_4$/TiH_x	0.01; 0.1	20
	SPE	Au/PVC/TBAHFPe	0.075	5
	SPE	C/PVC/TBAHFPe	0.08	2.2
	SPE	Au/Nafion/0.5 M H_2SO_4	n/a	100
	SPE	Au/Nafion/1 M $HClO_4$	0.2	7
SO_2	SPE	Au/Nafion, ADP/1 M NaOH	0.0005	0.1
	SPE	Au/Nafion/0.5 M H_2SO_4	0.0025	0.1

(*continued on following page*)

Table 1.4. (*continued*)

Analyte	Type	Arrangement	Detection limit (ppm)	Upper limit of dynamic range (ppm)
	SPE	Pt/Nafion/1 M $HClO_4$	0.18	4,500
	GDE	Teflon/Au/5 M H_2SO_4 in DMSO	0.5	200
	SPE	Teflon/Au, Au/Nafion/4 M H_2SO_4	n/a	50
	GDE	Teflon-bonded Au/0.33 M H_3PO_4	n/a	500
H_2S	SPE	Ag/Nafion/0.01 M $HClO_4$ + 0.99 M $NaClO_4$	0.045	450

[a] Galvanic mode.
[b] (Absorptive) preconcentration step followed by anodic oxidation or cathodic reduction.
[c] With porous Teflon membrane as additional diffusion barrier
[d] Operating temperature >150°C.

Source: Reprinted with permission from Knake et al. 2005. Copyright 2005 Elsevier.

6.1.2. Nonaqueous Electrolytes

Numerous experiments have shown that liquid electrolytes are limited in their specificity, service life, operating temperature range, and electrical potential range. As a result of the problems and limitations associated with aqueous electrolytes, sensor research benefits from a focus on the design and development of alternative electrolytes. By the middle 1970s, nonaqueous and solid polymer electrolytes emerged for electrochemical gas sensors (Niedrach and Alford 1965; Scheider 1978; La Conti 1979; Albery 1982; Venkatasetty 1985; Otagawa et al. 1985; Schmidt et al. 1985; Campbell et al. 1986; Alberti and Casicola 1993).

One of the earliest amperometric sensors employing a nonaqueous electrolyte was described by Schneider in 1978. The novel electrochemical cell, used for the detection of chlorine, contained a nonaqueous electrolyte composed of lithium or sodium perchlorate as supporting electrolyte dissolved in an organic solvent selected from the group consisting of γ-butyrolactone, sulfolan, or propylene carbonate.

All these solvents have a high boiling point (>200°C) and possess a high anodic limit with a Pt electrode. This sensor design was superior to previously designed chlorine sensors, which frequently failed because the electrode materials selective to chlorine often dissolved in the aqueous electrolyte medium. The new sensor was effective in detecting chlorine down to the parts-per-million range, had a fast response time of <1 min, and had an extended useful life of >1 year. A word of caution must be added that the use of perchlorates in organic solvents always represents an explosion hazard, particularly when the assembly is, inadvertently, allowed to dry up or be exposed to high temperatures. Similarly, Venkatasetty described the invention of a carbon monoxide sensor incorporating a nonaqueous electrolyte (Venkatasetty 1985). This sensor, based on an aprotic electrolyte system, also amperometrically

detected toxic gases such as nitrogen oxides, SO_2, and H_2S. Other electrochemical cells employing nonaqueous electrolytes were also introduced during the same time period. These systems were used to fabricate amperometric sensors for several gases such as methane (Otagawa et al. 1985) hydrazine, and carbon dioxide (Scheider 1978). In addition to inorganic materials, electrochemical gas sensors can also utilize biological materials such as hydrogenases (Bonanos 2001), a class of enzymes that catalyze the interconversion among H_2, protons [H^+], and electrons. The enzymes can be found in many phylogenetically different microorganisms, including *Thiocapsa roseopersicina, Allochromatium vinosum, Clostridium pasteurianum,* and *Ralstonia eutropha.* This branch of amperometry using biomaterials has addressed many sensing problems in medical applications, but this particular design has limited sensitivity and stability and will require additional research to achieve practicality in many of the known field applications for gas sensing.

6.1.3. Ionic Liquids for Electrochemical Gas Sensors

No commercial sensors use ionic liquids (ILs), but the research into their use is gaining momentum rapidly as of this writing (Welton 1999). Room-temperature ionic liquids (RTILs) are a unique class of compounds containing organic cations and anions, which melt at or close to room temperature. Ionic liquids possess some unique properties and can be classified as a special category of nonaqueous electrolytes as well as serve as a solvent or a gas-permeable membrane. The high boiling point and thermal stability can combine the benefits of both solid and liquid electrolytes. Some of the immediately obvious benefits of ILs include the following.

1. ILs have high ion conductivity, wide potential windows (up to 5.5 V), high heat capacity, and good chemical and electrochemical stability, and they have been explored as media in electrochemical devices including supercapacitors, fuel cells, lithium batteries, photovoltaic cells, electrochemical mechanical actuators, and electroplating (Buzzeo et al. 2004; Wei et al. 2008).
2. ILs have negligible vapor pressure, so that there is no "drying out" of the electrolytes, thus reducing hazards associated with flash points and flammability (Baker 2005; Anastas 2007). The low volatility of ILs has been demonstrated in gas-separation membranes for separation of SO_2 and CO_2 (Jiang et al. 2007). The SO_2 selectivity of separations using IL membranes has been shown to be 9–19 times that of CO_2.
3. ILs possess high thermal stability, which allows regeneration and decontamination of the sensor electrolyte as well as enabling operation at elevated temperatures, thus increasing the rate of mass transfer and hence signals (Yu et al. 2005; Jin et al. 2006).
4. ILs suppress conventional solvation and solvolysis phenomena and provide a medium able to dissolve a vast range of molecules to very high concentrations (Welton 1999; Kou et al. 2006).
5. ILs are excellent solvents that can support many types of solvent–solute interactions (hydrogen bond, π–π, dipolar, ionic, dispersive forces) (Welton 1999).

The use of ILs as electrolytes can also eliminate the need for a membrane and added supporting electrolytes, which is needed in conventional "Clark"-type gas sensors. The negligible vapor pressure and

high thermal stability make the gas sensors based on ILs promising in more extreme operating conditions, such as high temperature and pressures (Buzzeo et al. 2004). Unlike the oxide electrolytes in solid-state gas sensors, which operate at temperatures of several hundred degrees, the high ionic conductivity at room temperature allows ILs to be excellent electrolytes for the fabrication of quasi-solid-state electrochemical gas sensors working at ambient temperatures. As shown in Table 1.5, electrochemical oxidation of NH_3, NO_2, and SO_2 and electrochemical reduction of O_2 in ILs have been reported. The oxygen was found to be reduced into a superoxide radical at glassy carbon (Wang et al. 2004), Au (Buzzeo et al. 2004), and Pt (AlNashef et al. 2002) electrodes in various ionic liquid electrolytes, including BmimHFP and dmbimHFP. A solid-state O_2 gas sensor based on a porous polyethylene–supported 1-ethyl-3-methylimidazolium tetrafluoroborate ($EmimBF_4$) or 1-*n*-butyl-3-methylimidazolium hexafluorophosphate ($BmimPF_6$) membranes was developed. The sensor has a wide detection limit, high sensitivity, and excellent reproducibility (Wang et al. 2004). Moreover, upon increasing the concentration of CO_2 in the sample, the cathodic peak in cyclic voltammery increased while the reverse peak current of the oxidation decreased due to the reaction between the oxygen radical and CO_2. This mechanism provides an alternative way to perform the amperometric detection of CO_2.

Electrochemical detection of ammonia based on its interaction with hydroquinone in DMF or 1-ethyl-3-methylimidazolium bis(trifluoromethylsulfonyl)imide ($EmimNTf_2$) ionic liquid was also reported. It is suggested that ammonia reversibly removes protons from the hydroquinone molecules, thus facilitating the oxidative process with the emergence of a new wave at less positive potentials in the $EmimNTf_2$. A chemically sensitive field-effect transistor for the sensing of ammonia gas based on a composite of camphorsulfonic acid (CSA)-doped polyaniline (PAN) and an IL of 1-butyl-3-methylimidazolium bis(trifluoromethanesulfonyl)-imide, $BMI(Tf_2N)$ was developed recently. Ammonia gas concentrations from 0.5 to 694 ppm in air were characterized by using the IL-PAN–based gas sensor. The addition of the IL to the sensor structure results in enhanced sensitivity, lower detection limit, and fast response time.

In addition, the electrochemistry of several important gas analytes such as SO_2, H_2 (Silvester et al. 2008; O'Mahony et al. 2008), H_2S, NH_3 (Marisa et al. 2004), NO_2 (Broder et al. 2007), Cl_2 (Huang

Table 1.5. Electrochemistry of gases in ionic liquids or nonaqueous solvents

Gas	Conditions	Mechanism
O_2	BmimHFP; dmbimHFP, Au, Pt, and glassy carbon electrodes	$O_2 + e \rightarrow O_2^-$
SO_2	$BmiBF_4$, Pt electrode	$SO_2 + O_2 + 2e \rightarrow SO_4^{2-}$
NH_3	$EmimNTF_2$, glass carbon electrode	QH_2 (hydroquinone) + $2NH_3 \rightarrow 2NH_4^+ + Q^{2-}$ or $4NH_3 \rightarrow 3NH_4^+ + \frac{1}{2}N_2 + 3e$
NO_2	$C_2mimNTF_2$, Pt electrode	$NO_2 \rightarrow NO_2^+ + e$
CH_4	Nonaqueous 2 M $NaClO_4$ in γ-butyrolactone, Pt black electrode	$CH_4 \rightarrow CH_3(ad) + H^+ + e$

et al. 2008) were also investigated. In the ionic liquid [Emim][NTf2], the electrochemical oxidation of nitrogen dioxide gas (NO_2) on a Pt electrode follows a CE process, which involves the initial dissociation of the dimer to the monomer, followed by a one-electron oxidation. On an activated Pt electrode, the H_2 oxidation waves were nearly electrochemically and chemically reversible in a C(n)mimNTf_2 ionic liquid, chemically irreversible in C6mimCl and C4mimNO3 ILs, and showed intermediate characteristics in OTf^-, BF_4^-, PF_6^-, FAP^-, and other NTf_2^--based ionic liquids. Thus the IL has a profound influence on the observed electrochemistry, as expected. However, the important feature is that the design of ILs can be customized for optimum chemistry.

In several different ILs, a chemically irreversible reduction peak of H_2S was observed on a Pt electrode during the reductive sweep, followed by one or two oxidative peaks on the reverse scan. Potential-step chronoamperometry results indicate that the solubility of H_2S in the ILs was much higher than those reported in conventional molecular solvents, suggesting that room-temperature ionic liquids may be very favorable gas-sensing media for H_2S detection. As mentioned above, SO_2 also shows a very high solubility of 3100 (±450) mM in C4mimNO_3 IL, and a cathodic peak at 1.0 V (versus a Ag-wire reference electrode) is observed on a Pt microelectrode. The activation energy for the reduction of SO_2 in C4mimNO3 was measured to be 10 (±2) kJ/mol using chronoamperometric data at different temperatures. The stabilizing interaction of the solvent with the reduced species from SO_2 leads to a different mechanism than that observed in conventional aprotic solvents. The high sensitivity of the system to SO_2 also suggests that [C4mim][NO_3] may be a viable solvent in gas-sensing applications (Barrosse-Antle et al. 2008).

A promising property of ILs in electrochemical gas sensor development is that the physicochemical properties of ILs depend on the structure and size of both their cation and anion, which can be easily tuned by controlled organic synthesis. There are potentially many more useful ionic liquids; for example, at least a million binary ILs, and 10^{18} ternary ILs, are potentially possible. Therefore, it is likely that highly sensitive and selective determination of gaseous analytes can be realized with optimized ILs. For example, conductive polymers are often regarded as polyions after they are doped. A recent study by (Yu et al. 2008) shows that PAn in its doped state is a positively charged polymer, and the negatively charged anions of the ionic liquid butylmethylimidazolium camphorsulfonate (BMICS) can strongly absorb on the PAn polymer backbone as counter ions. The electrostatic interactions and the van der Waals interactions (π–π, alkyl–π, and alkyl–alkyl interactions and hydrogen bonding) between the IL and the charged conductive polymer template not only help increase the wetability of IL film electrolytes but also increase the selectivity by forming IL-PAn composite porous structures.

Sensitivity toward methane was measured on a polyaniline (PAn) and ionic liquid BMICS composite sensing material using quartz crystal microbalance (QCM) transducers (sensitivity is based on the frequency change) (Yu et al. 2008; Jin et al. 2008). UV-visible and Fourier-transform infrared (FTIR) spectroscopic results support observations that the anion of BMICS, camphorsulfonate, can form hydrogen bonds with the "nitrogen" sites of a protic acid–doped PAn. These hydrogen bonds align the camphorsulfonate anions in a comblike manner along the PAn backbone and therefore enhance the long-range π-orbital conjugation in the PAn. Methane molecules absorbed into the PAn/BMICS can occupy the "space" between the aligned anions and cations of BMICS. Such a mechanism of interaction is also supported by molecular mechanical simulation, spectroscopic, and thermodynamic measurements.

6.1.4. Two-Dimensional Gas Sensors with Ionic Liquids

Electrochemical gas sensors have historically proven to be very effective for measuring airborne trace compounds. However, they are also known to suffer from interference and limited specificity. To overcome these critical limitations of existing technology, electrochemical sensors can be combined with other classes of transduction using a single platform. Heterogeneous sensor arrays have been known for some time (Stetter et al. 1985). However, ionic liquids satisfy the requirements for both the electrolytes and the selective sorption coatings (Wang et al. 2003; Barisci et al. 2004), permitting two-dimensional (i.e., electrochemical and piezoelectric) sensing of gases with a single device. The unique properties of ionic liquids allow realization of both the electrolyte for amperometric detection and the sorption material for piezoelectric QCM detection, enabling a single gas sensor with multidimensional data (electroactivity and weight change upon adsorption), which can lead to enhanced sensitivity and specificity. Additional selectivity can be obtained by selecting an IL electrolyte and solvent with a specific structure on the surface of the working electrodes to enhance the reactivity. Simultaneous sensing with these two orthogonal methods provides additional selectivity to the sensor and can significantly increase the accuracy of the detection at little or no power cost. For example, an explosive vapor, 1-ethyl-2-nitrobenzene (ENB), was selected as the analyte to validate this approach (Yu et al. 2009).

As shown in Figure 1.13, the redox mechanisms of ENB in IL $BMIBF_4$ has two major processes: (1) a reversible one-electron reduction to a nitro radical anion and (2) a further irreversible one-electron

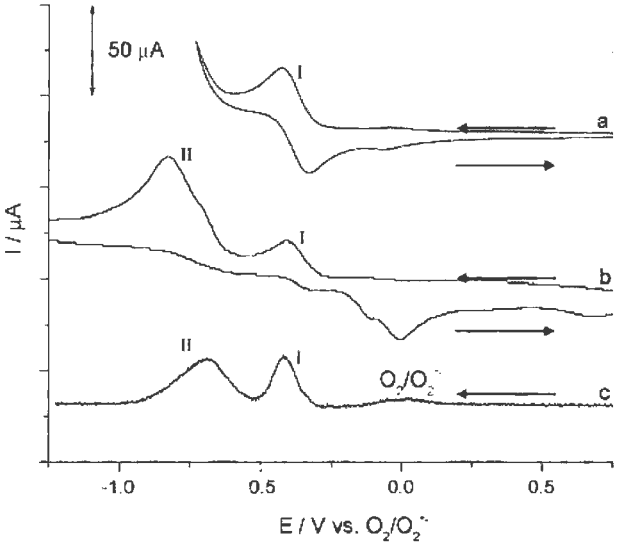

Figure 1.13. CVs of 1 mM ENB solution in $BMIBF_4$ (a) from 0 V to −1.5 V, (b) from 0 V to −2.0 V, and (c) DPV of 1 mM ENB solution in $BMIBF_4$. The reduction of oxygen was used as an internal reference, since the oxygen concentration is always saturated in the $BMIBF_4$ electrolyte. The working, counter, and quasi-reference electrodes were gold disk, platinum wire, and silver wire, respectively. (Reprinted with permission from Yu et al. 2009. Copyright 2009 Elsevier.)

reduction process to a nitro dianion. Figure 1.14 shows that in $BMIBF_4$, water (humidity) has no effect on the first processes but does affect the second process.

Due to the excellent thermal stability of ILs, as shown in Figure 1.14, by increasing the temperature, the baseline can be obtained again. Thus the problem of fouling by organic compounds or water can be minimized or eliminated by heating to regenerate the ionic liquid in an operational sensor. QCM results showed that ENB vapor is strongly sorbed into the various IL films, very likely because the anions of both BMICS and $BMIHSO_4$ can form hydrogen bonds with ENB. The absorptions of ENB in both ILs are stronger than occurs in the ILs $BMIBF_4$ and $BMIPF_6$, and the absorption of ENB on BMICS is the strongest. This result confirmed that the strength of the absorption of analyte in ILs depends directly on the specific chemical structure of the IL. The differing chemical structure of the IL can increase or decrease the IL–gas partition coefficient and provide needed partial specificity for use in sensor arrays with pattern recognition methods.

Figure 1.15 shows the integrated EQCM electrode chip with the concentric gold ring disk electrodes deposited on one side of a piece of quartz substrate. On the other side, a single gold disk electrode was formed to align exactly with the disk electrode on the opposite side. A tiny drop (2–4 μL) of $BMIBF_4$ was deposited on the ring-disk side and spread to form a thin film. The piezoelectric electrodes for mass sensing and the electrochemical electrodes for amperometric detection were fabricated on a single quartz plate to demonstrate the two-dimensional sensing (QCM mass sorption and amperometric electrochemical reactivity) (Yu et al. 2009). The resulting integrated EQCM electrode functioned both as an amperometric sensor and as a QCM sensor. Results of testing this device demonstrated that this EQCM gas sensor, which integrates both amperometric and QCM sensing modes on a single

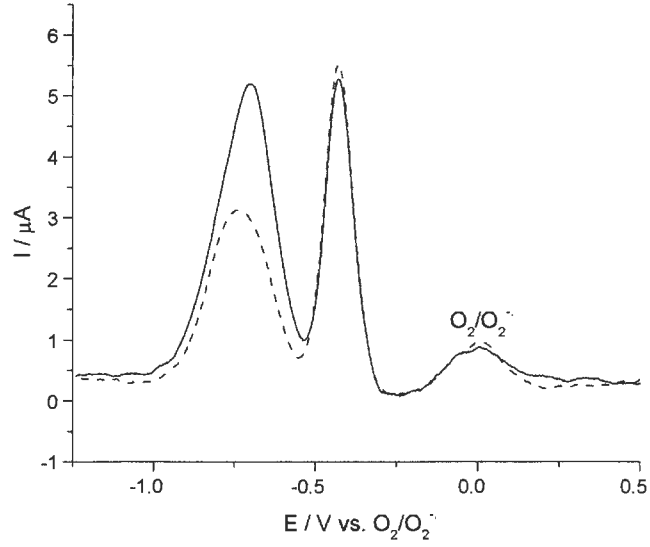

Figure 1.14. SWVs of ENB in pure $BMIBF_4$ (solid) and $BMIBF_4$ containing 0.01% (volume) of water (dashed). (Reprinted with permission from Yu et al. 2009. Copyright 2009 Elsevier.)

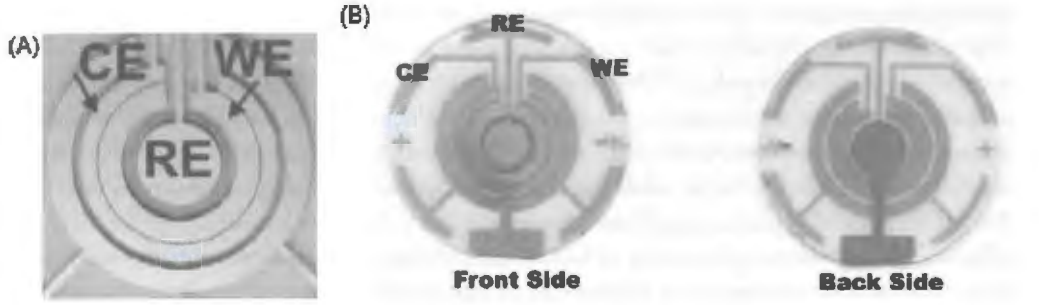

Figure 1.15. Images of integrated EQCM electrode chip: (A) Pattern of electrodes on an RsDE and (B) on front and back sides of an EQCM electrode. (Reprinted with permission from Yu et al. 2009. Copyright 2009 Elsevier.)

piece of quartz, can cross-validate the measurement and increase the accuracy of detection. Further miniaturization of the EQCM detection device incorporating both amperometric and QCM methods might lead to highly sensitive, specific, and rapid-detection gas sensor devices and systems with fewer false alarms than existing simple sensing systems.

6.1.5. Polymer Electrolytes

One of the approaches to design a room-temperature electrochemical gas sensor is the employment of solid electrolyte polymers (SEPs) (Samec et al. 1995; Opekar and Stulik 1999; Limoges et al. 1996; Liu et al. 2002; Sundmacher et al. 2005). Bobacka (2006) reported the following reasons to explain the utility of using conducting polymers in electrochemical sensors: (1) Conducting polymers can form an Ohmic contact to materials with high work function, such as carbon, gold, and platinum; (2) conducting polymers can be conveniently electrodeposited on the electronic conductor by electrochemical polymerization of a large variety of monomers; (3) several conducting polymers are soluble and can therefore be deposited from solution; and (4) conducting polymers are often materials with mixed electronic and ionic conductivity, which means that they can transduce an ionic signal into an electronic one in the solid state. These multifunctional properties are advantageous for ion-to-electron transduction solid-state devices such as sensors.

Solid polymer electrolytes became important during the mid-1970s because of their promise to overcome the inefficiencies and maintenance requirements of liquid electrolytes. Originally, a solid polymer electrolyte (SPE) was described as a solid plastic sheet of perfluorinated sulfuric acid polymer that, when saturated with water, became an excellent ionic conductor. Ionic polymers in contact with a conductive medium such as a metal allow electrochemical reactions at this interface. Early SPEs, e.g., Nafion, were not electronic conductors. Nafion, a typical solid polymer electrolyte, is a hydrated copolymer of polytetrafluoroethylene (PTFE) and polysulfonyl fluoride vinyl containing pendant sulfonic acid groups (DuPont). Nafion is a cation exchanger containing hydrophilic SO_3^- radicals firmly bound to

the hydrocarbon backbone, whose charge is compensated by counter ions (mostly H^+). The counter ions are dissociated and solubilized by water present within the polymer structure and give rise to the ionic (proton) conductivity of the polymer. The water required for proton solubility is bound in the hydration spheres of the ions present and thus the polymer is a solid which contains no macroscopic liquid phase unless excess water is present (Opekar and Stulık 1999). Nafion has good proton conductivity, high gas permeability, outstanding chemical stability, and good mechanical strength, and it has been widely used in chlorolkali, fuel cell, and sensor applications.

However, the geometric dimensions of Nafion and its electrical properties (primarily its ionic conductivity) are strongly dependent on the amount of water contained in the polymer. The maximum water content, corresponding to 22 water molecules per single sulfur group of the polymer, is attained by boiling Nafion in water, and this number decreases to 14 for the polymer in contact with a gaseous phase saturated with water vapor; the water content fluctuates with the relative humidity of the surrounding medium (Zawodzinski et al. 1993). In general, perfluorated polymer membranes show high ionic conductivities at high water vapor pressure (Anantaraman and Gardner 1996). Nafion electrolyte gas sensors, because Nafion conductivity is a function of RH, typically produce a gas response that depends on the RH (Opekar 1992; Yasuda et al. 1992; Yan and Liu 1993; Samec et al. 1995) The RH response is not desired for an ambient air sensor, where the RH can change over wide limits and typically is either eliminated or compensated.

Nafion and polymer electrolytes such as sulfonated polybenzimidazole (PBI), sulfonated polyether ether ketone (S-PEEK) (Bouchet et al. 1999, 2000, 2002; Alberti and Casciola 2001; Sundmacher et al. 2005), and PVA/H_3PO_4 can be used in H_2 sensors (Ramesh et al. 2003, 2004). Some of these solid polymer electrolytes have excellent mechanical and thermal properties and good protonic conductivity even in dry atmospheres (Bouchet and Siebert 1999; Rosini and Siebert 2005). The remarkable properties of these polymers and composites lie in the combination of the high hydrophobicity of the perfluorinated polymer backbone and the high hydrophilicity of the sulfonic acid branch. The hydrophilic branches act as a plasticizer and the backbone retains strong mechanical properties (Colomban 1999). More detailed information about polymers used in electrochemical gas sensors can be found in various reports in the literature (Josowicz 1995; Shi and Anson 1996; Colomban 1999; Wroblewski et al. 2004; Lukow and Kounaves 2005; Maksymiuk 2006; Michalska 2006).

In some cases, hydrogels or an electrolyte inside a porous matrix are used to replace free liquid electrolytes in order to raise viscosity, lower evaporation rates, and resist leakage of the electrolyte from sensor devices. The polymers or hydrogels can prevent the evaporation of electrolyte during sensor fabrication, especially for microsensor devices in which very small amounts of electrolyte are used. Using polymer electrolytes provides opportunities for the design of planar sensors and the applications of standard microelectronic fabrication technologies (Shi and Anson 1996). Polymers allow decreasing essentially both the size and the weight of electrochemical sensors. In addition, polymer electrolytes allow a larger range of operating temperatures for the electrochemical sensor. As research has shown, polymer-based electrochemical gas sensors operate successfully in the temperature range from room temperature to 100°C (Sakthivel and Weppner 2006b; Ramesh et al. 2008) and, compared to liquid electrolytes, solid polymer electrolytes can be used as separators in electrochemical cells, do not dissolve impurities from the gas as easily, and permit the construction of miniaturized devices that are leakproof to help avoid premature sensor failure.

6.1.6. Solid Electrolytes

Solid electrolyte electrochemical sensors function much like their liquid and polymer electrolyte counterparts except that the mobility of ions in crystalline or polycrystalline solids is typically much lower than in liquids. This often requires solid electrolyte sensors to operate at higher temperature in order to have high concentrations of mobile ions in the bulk solid phase (Alberti and Casciola 2001). The solid-state ions participate in the electrode reactions involving gaseous components and electrons, and the electrodes act as a catalyst for the electrode reactions in a manner very similar to that of their liquid electrolyte sensor counterparts. There are a few examples of room-temperature solid ionic conductors (e.g., AgRbI and similar salts), and there have been attempts to use them in room-temperature solid ionic conductor gas sensors.

Most of the gas sensors that use solid electrolytes are operated potentiometrically. The simplest scheme for such a sensor is represented in Figure 1.16.

Similar to liquid systems, solid-state electrochemical cells for gas sensing are typically constructed by combining a membrane of solid electrolyte (proton or ion conductor) with a pair of electrodes (electronic conductors). As is typical of electrochemical systems, the interface between the solid electrolyte and the electrode plays a very important role in determining the gas sensor's analytical characteristics. The voltage produced is from the concentration dependence of the chemical potential, which at equilibrium is represented by the Nernst equation [see Eq. (1.22)]. Such a potentiometric (Nernst-type) sensor is often called a concentration cell, and the gas activity at the sensing electrode can be obtained from the open-circuit potential E (EMF).

Electrochemical sensors based on solid electrolytes will be considered in detail in Chapter 2 of this volume and therefore are not discussed further here. We need only say that the majority of electrochemical gas sensors are based on ion and proton conductors, and there are quite a large number of solid-state materials that can potentially meet the requirements for application in solid electrolyte gas sensors.

Examples of solid electrolytes with proton conductivity, which can be used to design H_2 sensors, are given in Table 1.6.

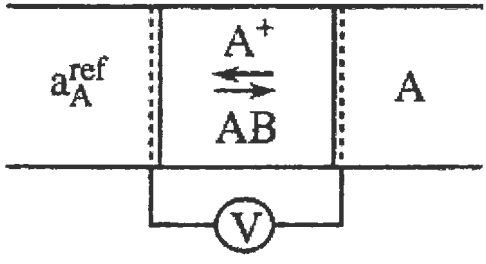

Figure 1.16. Diagram illustrating a potentiometric sensor mechanism: A is the analyte with variable activity/concentration, a^{ref} is a constant activity of analyte A in the reference side of the solid electrolyte membrane; AB is a solid electrolyte membrane (A^+ ion conductor); and the electrodes facilitate the reaction $A^+ + e^- = A$; when the activity of A is different on each side of the membrane, a potential, V, is observed. (Reprinted with permission from Korotcenkov 2009. Copyright 2009 American Chemical Society.)

Table 1.6. Solid electrolytes used in electrochemical solid electrolyte H_2 gas sensors

Solid electrolyte	Temperature of stability (°C)	Type of gas sensor
$HUO_2PO_4 \cdot 4H_2O$	<100	P; C
$Sb_2O_5 \cdot 4H_2O$	<100	P; A
$Sb_2O_5 \cdot H_2O\text{-}H_3PO_4$	<100	P
$Zr(HPO_4)_2 \cdot nH_2O$	<350	P; A
$H_4SiW_{12}O_{40} \cdot nH_2O$	100	P
$Me_xH_{3-x}PW_{12}O_{40} \cdot nH_2O$	100	P
$(NH_4)_2HPW_{12}O_{40} \cdot nH_2O$	100	P
Hydronium NASICON	100	P
$5P_2O_5 \cdot 95SiO_2$ glass		P
Na_3PO_4	>600	P
K_3PO_4	>600	P
In^{3+}-doped SnP_2O_7		
YSZ	>1000	
α-Al_2O_3:Mg	>1500	
$Ce_{0.8}Gd_{0.2}O_{1.9}$	>1000	P
Perovskites:		
$SrCeO_3$	>1000	P
$SrCeO_3$:Yb	>1000	C, P
$CaZrO_3$	>1000	P
($CaZrO_3$:In)		P
$BaCeO_3$	>1000	P
$BaCe_{0.8}Gd_{0.2}O_3$	>1000	P
$BaZr_{0.4}Ce_{0.4}In_{0.2}O_3$	>1000	
$Ba_3Ca_{1.18}Nb_{1.82}O_{9-\delta}$	>1000	P
$KCa_2Nb_3O_{10}$	>1000	P

P, potentiometric; A, amperometric; C, conductometric; NASICON, $Na_3Zr_2Si_2PO_{12}$

Source: Reprinted with permission from Korotcenkov et al. 2009. Copyright 2009 American Chemical Society.

Each solid material has its own range of temperatures over which it possesses the required proton conductivity and is stable. The proton mobility is a function of temperature. Figure 1.17 illustrates this for some solids versus liquids and polymers, and each material has an optimum temperature or temperature range for operation. For example, the working temperature range of the $BaCeO_3$-based sensor, due to the high protonic conductivity of $BaCeO_3$, varies from 200 to 900°C (Iwahara et al. 1991). Also, the electrical conductivity measurements of $BaZrO_3$:Y showed predominantly proton conduction at temperatures below 500°C, which is suitable for hydrogen sensor operation (Wang and Virkar 2005). Many of these materials compare favorably to Nafion and should be suitable for H_2 sensing applications.

Typical solid electrolytes for high-temperature gas sensors include yttria-stabilized zirconia (YSZ) and perovskites that become sufficiently conductive only when the temperature exceeds 400°C (Tejuca and Fierro 1993; Iwahara 1995; Post et al. 1999; Kosacki and Anderson 1998; Hashimoto et al. 2001; Schober 2003; Fergus 2007). They have high ionic conductivity and high activity for gas sensing over a wide range of temperatures. They often have high melting and/or decomposition temperatures and can provide microstructural and morphological stability to improve the reliability and long-term performance of sensors. The perovskite structure has two different-sized cations, which makes it amenable to a variety of dopant additions. This doping flexibility allows controlling the transport and catalytic properties to optimize sensor performance for particular applications (Fergus 2007).

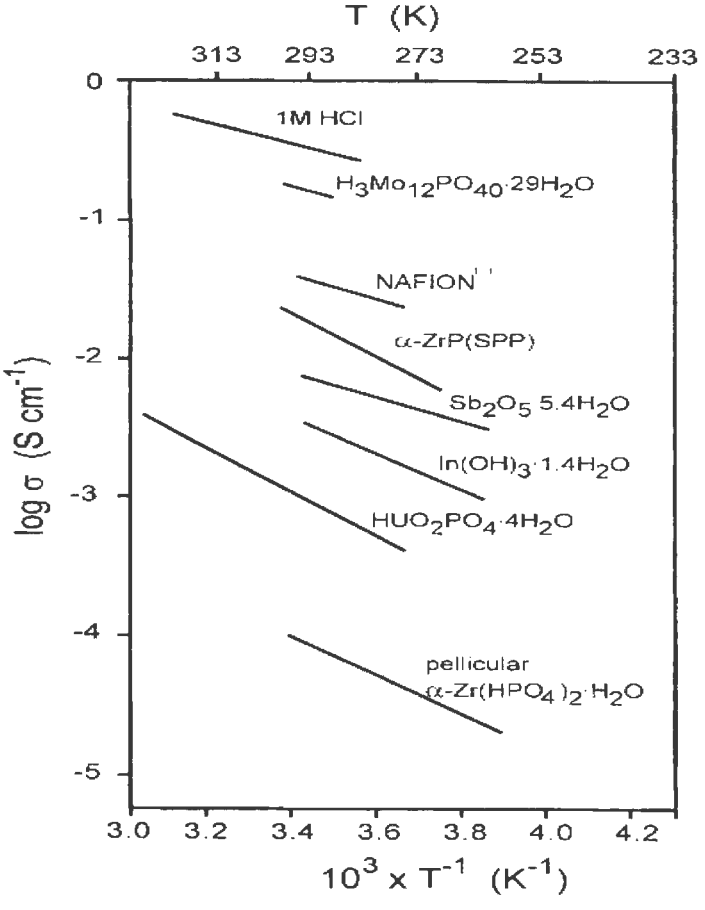

Figure 1.17. Conductivity as a function of temperature for some proton conductors. (Reprinted with permission from Alberti and Casciola 2001. Copyright 2001 Elsevier.)

6.2. MEMBRANES

A gas-permeable membrane can be used to regulate the gas flow into the sensor and can aid selectivity, allowing only the analyte gas to pass, as well as providing a barrier to prevent leakage of the electrolyte from the interior of the sensor. Hydrophobic porous membranes are used with aqueous electrolytes, since the pores are not wetted by the aqueous solution but allow the transport of dissolved gases to the electrode–electrolyte interface. The choice of membrane, its pore size and its thickness, can determine sensitivity and response time of the sensor. For example, a low-concentration gas sensor with very high sensitivity uses a coarse, high-porosity hydrophobic membrane and less restricted capillary to allow more gas molecules to pass through per unit time to produce higher sensitivity. However, this design also allows more of the electrolyte's water molecules to escape out to the environment, so the sensor can dry out faster. Depending on the electrolyte, dryout can change the electrolyte concentration, the solubility of the analyte, and the conductivity of the electrolyte, and these changes will often negatively affect the sensor signal-to-noise ratio and can lower sensitivity and response time.

Several types of porous and gas-permeable membranes exist and can be made of polymeric or inorganic materials. Most common are the commercially available very thin solid Teflon films, microporous Teflon films, or silicone membranes. Issues in the choice of membrane include permeability to the analyte of interest, ability to prevent electrolyte leakage, manufacturability, and the thickness and durability of the membrane. For example, a semipermeable membrane composed of an acrylonitrile butadiene copolymer can be used to selectively detect the partial pressure of oxygen in blood samples by allowing oxygen transport and effectively preventing the transport of other species present in the sample. In a number of cases, the rate of mass transport through the membrane controls the limiting current and, hence, the sensitivity of the sensor. As can be seen from the data presented in Figure 1.9, an increase in membrane thickness decreases the sensor sensitivity. Ideally, the gas membrane must have a constant permeability to the target gaseous analyte during sensor operation over a wide temperature range and must possess mechanical, chemical, and environmental stability. Electrochemical hydrogen sensors typically use membranes of Teflon (see Table 1.3). The expanded polytetrafluoroethylene (ePTFE) membrane is a chemically stable substance and has high gas permeability without permeation of aqueous electrolytes.

6.3. ELECTRODES

6.3.1. Sensing Electrodes

Electron transfer takes place at the interface between the sensing electrode and the electrolyte. The function of the sensing electrode varies with the methodology. In conductometry, the electrodes are generally not modified. The rate of electron transfer or the current (I) is proportional to the potential difference (U) between the sensing electrode and the auxiliary electrode. The conductance of electrolyte is the ratio of current to the potential difference. In practical use, the relative resistance change is usually monitored and reported in conductometry. Resistance, the ratio of U to I, is the reciprocal of conductance. The relative resistance change is expressed as $\Delta R/R_0$, or $(R - R_0)/R_0$, where R is the present resistance and R_0 is the resistance in the absence of analyte gases. Note that the signal is defined as the resistance with

analyte present minus the signal with no analyte, and that the sensitivity is the slope of the signal-versus-concentration graph.

In potentiometry and amperometry, the sensing electrode is usually has a chemically modified surface. The modification is a thin film or layer of certain materials that is ideally selectively permeable to the analyte gas molecule. This modification ensures the selectivity of the gas sensor. The modifying films or layers may also incorporate some catalysts, including enzymes in some cases, facilitating the reduction or oxidation of the analyte gas.

In gravitometry, the electrode surface is also chemically modified. The modifying films or layers trap the gas molecules of interest. The change in mass on the electrode surface is the signal for gas sensing (see the discussion of the QCM in the section on ionic liquids).

6.3.1.1. CHARACTERISTICS OF SENSING ELECTRODES FOR SENSORS WITH LIQUID ELECTROLYTES

Many liquid-electrolyte gas sensors use designs that are derived from modifications of the Clark electrode (Hitchman 1978), especially those that utilize metallized membranes for electrodes (Stetter and Blurton 1976, 1977; Vaihinger et al. 1991; Cao and Stetter 1991; Cao et al. 1992; Chang et al. 1993; Stetter and Li 2008). In the latter cells, the precious-metal electrode is evaporated or sputtered directly onto the electrolyte-facing side of a polymer membrane (Cao and Stetter 1991; Cao et al. 1992). The common feature of the Clark type of gas sensor is an interface at the working electrode (WE, or sensing electrode, SE) that facilitates rapid transport of the gas to the WE/electrolyte interface. Gas sensors with electrodes made as a back-side metallized porous membrane are not affected by evaporation of water from the electrolyte as much as those electrodes that are open to the analyte or air, because the electrode is in direct contact with the bulk of the electrolyte solution. The mass transfer of analyte from the sample to the working electrode can be fast, but even faster in electrodes open to the air, resulting in short response times and high sensitivity.

Sensors employing fuel-cell electrode technology or gas diffusion electrodes (GDEs) are also well studied (Mosley et al. 1991; Sundmacher et al. 2005). These are generally composed of a sintered composite (e.g., powdered Teflon and noble-metal black) with two or three similar gas diffusion electrodes separated by an aqueous electrolyte or an ion-conducting membrane. The GDE combine the following functions (Sundmacher et al. 2005):

- There is a catalytic function within the electrode structure for electrochemical reactions.
- Electrons released in the anodic reaction or consumed in the cathodic reaction at the reaction sites have to be collected; i.e., the electrode composite must be electrically conductive.
- Ions in the membrane must be transported toward the reaction sites; i.e., the electrode needs to house some electrolyte to have ionic conductivity.
- Noncharged reactants have to be transported toward the reaction sites, primarily via pore diffusion inside the electrode structure.

Optimal electrode design requires a perfectly executed balance of the different functions. This is often achieved by preparing mixtures of ion-conducting particles (made of the membrane material),

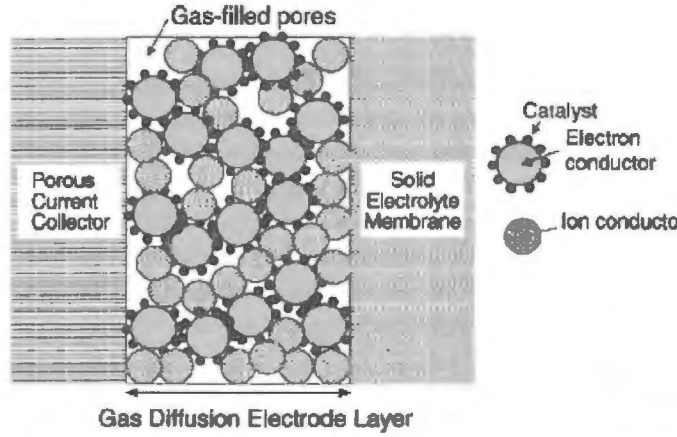

Figure 1.18. Schematic illustration of gas diffusion electrode (GDE). (Reprinted with permission from Sundmacher et al. 2005. Copyright 2005 Elsevier.)

particles of an electron conductor or metal, and catalytic particles that are either the same as the metal or different. By using well-defined particle size distributions, one can adjust the electrode pore structure. This in turn offers the possibility to optimize the transport properties of the GDE with respect to the noncharged reactants. As a result, the catalytically active surface area of the electrode can be several orders of magnitude greater in comparison with standard electrodes, allowing species with relatively poor electroactivity to produce measurable currents. Figure 1.18 shows a schematic of a typical GDE.

Gas-diffusion electrodes, manufactured much like fuel cell electrodes, have highly efficient three-phase boundaries (Vielstich et al. 2003), where the reacting gas, metallic electrode, and electrolyte meet together. The design of GDE electrochemical sensors has been shown to provide fast responses, high sensitivities, and low detection limits (Stetter et al. 1977; Blurton and Stetter 1978). The mechanism of transport is often modeled as a process consisting of diffusion through the air-filled pores of the porous current collector, diffusion to the triple phase boundary, and electron transfer occurring just as the analyte reaches the three phases where electrodes, ion-exchange membrane or electrolyte, and gas phase meet.

The GDE was first deployed for reducing gases by Blurton et al. (1972) with free electrolyte and also for H_2 sensors using a Nafion polymer electrolyte by La Conti and Maget (1971). In this work, a fuel cell could also be used as a gas sensor if the configuration is appropriate. A description of the most frequently encountered Pt-black gas-diffusion electrodes is given in Table 1.7. Platinum-based metal nanoparticles of around 2–5 nm supported on high-surface-area carbon (40- to 50-nm particles) are often used for the fabrication of gas diffusion electrodes (Kordesch and Simader 1996; Paganin et al. 1996), as is typical in fuel cells. It is important to note that over the last 20 years, the content of Pt in GDEs, expressed as mass of Pt per unit of geometric area, has decreased more than 10 times, from 5 mg Pt/cm^2 to 0.2–0.4 mg Pt/cm^2.

The gas diffusion electrodes used in amperometric sensors are semihydrophobic with a very developed microporous structure (Kordesch and Simader 1996; Bay et al. 1972; Paganin et al. 1996). Usually they are composed of two layers deposited on an appropriated support. A diffusion layer is prepared with a suspension of PTFE (e.g., DuPont TM 30) with high-surface-area carbon (Cabot XC-72, 250 m^2/g). The mixture is filtered on a support (a carbon cloth or a carbon paper or Teflon film that is totally

Table 1.7. Standard gas diffusion electrodes

ELECTRODE	ETEK	SORAPECH2	SORAPECO2
Platinum loading (mg/cm^2)	0.5	0.2	0.35
NAFION (mg/cm^2)	Unknown	1	0.8
Roughness factor	5	80	150
Active layer (10^{-6} m)	10	5	5
Diffusion layer (10^{-6} m)	250	250	250

Source: Reprinted with permission from Rosini and Siebert 2005. Copyright 2005 Elsevier.

hydrophobic). The catalytic layer is deposited onto the hydrophobic layer using one of several procedures (Paganin et al. 1996; Ren et al. 1996). The catalytic layer contains metal nanoparticles anchored on a carbon support and may incorporate Nafion, which is a proton-exchange material and thus an ionic conductor. The result is a matrix which has pores, electrolyte channels, electronic pathways, and electrocatalytic surfaces intermixed. The composite material is a good electronic conductor, porous to gases, and can conduct ions in and around the catalyst, which has a very large electroactive area. Because the electrochemical oxidation of hydrogen takes place only at the triple-phase boundary, where the Pt catalytic sites, electrolyte or Nafion, and H_2 meet in the amperometric gas sensor, the effective electrode surface area should be as large as possible.

6.3.2. Auxiliary Electrode

Most gas sensors use a two-electrode system with a sensing electrode and an auxiliary electrode. Auxiliary electrodes function as counter electrodes in condutometry and as the reference electrodes concurrently in potentiometry and some cases of amperometry. When used as a reference electrode, the potential of the auxiliary must not be significantly affected by any component in the environment unless the gas sensor utilizes a mixed potential mechanism.

In a mixed potential mechanism, the potential of the auxiliary electrode is partially determined by one or more components other than the analyte gas in the environment. The concentrations of these components do not change during the process of sensing or the components affect the sensing electrode potential and the auxiliary electrode potential to the same degree. Therefore, the potential of the sensing electrode versus the auxiliary electrode is affected only by the concentration of the analyte gas in the environment.

6.3.3. Materials for Electrodes

The material of choice for the sensor's electrodes can be different for each function. The reference electrode needs to be able to establish a stable potential. The counter electrode or auxiliary electrode should

be able to catalyze its half-cell reaction over a long time. And, of course, the sensing or working should be the ideal catalyst for its sensing reaction and be selective for it. All of the electrodes need to be stable, manufacturable, and provide stable and facile interfaces for the electrochemistry.

In an electrochemical sensor, the working electrode is typically made from a noble metal, such as platinum or gold, that is capable of making a defined interface with the electrolyte in the cell and is in a porous structure to allow efficient diffusion of the gas phase to a large-area and reactive electrode/electrolyte interface. The noble metals generally exhibit excellent stability under polarized potentials that may be corrosive to other metals. The noble metals are also excellent catalysts for many analyte reactions. Carbons, including graphite and glassy carbon, are also popular materials for working electrodes, especially for sensing bioanalytes, since many forms of carbon are biocompatible. Using Pt/C composites and nanoscale materials in gas diffusion electrodes maximizes the effective electrode surface area and, because carbon is conductive, the electrode can achieve an optimum combination of such properties as conductivity-porosity (Lu et al. 2005). Carbon provides good electrical contact between the grains of the noble metal in the porous matrix. Using a thick-film technology, a few milligrams of a carbon slurry paste can be added along with Pt grains to make an effective electrode.

The counter electrode must also be stable in the electrolyte and efficiently perform the complementary half-cell reaction that is the opposite of the analyte reaction (Stetter et al. 1993). A Pt electrode is very often used as the counter electrode in electrochemical gas sensors. In addition to the working electrode and the counter electrode, a reference electrode is also present when a potentiostat is used.

Table 1.8. Reference and sensing electrode materials used in H_2 electrochemical sensors

Electrode material	Electrode type	Examples	Working temperature
Ag/Ag^+	RE	($Ag/AgSO_4$; Ag/AgCl)	RT
Hydrated oxides	RE	(NiO; PbO_2; etc.)	RT
Ag	SE	Ag-loaded epoxy resin	<100°C
Au	SE; RE		<500°C
Pd	SE (WE)		>600°C
Pt	SE; RE		>600°C
Pt/C	SE (WE)	Pt-carbon	
Pt-alloy	SE (WE)	Pt-Au;Ag;Cu;Ni	>500°C
Transition metal hydrides	RE; CE	(ZrH_x; TiH_x; ThH_x; NbH_x)	
Metal oxides	SE (WE)	ITO, ZnO, SnO_2, CdO	Up to 700°C
Nanocomposites	SE	(Au/CuO; Au/Nb_2O_5; Au/Ga_2O_3; Au/Ta_2O_5)	Up to 700°C

RT, room temperature; RE, reference electrode; SE, sensing or working (WE) electrode; CE, counter electrode.

Source: Reprinted with permission from Korotcenkov et al. 2009. Copyright 2009 American Chemical Society.

The reference electrode must form a stable potential with the electrolyte, be compatible with the sensor manufacture, and, generally, not be sensitive to temperature (T), pressure (P), relative humidity (RH), or other contaminants or reactants in the sensor system.

The reference electrode also presents challenges for electrochemical sensors and especially miniaturized sensors. A small, stable, and long-lived RE is needed. The RE must be able to maintain the working electrode at a constant electrochemical potential during the sensing application. Silver/silver chloride (Ag/AgCl), which shows good reversibility, has been used as a reference electrode in many electrochemical applications, but it maintains a fixed potential only when the chloride concentration is fixed, and its lifetime is limited because silver chloride can gradually dissolve in aqueous solutions. The other popular reference electrode is a Pt/air electrode, which is not a classical reference electrode but is sometimes called a pseudo-reference electrode (Bay et al. 1972) because, while it forms a stable potential, the potential is not that of a well-defined thermodynamic reaction and the electrode must be calibrated with an electrode of known potential in order to know the exact potential. In a two-electrode system, a single electrode, called the auxiliary electrode, can function as both the RE and the CE for the purposes of a given analytical experiment.

The selection of the WE, RE, and CE materials is, therefore, based on the electrochemical and electrocatalytic properties as well as stability and manufacturability. Materials used as reference or sensing electrodes in H_2 electrochemical sensors are presented in Table 1.8.

6.3.4. Fabrication of Electrodes

As can be seen in the literature, there are many approaches that can be taken to create electrodes in electrochemical sensors. Opekar and Stulık (1999) emphasize four of the most often used methods:

- *Mechanical procedures.* An electrode of a suitable shape and material, e.g., a fine mesh, can be pressed, under ambient or elevated temperature, onto the surface of a membrane, or a wire can be tightly wound around a solid or polymer electrolyte tube. Screen printing is also a mechanical procedure for depositing material from an ink onto a surface.
- *Physical vapor deposition (PVD) and chemical vapor deposition (CVD) plating.* These procedures permit formation of electrodes of various shapes on the surface of membranes and solid electrolytes, but the electrodes often have poor mechanical stability and are destroyed by changes in the membrane dimensions due to test-medium humidity variations. However, vacuum evaporation (or sputtering) is one of the principal methods for preparation of planar sensors, with electrodes produced photolithographically on an inert support (glass, ceramic).
- *Chemical deposition.* A metal can be deposited from a solution, especially in cases where the electrode is produced on the surface of membranes and solid electrolytes, by chemical reduction of a suitable metal compound. This approach was patented for platinum and gold electrodes, but it also can be used for other metals (e.g., Ni, Cu, Ag).
- *Impregnation.* The polymer or solid electrolyte membrane is immersed in a solution of a suitable compound of the metal to be deposited and is saturated with the solution; the saturation can be accelerated for Nafion by adding methanol to the solution. The membrane is then immersed,

one or both sides, in a solution of a strong reductant so the metal deposits where the reductant is placed. The procedure can be repeated to obtain a thicker metal film.

In addition, the GDE of the fuel cell can be sprayed onto the substrate or vacuum filtered onto the substrate with subsequent curing to bond the electrode structure together. Of course, every method has both advantages and disadvantages, and some detailed information is available in reviews (Opekar and Stulık 1999).

7. ANALYTICAL CHARACTERISTICS OF ELECTROCHEMICAL SENSORS

As has been shown in previous sections, the response of an electrochemical gas sensor can be described by the following eight steps (Chang et al. 1993).

1. Introduction of the gas- or vapor-phase compound to the sensor through the filter (The filter can enhance the selectivity of the sensor system by removing unwanted electroactive contaminants and also protect the sensing electrode from particulate contamination.)
2. Transfer of the reactant from the gas chamber to the back of the sensing electrode and diffusion to the gas/electrolyte interface (Laminar flow characteristics dominate in gas chambers of typical geometries. There may be a membrane or capillary somewhere between the gas chamber and the electrode, and transfer across the membrane or capillary is usually characterized as a diffusion process.)
3. Dissolution of the electroactive species in the electrolyte (The rate of mass transfer across the gas/liquid boundary and the solubility of the gas in the electrolyte can affect the sensor sensitivity and response time.)
4. Diffusion of the analyte to the electrode/electrolyte interface (in the liquid phase)
5. Adsorption onto the electrode surface
6. Electrochemical reaction with electron transfer
7. Desorption of the products
8. Diffusion of the products away from the reaction zone to the bulk of electrolyte or gas phase.

Any of these steps can be rate-limiting and thus determine the ultimate response characteristics of the electrochemical sensor. The parameters that most frequently influence the observed analytical characteristics of a sensor include sample flow rate, working electrode composition, type and amount of electrolyte, membrane porosity and permeability, and the electrochemical potential of the sensing electrode. By controlling these parameters, the sensor engineer can often achieve the desired and/or optimum sensor response characteristics for a particular compound in a given situation.

The response of an electrode may also be complicated by electrode poisoning processes and/or auto-catalytic reactions (observed as a change of steady-state signal response time and magnitude). In addition, the electrochemical reaction mechanism may change with sensor operating conditions. For example, at low analyte sampling rates, the sensor may electro-oxidize all of the available analyte and act

as a coulometric device, being limited by the supply of analyte. Conversely, at high analyte flows, diffusion through the electrolyte may limit response; and at low electrocatalytic activity, the rate of reaction at the electrode surface may limit the observed current (i.e., signal).

7.1. SENSITIVITY (LOWER DETECTION LIMIT)

Sensitivity is defined as the slope of the signal-versus-concentration graph. For nonlinear sensors, the concentration at which the sensitivity is determined must also be reported. The lower detection limit (LDL) is often reported as the concentration corresponding to three times the noise level, but this only takes into account false negatives. A true detection limit should also consider the selectivity of the analytical method and take into account the probability of both false positives and false negatives. While the subject of the LDL is somewhat controversial, whenever a sensitivity is reported, the noise level should also be reported so that an estimate of the detection limit can be made.

The lower detectable limit for an electrochemical sensor for a particular gaseous compound is related to several factors, including mass transport of the compound within the detection system, electrocatalytic activity (catalyst material, form, and potential of operation), Faradaic equivalents per mole transferred during reaction, analyte solubility and mobility in the electrolyte, the physical geometry of the sensor, and the "method" of operation (including semipermeable membranes or filters). It is the optimization of these parameters which leads to the maximum signal-to-noise ratio (S/N) for a given analytical system.

Sensitivity is typically not limited by the Faradaic or electrocatalytic signal. For example, using Faraday's law [Eq. (1.16)], the current achieved (i.e., sensitivity) by reacting a 1-ppm CO/air mixture at 1% efficiency in a gas stream at 600 cm^3/s is about 1 μA.

Clearly, a current of 1 μA can be easily measured with existing electronic capabilities. However, the background current and fluctuations thereof cause most sensors to have a detection limit around the 1-ppm range. Thus, the practical LDL for most sensors is the relatively large magnitude of the background and noise current and not the size of the signal. Possible causes of background current in amperometric gas sensors can include (Chang et al. 1993):

1. Impurities in the electrolyte, such as traces of dissolved oxygen, and/or slow oxidation or reduction of solvent at the sensing electrode, such as the slow evolution of hydrogen or oxygen from an aqueous solution
2. Corrosion of the electrode, such as slow growth of the oxide layer on the surface of a noble or passivated metal electrode catalyst in the anodic potential range
3. Diffusion of the reactant or reaction products from the counter electrode, such as the diffusion of dissolved peroxide toward the sensing electrode from an oxygen-reducing counter electrode

A 1-ppm LDL is not sufficient for many applications, and in recent years, improvements have been reported (Hodgson et al. 1999; Stetter and Li 2008). The design of advanced amperometric cells has been shown to give fast responses, higher sensitivities, and better detection limits than previously reported arrangements. As a result, lower detection limits for current amperometric gas sensors have been

extended to parts-per-billion levels for certain analytes such as NO_2, $C1_2$, H_2S, ozone, and many other gases (Chang et al. 1993; Knake et al. 2005; Stetter and Li 2008).

For species with very slow reaction kinetics, in some cases, the sensitivity can be enhanced by preconcentration of the analyte on the electrode by setting it to a potential at which partial oxidation or reduction takes place, followed by a potential sweep during which the accumulated analyte is completely oxidized or reduced and the resulting current is integrated. Examples include demonstrations by (1) Vielstich and co-workers (2003) for the determination of CO_2 on a Pt electrode; (2) Kuver et al. (1993) and Schiavon et al. (1995) for the determination of H_2S on Ag; (3) Baltruschat et al. (1997) for a number of unsaturated hydrocarbons on Pt or Pd; (4) Jordan and Hauser (1997) for acetylene on gold; and (5) Jacquinot et al. (2001) for methane and other small saturated hydrocarbons on Pt. Preconcentration may also be carried out externally in systems with forced gas flow. Jordan et al. (1997) demonstrated the preconcentration of ethylene on silver, from which it was flushed by heating the cartridge, and a similar arrangement was used by Knake and Hauser (2003) for preconcentration of acetylene. Note that preconcentration generally leads to higher selectivities as well.

7.2. SELECTIVITY

Selectivity can be quantified as the ratio of the signal for the target analyte to another or several other electroactive species that may be simultaneously present in the sample. Electrochemical sensors are useful for detection of more than a dozen electroactive analytes. The levels of all electroactive species possibly co-present in the environment in a particular application must be known, so that interference in the desired measurement can be minimized. Therefore the selectivity of the sensor to a specific gas is necessary for the success of the sensor. However, it is generally difficult to achieve "perfect" selectivity, as many electroactive species tend to react under similar conditions, i.e., oxidations or reductions (Knake et al. 2005).

Interferences can be generally kept to an acceptable level either by selecting the proper electrocatalyst, electrochemical conditions, or method, or by using a selective adsorbent in the instrument inlet to remove undesirable electrochemically active contamination. In a sulfur dioxide sensor, for example, it was found that the use of a basic electrolyte solution enhanced the oxidation wave in the region of "AuO"' formation, because the major electroactive species is SO_3^{2-} (*aq*) as opposed to physically dissolved $SO_2 \cdot H_2O$, which is almost solely present in acid electrolyte solutions. Sulfite ions, in fact, react chemically with the oxide layer on the gold surface (Bard 1978). This is not the case, however, for the other interfering species in acid solutions, such as NO, NO_2, and CO, which, in a basic electrolyte, still react mainly in the double-layer region. The use of a basic electrolyte for the detection of SO_2, therefore, not only increases the current sensitivity but also improves the selectivity, with cross-sensitivities decreasing from 0.5% to 0.2% for NO, and from 3% to 0.3% for CO (Hodgson et al. 1999b).

The selectivity of amperometric gas sensors can be improved by careful manipulation of thermodynamic and/or kinetic reaction parameters; that is, some degree of selectivity can be obtained by careful choice of the applied potential within the available range, which is bound by the reduction and oxidation of water (Chang et al. 1993; Knake et al. 2005). The selectivity of an amperometric sensor can also

be altered to some degree by the choice of electrode material and electrolyte solution. Such approaches have been discussed (Blurton and Sedlak 1974), and a brief example is offered here. Carbon monoxide oxidation occurs on a platinum electrocatalyst at 0.9–1.5 V versus NHE (normal hydrogen electrode). However, the CO reaction proceeds 100 to 1000 times slower on a gold electrocatalyst. On the other hand, H_2S reactivity is high for both Au and Pt electrocatalysts. Thus, H_2S can be monitored even in the presence of CO by using a gold electrocatalyst. This is an example of kinetic selectivity. The NO oxidation reaction on gold does not occur at potentials below about 1.0 V versus NHE, but NO_2 can be reduced at potentials about 0.8 V versus NHE (Roh and Stetter 2003). Thus, NO_2 can be detected even in the presence of NO using a gold electrocatalyst operated at 0.8 V versus NHE.

However, favorable kinetics or thermodynamics are not the only two sources of inherent sensor selectivity. There are also many other approaches, which involve different methods of piefiltration or pretreatment of the gaseous analyte prior to sensor entry. For example, commercial sensors based on gas diffusion electrodes often contain chemical filters, substances which scrub interfering species from the sample gas. An elegant solution, also used in commercial devices, is the use of an additional auxiliary electrode for this purpose. This is poised at a lower potential then the working electrode so that, SO_2 is removed to allow the selective determination of NO at the working electrode. Chemical and electrochemical filtering may also be used external to the sensor cell itself if the latter is connected to a manifold through which the sample gas is guided (Knake and Hauser 2003; Jacquinot et al. 2001). Selectivity can also be obtained through separation of the analytes. In fact, several groups have described the use of amperometric gas sensors as detectors in gas chromatography (Blurton and Stetter 1978; Criddle et al. 1995).

7.3. PRECISION AND ACCURACY

Accuracy generally refers to the "true" value and how well any given sensor or method provides the true value for the analysis. The precision is often stated in terms of repeatability of a given measurement, and the statistical definitions of precision and accuracy are provided in many textbooks on analytical science.

The accuracy of amperometric gas sensors is typically limited by the preparation of standards, while the precision is a function of the operating conditions, the concentration of analyte, and the care taken by the operator in making the measurement. Performance in general is a function of the entire analytical system and the method employed. In field monitoring situations there is often no opportunity for repeat readings and, indeed, the sensor must often operate unattended, gathering data over a long period of time. Instrument precision must be known in order to quantify the analyte and assess the reliability of each independent measurement. The precision of amperometric gas sensors for a variety of gases has been evaluated, and for signals that are 10–100 times greater than the background current, a precision that is typically within 1% of the signal can be obtained (Sedlak and Blurton 1976a; Stetter et al. 1979).

The accuracy of an individual datum point is often limited by the ability to calibrate the instrument. Calibration is achieved when an unambiguous relationship between the instrument signal and the actual gas concentration is established. For an electrochemical sensor system we may assume that

the response-versus-concentration function is linear (if the sensor materials and geometry are properly chosen) over about two orders of magnitude. Typical least-squares representations of signal versus concentration data produce nearly ideal slopes and intercepts, with correlation coefficients of near unity (Rieger 1987; Skoog et al. 1988).

The range of linear response of the sensor varies with the particular gas or vapor being monitored. In most cases, linear response is observed in the low parts-per-million range and may extend to as high as 5000 and 10,000 ppm. For example, the linear response of a H_2S sensor was evaluated in the concentration ranges 0–0.277 ppm and 0–153 ppm, and the signal was directly proportional to the H_2S concentration (Sedlak and Blurton, 1976a).

Determinations of linearity are often limited by the ability to synthesize an accurate calibration for gas mixtures. For highly reactive gas mixtures such as hydrazine, it is difficult to prepare an accurate gas mixture even under ideal laboratory conditions. U.S. National Bureau of Standards (NBS) gas standards are available with an accuracy certified as f 2% for certain mixtures such as CO/air.

In conclusion, the accuracy, precision, and typical linear response of the amperometric gas sensor system is very important because it makes the following possible (Chang et al. 1993):

1. Reliable and accurate instrument calibration with only a single datum point; i.e., only one standard gas sample is necessary, making field use simple
2. Simplified electronic design to measure, amplify, record, manipulate, and report (display) the output signal
3. Simple additivity of responses when used in a sensor array, where one records responses to various compounds and simple mixtures of compounds

7.4. STABILITY

The stability of an amperometric gas sensor relates to its ability to retain its original response characteristics over long time periods and under changing environmental conditions. Stability should be measured in all of the dimensions of intended use for the sensor.

Stability is generally divided into short-term and long-term fluctuations. The stability of certain sensors has been reported (Sedlak and Blurton 1976a, 1976b; Stetter et al. 1978, 1979; Barsan et al. 1999). The causes of zero drift (i.e., drift in background current) and span drift (i.e., fluctuations in signal magnitude or changes in the steady-state current) are not well characterized. It is known that drift can be caused by temperature fluctuations, sensor operation at extreme relative humidities over long time periods (under- or overhumidification of the membrane or the gas diffusion electrode), catalyst degeneration or fouling, and electrolyte contamination. In addition, if the counter-electrode reaction consumes an electroactive substance of limited supply (such as the metal/metal oxide electrode), the lifetime of the sensor will be limited and extreme drift can be observed near the end of the sensor life. Even the input current of an operational amplifier can exhaust the capacity of a small-size reference electrode after long-term continuous operation (Lucisano et al. 1987). In spite of such problems, however, amperometric sensors may last many years in demanding industrial environments and still retain good analytical performance.

8. EXAMPLES OF ELECTROCHEMICAL GAS SENSORS

For illustration, we have selected hydrogen sensors, which currently have high interest due to intensive development of hydrogen energy technology.

8.1. ELECTROCHEMICAL H_2 SENSORS WITH LIQUID ELECTROLYTES

The development of an amperometric sensor demonstrates, by example, many of the important considerations in the fabrication of a practical hydrogen sensor (Chao et al. 2005). As illustrated in Figure 1.19, three sensor designs address three issues in liquid electrolyte hydrogen sensors that can be generalized to all amperometric gas sensors.

In device I, the WE, RE, and CE were Pt electrodes deposited on to the same side of a 1.5-cm-diameter Teflon membrane. The Teflon membrane with Pt electrodes was mounted into a polypropylene cell body and sealed. The backside of the cell body contained a reservoir into which 0.5 ml of 30% (w/w) H_2SO_4 electrolyte was added. The electrolyte was in direct contact with the electrodes. Device II was identical to device I except that a 2-mil (50-μm)-thick semipermeable fluorinated ethylene-propylene (FEP) membrane (Type 200A, DuPont, Circleville, OH) was mounted over the gas inlet hole. And device III was identical to device II except that an alternative RE was inserted.

Electrodes were fabricated from a suspension prepared with 60 mg of platinum black (Englehard, fuel cell–grade Pt black), 400 L of Teflon suspension (Type 30, DuPont, Circleville, OH), and 1600 L of

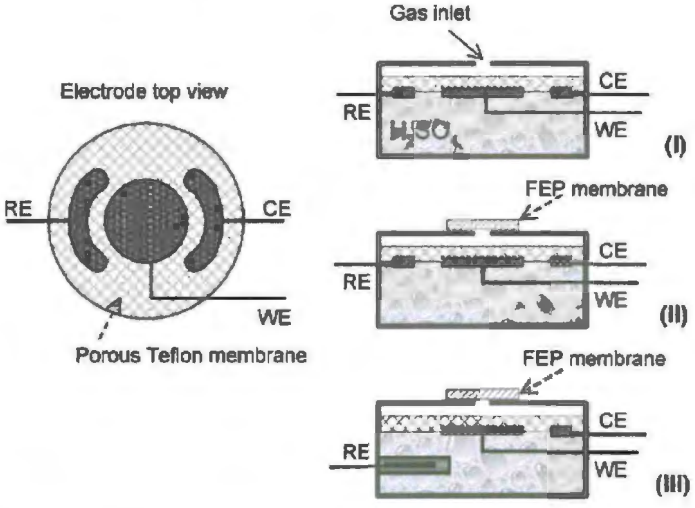

Figure 1.19. Schematic diagram of the AGS. (Left) Orientation of the WE, CE, and RE on a porous Teflon membrane. This electrode structure was mounted into polypropylene cells. (Right, top) Device I simulated a commercial sensor design. (Right, middle) Device II incorporated a semipermeable FEP membrane. (Right, bottom) Device III incorporated a semipermeable FEP membrane and an alternative and stable RE. (Reprinted with permission from Chao et al. 2005. Copyright 2005 Elsevier.)

18 M deionized water prepared with a commercial water purification system (model D7381, Barnstead Thermolyne Corp., Dubuque, IA) using a well-known procedure (Roh and Stetter 2003). Electrode structures were fabricated directly on porous Teflon membrane sheets as the supporting material (Type G110, Northern Performance, Wayne, NJ) using a vacuum filtration apparatus with a precut die that outlined the electrode shapes and positions. Three individual electrodes, which served as the WE, the CE, and the RE, were simultaneously deposited on the same side of the Teflon membrane in a planar geometry as illustrated in Figure 1.19. Once formed, the electrode–membrane structure was sintered at 310°C for 90 min and had a platinum black loading of about 7 mg/cm^2.

The results obtained with sensors I, II, and III clearly demonstrate the issues resolved by each unique sensor design. Sensor design I had a response to H_2 (see Figure 1.20) that illustrates using a standard configuration (device I) does not provide a stable or selective hydrogen detector. The Pt WE was sensitive to both CO and H_2 (Dabill et al. 1978; Bui et al. 1997; Park et al. 1999), and as a result, the presence of CO interfered with the H_2 measurement. For example, as shown in Figure 1.20, the H_2 signal was dramatically affected by low concentrations of CO. Upon exposure to only 50 ppm of CO, the signal magnitude dropped by nearly 33% while the hydrogen concentration was kept constant.

Embedding a solid FEP membrane (device II), to prevent CO and other gases from reaching the WE, made the sensor very selective to H_2 gas. Hydrogen has a much higher permeability through polymeric films such as FEP Teflon than CO and other gases (McCandless 1972; Hartel et al. 1996; De Vos and Verweij 1998; Hartel and Puschel 1999; Wesselingh and Krishna 2000; Pages et al. 2001; Orme et al. 2003). This modification fixed the first problem of the traditional amperometric H_2 sensor, its selectivity, and it also reduced the large amount of H_2 getting into the sensor. Device II exhibited a response to 100% H_2 and 2% H_2 in air and no detectable response to 10% CO over a 10-min exposure (Figure 1.21). So, it is seen that the FEP membrane was effective at improving selectivity.

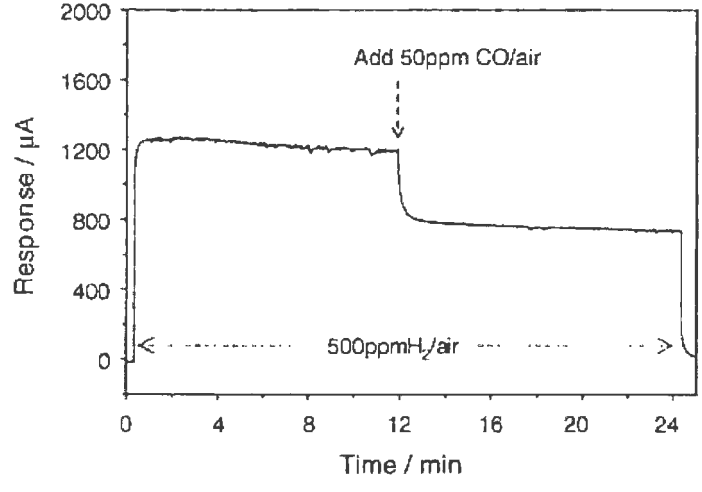

Figure 1.20. Response of device I to 500 ppm H_2/air for 24 min. At 12 min, the gas mixture was changed from 500 ppm H_2/air to 500 ppm H_2 with 50 ppm CO in air and finally to zero-filtered air at 24 min. (Reprinted with permission from Chao et al. 2005. Copyright 2005 Elsevier.)

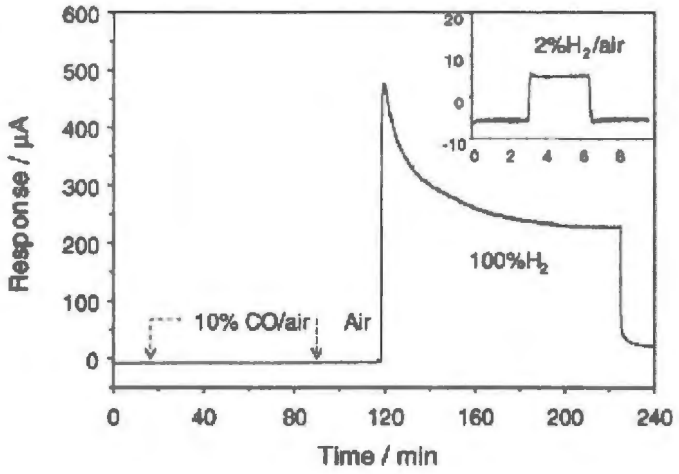

Figure 1.21. Response of device II to CO and hydrogen in air and then to zero-filtered air. (Reprinted with permission from Chao et al. 2005. Copyright 2005 Elsevier.)

However, simply embedding an additional membrane does not resolve a second important problem of hydrogen sensors with Pt electrodes, i.e., that related to diffusion and adsorption of hydrogen molecules on the Pt–air RE. This results in a sizable shift in the thermodynamic potential of the reference electrode. The shift in the RE potential immediately translates into a shift in the thermodynamic potential of the WE because the bias (e.g., the potential difference between the WE and RE) is held constant by the potentiostat circuit. The potential shift of the RE can be observed at even moderate hydrogen concentrations and is a reason for the unstable hydrogen signal from the design I and II sensors. As a result, device II, similar to device I, showed dramatic decreases in signal magnitude during extended exposures at high H_2 concentration (Figure 1.21). A measurable change in the reference potential was observed almost immediately following the hydrogen exposure. Over time, the magnitude of this drift could become quite large (more than 150 mV). Because of the unstable signals, a reliable hydrogen calibration curve was limited to concentrations less than 3% H_2 with sensor designs I and II (Figure 1.22).

This second deficiency of design, the hydrogen-induced potential drift of the RE, was eliminated by replaceing the Pt-based RE with an RE that was not sensitive to hydrogen gas, such as the Ag/AgCl electrode. This change led to device III of Figure 1.19 with an Ag/AgCl RE, whose performance is shown in Figure 1.22. Device III was identical to device II but incorporated the alternative RE by mounting the Nafion-coated Ag/AgCl wire into the bulk electrolyte through a hole in the side of the sensor body.

The Ag/AgCl reference electrodes were prepared by modification of an electrodeless chloridization method (Yao and Wang 2002). The chloridization of Ag wires was carried out for 24 h in a 1 M $FeCl_3$/0.1 M HCl solution. The wires were rinsed with deionized water, and put in a saturated AgCl solution for 24 h to remove traces of $FeCl_3$. Finally, the wires were dried at 100°C overnight. A uniform gray-black layer of AgCl developed on the surface of the Ag wire. The chloridized wires were dipped in a 5% Nafion 117 solution (Aldrich, Milwaukee, WI) and allowed to dry at room temperature. Immersion of the wires in the Nafion solution and air drying was repeated several times to make a uniform Nafion coating on the wires.

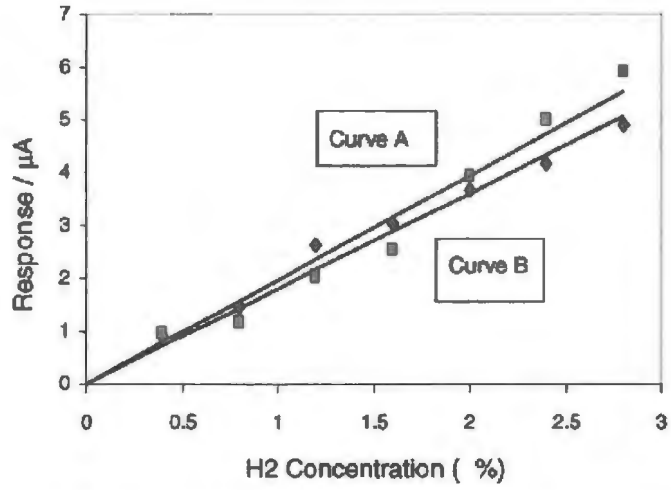

Figure 1.22. Hydrogen calibration curves for device II. The CO concentration in curve A was 0 ppm and was maintained at 1000 ppm in curve B. (Reprinted with permission from Chao et al. 2005. Copyright 2005 Elsevier.)

Testing showed that design III sensors exhibited a reversible, drift-free response even at high levels of H_2 with negligible cross-sensitivity to CO (see Figure 1.23). The steady-state signal remained constant for more than a 2-h continuous exposure to 100% H_2, and no detectable interfering CO responses were observed for device III as gas mixtures of 0.5–2.5%CO + 50% H_2/air were introduced. The sensor responses to H_2 before and after CO (5%) exposures were the same. It was noted that device III also

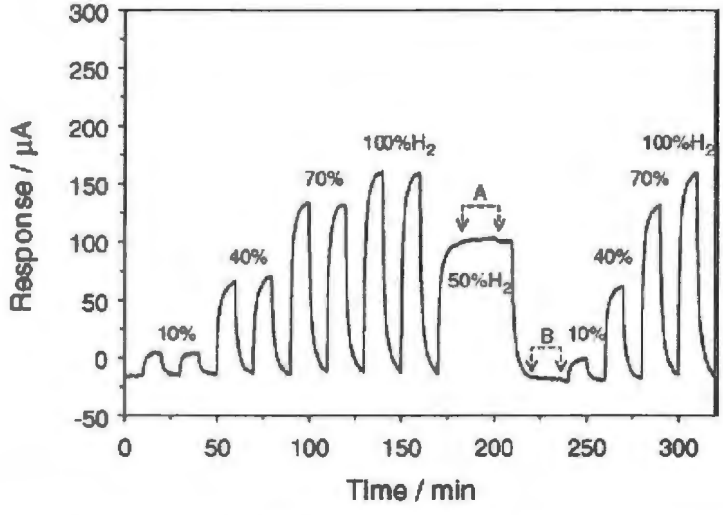

Figure 1.23. Response of device III to various concentrations of H_2 and CO mixtures in air. In region A, the gas mixtures were 50% H_2/air with 0.5, 1, 2.5% CO (each for 15 min). In region B, the gas mixture was 5% CO/air. (Reprinted with permission from Chao et al. 2005. Copyright 2005 Elsevier.)

showed no detectable responses to 500 ppm of NH_3 or 500 ppm of H_2S in air when exposed for over 10 min to these potential interferants.

The AgCl electrode had to be designed specifically for this amperometric sensor (Chao et al. 2005). While the Ag/AgCl electrode is a well-known standard reference electrode (Ives et al. 1961), the basic design of the Ag/AgCl RE is unstable in many electrolytes. The AgCl layer may dissolve in an electrolyte such as sulfuric acid, causing the Ag/AgCl RE potential to change as the chloride layer is dissolved. In addition, free chloride ions in the electrolyte may form complexes with the platinum particles on the WE and CE. This can have deleterious effects on the chemical stability of the electrodes and adversely affect the sensor performance. Nafion is a cation-exchange membrane that allows only small cations such as protons in the electrolyte to move freely from the bulk solution to the Ag/AgCl wire surface. Anions such as Cl^- will not readily diffuse into the electrolyte because of the electric repulsion (Donnan exclusion) within the positively charged Nafion ion-exchange layer. The protective Nafion coating both minimizes the dissolution of chloride ions into the bulk solution and, at the same time, maintains ionic contact between the RE and the bulk solution. In addition, the geometric placement of this Nafion-coated Ag/AgCl RE was further from the WE than the RE in device II, and this also minimized the chance of significant hydrogen levels reaching the RE. The solid Teflon membrane was effective at providing differential selectivity, but it slowed the response time of the sensor from 5–90% signal from a few seconds to a few minutes.

8.2. CHARACTERISTICS OF ELECTROCHEMICAL H_2 SENSORS FABRICATED USING POLYMER ELECTROLYTES

The electrode reaction in polymer-based electrochemical sensors, i.e., electron-transfer reaction at the working electrode, is part of a mechanism of response that is similar to all amperometric gas sensor technology and has several steps, including gas diffusion to the electrode–electrolyte interface, dissolution of the analyte gas, adsorption of the analyte onto the surface, electroreaction at the triple-phase boundary, and desorption of products from the electrode surface (Stetter and Blurton 1976, 1977; Vaihinger et al. 1991; Chang et al. 1993; Stetter and Li 2008). Similar reactions in air are proposed for the anode and cathode, respectively. Actual electrode reactions at the electrode surface are dependent on the nature of the electrode material, the electrolyte solution, the thermodynamic potential, the electrode–electrolyte interface, and, of course, the analyte, which in this case is hydrogen. If the products of the reaction are sensor poisons, the sensor lifetime or response characteristics may be severely limited, but in this case, the hydrogen sensor produces water and is a very "green" system, which makes the choice of materials and methods for the electroanalytical processes simple.

Metallization of the polymer, i.e., how the electrode is deposited, is a most important process in the manufacturing of polymer sensors. The Nafion surface has to be metallized by noble metals to create the reference, counter, and sensing electrodes. A laminated structure or one with intimate contact of electrode and electrolyte is required. This contact between the two solids, i.e., the membrane and the catalytic metal, with a provision for gaseous contact, is a very critical factor in obtaining performance. To obtain optimal performance, the Nafion itself must also be cleaned by leaching/cleaning with ethanol for several hours, boiling in nitric or perchloric acid, or sometimes by mechanical abrasion (Opekar and Stulik

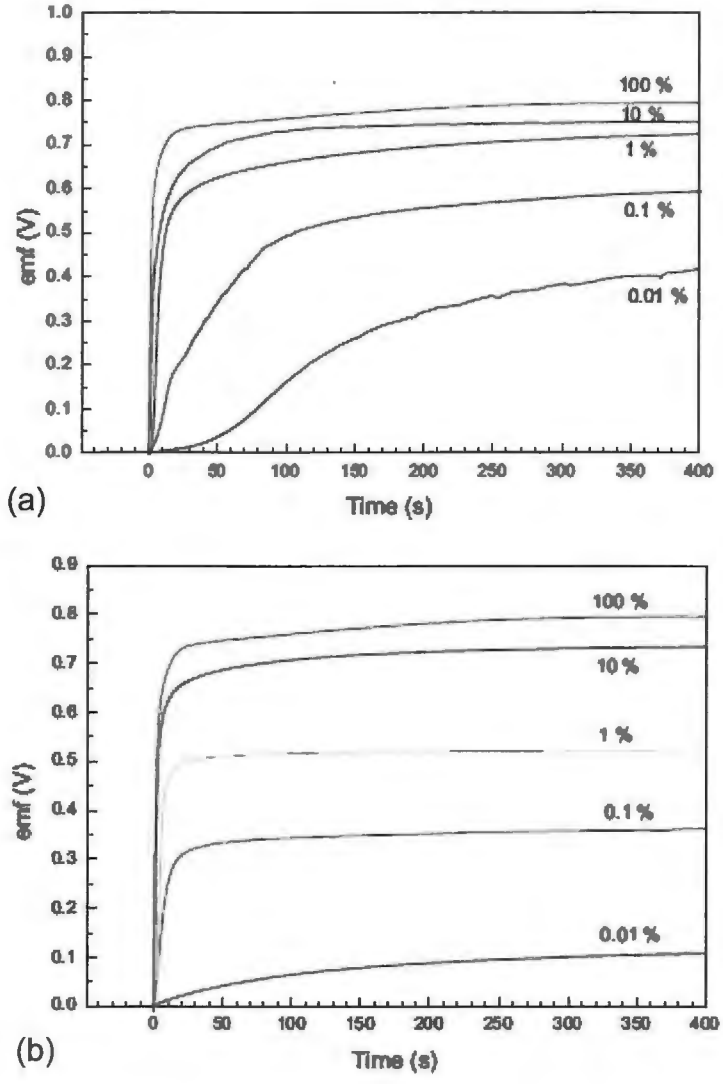

Figure 1.24. Response time of the sensor with (a) Ag and (b) Pd reference electrodes to various concentrations of hydrogen in nitrogen; (a) for short exposure times. The sensor was flushed with air prior to the introduction of each new hydrogen gas mixture. (Reprinted with permission from Maffei and Kuriakose 2004. Copyright 2004 Elsevier.)

1999). Various noble metals, including Ag, Pd, and Pt, are typical electrode materials. However, Pt and Pd electrodes seem to have better stability, reliability, and rate of response (Maffei and Kuriakose 2004). The performance for H_2 sensors made with the hydronium Nafion system is compared in Figure 1.24.

Figure 1.24 shows that this potentiometric H_2 sensor with Ag electrodes does not reach equilibrium at very low hydrogen gas concentrations even after 1 h, while sensor response with Pd electrodes

is extremely rapid for all hydrogen concentrations from 1% to 100%. The response time is typically less than 10 s to achieve a signal level of 90%, and additional research on this system has indicated that, with Pt electrodes, the response time is even faster (Maffei and Kuriakose 1999). In some structures, the metal electrode is deposited directly onto the polymer electrolyte. Any one of several methods can be used for polymer/electrolyte metallization (see above discussions) during H_2 sensor fabrication, e.g., mechanical, electrochemical, and chemical reduction processes (Vork et al. 1986). Each method produces a different quality electrode and electrode–electrolyte interface and thereby affects the analytical performance of the resulting sensor. Potentiometric H_2 sensors prepared by sputtering, electroless plating, and Pt powder molding have been compared (Inaba et al. 1999). The sputtered electrode had the highest catalytic activity, and the sensitivity of the sensor was 16 times higher than that prepared by molding (Inaba et al. 1999). The sensitivity of the sensor was about 4 μA/100 ppm with a linear output from 0 to10^4 ppm. The sensors with electroless plating electrodes were unstable.

The most efficient method for electrode preparation is believed to be a chemical reduction process, which can be divided into two types, the Takenata-Torikai method (Ogumi et al. 1992) and the impregnation–reduction method (Millet et al. 1993). Both methods have low investment and production costs. Chemical reduction produces mechanically stable electrodes with good interfacial contact (Millet et al. 1993). Control of the reductant concentration provides control of the size of the resulting metal particles and their average grain size. As a result, it may be possible to optimize the gas sensor electrode performance. The average particle diameter increases with increasing reductant concentration. The increase in grain size is believed to be due to higher nucleation growth with fast reduction of the $[Pt(NH_3)_4]^{2+}$ in the electrode. The optimum particle size of 74 nm with good interparticle connections was found at 0.04 M concentration of $NaBH_4$, and this may correspond to the optimum electrochemical sensor performance. Smaller particles with enhanced surface area can be expected to have high electrocatalytic activity but were isolated from each other, resulting in an interruption of the electrical contact. In contrast, a Pd layer deposited at high concentrations showed good electronic contact, but as one may expect, when the particles were grown to micrometer size, surface area and electrocatalytic activity decreased.

Some polymer amperometric H_2 sensors discussed earlier used a microporous PTFE as a gas-permeable diffusion membrane and Pt/Ru mesh as a current collector (Lu et al. 2005). The sensor was prepared with a Pt/Ru mesh that was placed onto the PTFE membrane and its upper side was coated with a thin layer of the Pt/C catalyst mixture. Then the Nafion 117 membrane was placed onto the thin layer and the other side of the membrane was coated with a thin layer of the Pt/C catalyst mixture divided into two parts of different surface areas by an insulator. Afterward, two Pt/Ru meshes were placed onto the two parts of the thin Pt/C catalyst layer, making a CE and a RE. Finally, the assembly was placed in a hot-press at 110°C and kept in a nitrogen atmosphere for 10 min under a pressure of 40 kg/cm^2. The diameter of the sensor with 3.0-mg/cm^2 Pt loading was 15 mm, making the overall polymer–electrode–membrane (PEM) structure small and suitable for small portable H_2 sensor applications.

Performance of the assembled H_2 sensors illustrates a useful sensitivity, stable sensing current, short response and recovery times, and long-term stability (Figure 1.25) (Lu et al. 2005). For a step change of the hydrogen concentration, the t_{90} response time (the time required to reach 90% of the steady-state current) of the sensor is about 20–50 s, suitable for most monitoring applications (Lu et al. 2005).

The response of many polymer H_2 sensors is sensitive enough to detect less than 10 ppm and perhaps even 1 ppm with the appropriate electronics and controlled exposures (Ramesh et al. 2003;

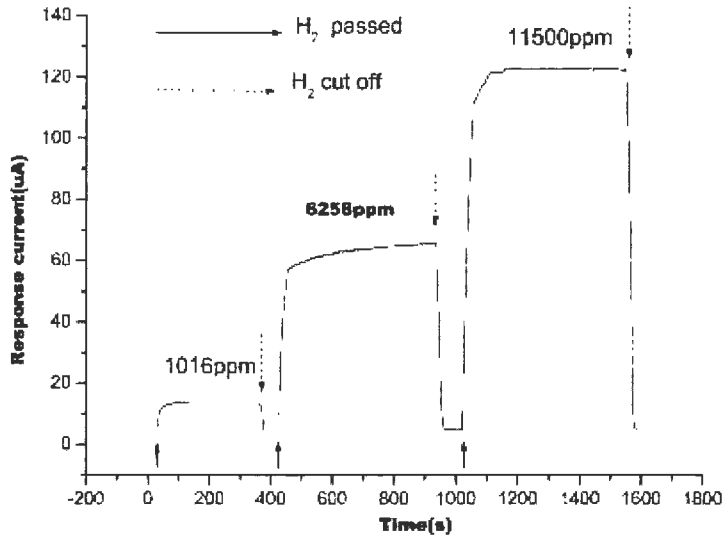

Figure 1.25. Response curves of the sensor for various concentrations of hydrogen. (Reprinted with permission from Lu et al. 2005. Copyright 2005 Elsevier.)

Sakthivel and Weppner 2006a). These results were obtained using a PVA/H_3PO_4 electrolyte that was prepared by casting the structure onto a Teflon sheet (Ramesh et al. 2003, 2004). The electrolyte film was fixed to a supporting ring and coated with palladium as an anode on the sensing side and platinum as a cathode on the counter electrode side. The electrolyte thickness was about 2 mm. The housing assembly for the sensor was made from polycarbonate. A schematic diagram of this sensor is shown in Figure 1.10. The palladium anode was deposited by vacuum vapor deposition. The thickness of the anode film in the sensor was of the order of 1000 Å. The cathode on the counter-electrode side of the sensor was platinum supported on carbon prepared by screen printing. Before coating, 20–25% of a Teflon emulsion was added to the mixture. The electrode was sintered at 100°C under vacuum. Two gold-coated nickel grids were used as current collectors on both sides. Pt was chosen as cathode material because of the lower overpotential for oxygen reduction and lesser solubility for hydrogen. Pd is not a suitable material for the cathode, since the cathodic overpotential for oxygen reduction at Pd is high and it does reach a diffusion-controlled electrode process because of the high solubility of hydrogen in palladium. Pd also exhibits a decrease in catalytic activity at the cathode due to the oxide formation on the air side. However, Pd can be effective as an anode, since its high solubility, large sticking coefficient, and fast diffusion coefficient for hydrogen are advantageous for sensing low concentrations of hydrogen in argon or another gas. The low overpotential for hydrogen oxidation on the Pd film anode was also found to provide sufficient catalytic oxidation rates to make the above sensor function well.

While many measurements of the rate of response are limited by the apparatus, in general, the rate of response of the polymer hydrogen sensor is at least 1 min to 90% signal. For example, Figure 1.26 shows cyclic exposure of the Pt|Nafion sensor element to 4% hydrogen and no hydrogen (Sakthivel and Weppner 2006b). Results (Figure 1.26) can be used to calculate the measurement precision during

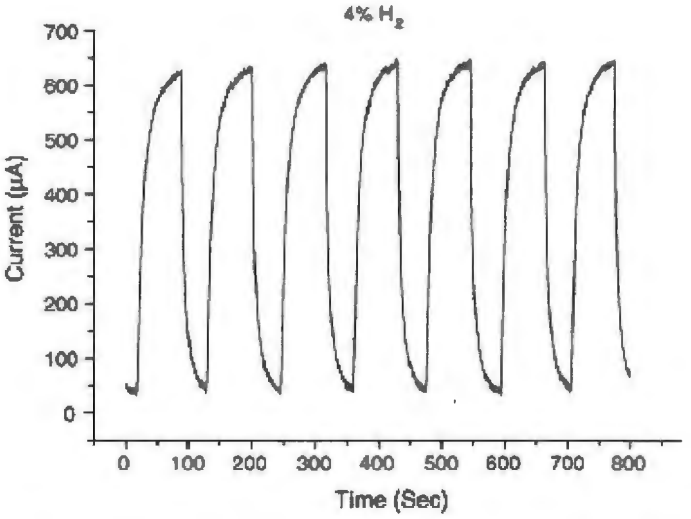

Figure 1.26. Cyclic behavior of 4% H_2 exposure to the sensor Pt|Nafion WE with an area of 2 cm^2 made from 0.01 M $Pt(NH_3)_4Cl_2$ and reduced with 0.04 M $NaBH_4$ in a 1-min time interval. (Reprinted with permission from Sakthivel and Weppner 2006b. Copyright 2006 Elsevier.)

cyclic exposures. Also, short-term and long-term drift (downward drift in the output current) under laboratory conditions was reported to be about 2% of signal per day.

The potentiometric response of a polymer sensor is given in Figure 1.27 and, as is typical for potentiometric sensors, H_2 can be detected over many orders of magnitude in concentration. The EMF

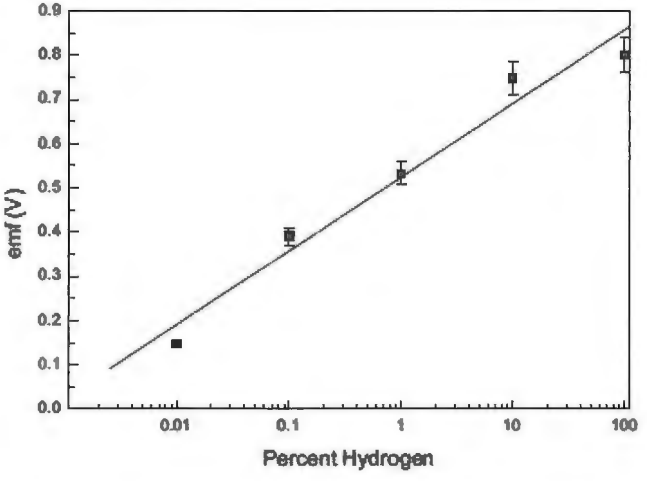

Figure 1.27. Equilibrium emf of Pd/Nafion-based sensor versus the logarithm of the hydrogen partial pressure for hydrogen–air gas mixtures. (Reprinted with permission from Maffei and Kuriakose 2004. Copyright 2004 Elsevier.)

dependence on the logarithm of the hydrogen partial pressure is very close to linear but is non-Nernstian. A nonlinear least-squares fit (NLLSF) of the data yielded a slope of 166 mV, well above the value predicted by the Nernst equation. If the data for 0.01% hydrogen is discarded, the value of the resulting slope is 145 mV, still significantly greater than the expected theoretical value. The reasons for the non-Nernstian behavior of this sensor to hydrogen–air mixtures are not clear. The fast, linear, reproducible, and large, stable output of the sensor makes it very useful for detection of hydrogen leaks in air. The sensor performance thus suggests that it can be incorporated into a fuel cell or into other hydrogen process applications to detect explosives levels of hydrogen gas.

However, it would be most advantageous if the sensor were to respond over the entire range of 0–100% hydrogen. Linearity of the semilog plot for the potentiometric H_2 sensor (Figure 1.27) is observed in the range 0.1–10%; outside this range, there appears to be what is often called a mixed potential (Bouchet et al. 2001). Over a wide range of hydrogen partial pressures, gas diffusion electrodes usually exhibit a sigmoidal response (Figure 1.28) on the semilog plot.

Calculations show that in ambient air, the hydrogen sensor sensitivity (defined as the slope of the *E*-versus-log[$P(H_2)$] curve) is always higher than that given by the Nernst equation, and the potential is influenced by electrode morphology. Electrodes deposited on Nafion exhibit a non-Nernstian open-circuit voltage (Opekar et al. 1994) that is characteristic of a mixed potential resulting from at least two simultaneous electrode reactions, e.g., a hydrogen oxidation reaction (HOR) and an oxygen reduction reaction (ORR) (Bouchet et al. 2000b).

According to this model, For low hydrogen partial pressure, the sensor potential varies linearly with the logarithm of the hydrogen partial pressure and the sensitivity, deduced from the ORR Tafel slope, and is of the order of 120 mV/decade. For high hydrogen partial pressure, the sensor potential varies linearly with the logarithm of the hydrogen partial pressure and the sensitivity is in agreement with the Nernst equation (30 mV/decade at room temperature). The abrupt change of potential between these two zones can be explained by mass-transport limitations of both the HOR and ORR reactions.

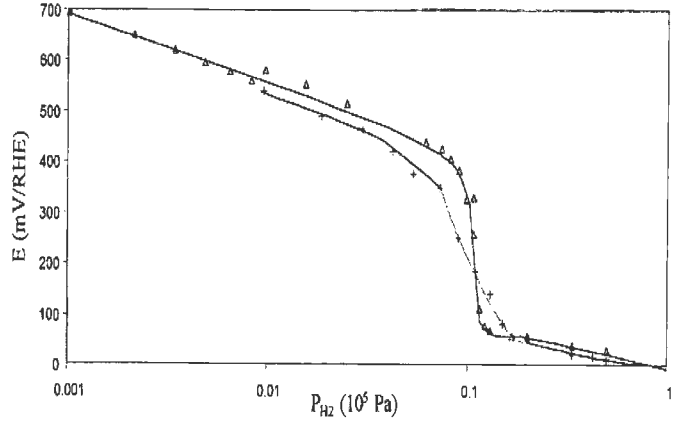

Figure 1.28. Potentiometric response of the Pt electrode (E-TEK) in PBI-H_3PO_4 electrolyte sensors to various H_2 partial pressures in dry air: Experimental response (Δ); curve is of the mixed potential mode (+). (Reprinted with permission from Bouchet et al. 2001. Copyright 2001 Elsevier.)

While some have suggested that these characteristics reduce the utility of Pt potentiometric hydrogen sensors (Rosini and Siebert 2005), there is hardly another metal better suited for the hydrogen oxidation reaction. The ideal metal would have a response for hydrogen reaction only; this is the challenge of selectivity.

8.2.1. Methods to Improve H_2 Sensor Performance

One can always improve on sensor performance in a given application. There are five general areas in which to improve sensors: (1) sensitivity, signal-to-noise ratio, and limit of detection; (2) selectivity; (3) response time; (4) stability for short- and long-term performance, including lifetime; and (5) logistical or application-specific properties such as cost, size, weight, power requirements, ruggedness, and packaging. Sometimes, improvements can come from packaging or software and include pumps or membranes to improve sensitivity and selectivity or even algorithms to predict steady-state values for improved response time. Overall, however, most electrochemical H_2 sensors are not perfect for all applications, and fundamental improvements to the sensor are always desired.

Control and improvement in amperometric sensors can be enhanced by physical optimization of the sensor package, e.g., diffusion holes (pores) can control the concentration range for H_2 sensitivity. This diffusion hole type of amperometric limiting current sensor has a linear current with P_{H2} (Weppner 1987; Park et al. 2003), and small changes in the hydrogen partial pressure may be measured with high accuracy (Liu and Weppner 1992; Sakthivel and Weppner 2006b). Several engineering designs targeted toward optimization of the H_2 sensor have also been suggested. A schematic diagram of the H_2 sensor designed by Sakthivel and Weppner (2008) is shown in Figure 1.29.

Decreasing the inlet diameter to 0.5 mm at a length of 5 mm, i.e., a length-to-diameter ratio (L/D) of 10, improved selectivity to H_2 with respect to CO_2. This same idea was used in a prefilter to gain

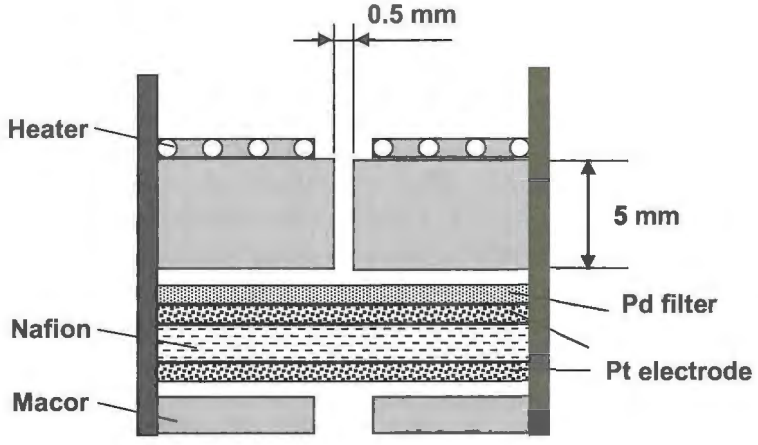

Figure 1.29. Schematic diagram of the cell construction showing top and side views of sensor DHS-IV with the heating element on top. (Adapted with permission from Sakthivel and Weppner 2008. Copyright 2008 Elsevier.)

selectivity for CO over H_2, using the prefilter to remove hydrogen (Stetter and Blurton 1976, 1977; Vaihinger et al. 1991; Chang et al. 1993; Stetter and Li 2008) Since hydrogen diffuses much more quickly than other gases, this diffusion barrier allows a significant (approximately factor of 4 for air) advantage to hydrogen over other gases. Further, catalytic electrode poisoning by CO_2 gas mixtures along with H_2 was eliminated with a Pd diffusion barrier on the top of the sensing Pt electrode (Sakthivel and Weppner 2008). The result was that the amperometric H_2 sensor performance was improved in environments containing high concentrations of CO_2 (Figure 1.30).

Additional improvements in this sensor include a screen-printed Pt heater to compensate for any temperature variation within the diffusion hole in the sensor chamber. The heater further kept the gas mixture and sensor measurements at a constant temperature. Decreasing the space between the Pd barrier and the diffusion hole avoided excessive condensation of water vapor from the reactor samples.

The membrane can also be optimized to improve sensor performance. Ion implantation of an ePTFE membrane is an effective way to improve H_2 selectivity (Okamura et al. 2007). Implantation of the PTFE membrane with various kinds of ions (N^+, N_2^+, O^+, and O_2^+; 1×10^{15} ions/cm^2) decreased the detection current for interfering gases such as H_2S, SO_2, NO, and NO_2 relative to H_2. It was proposed that structure modification of the ePTFE under ion implantation (Figure 1.31) could provide a high rate of H_2 permeation compared with permeation for other gases: H_2S, SO_2, NO, and NO_2. It is known that the chemical bonding structural change of ePTFE, especially the pore surfaces, influences the interactions between gas molecules and the polymer surface, which induces a change in permeability unique to each gas.

The required operating temperatures can add complexity to a gas sensor system. For example, sensors using Nafion 117 often do not reach a steady state at temperatures above about 50°C (Mika et al. 2007). This instability is caused by the rapid and continuous drying of the membrane in gas streams,

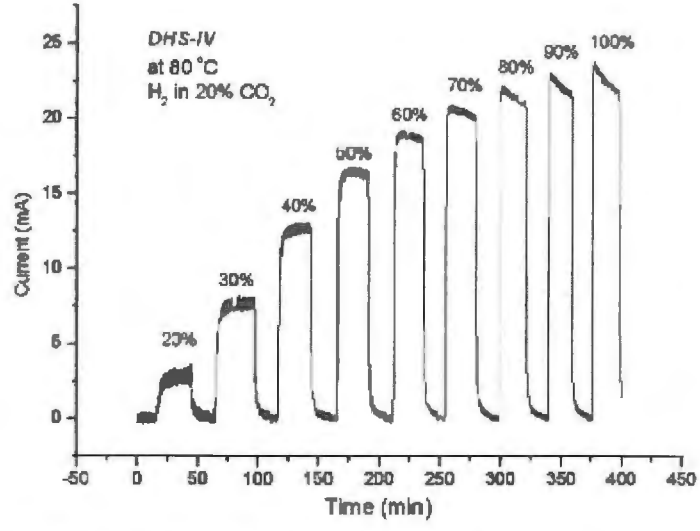

Figure 1.30. Typical step response of design DHS-IV up to 100% H_2 in Ar + 20% CO_2 measured at 80°C. (Adapted with permission from Sakthivel and Weppner 2008. Copyright 2008 Elsevier.)

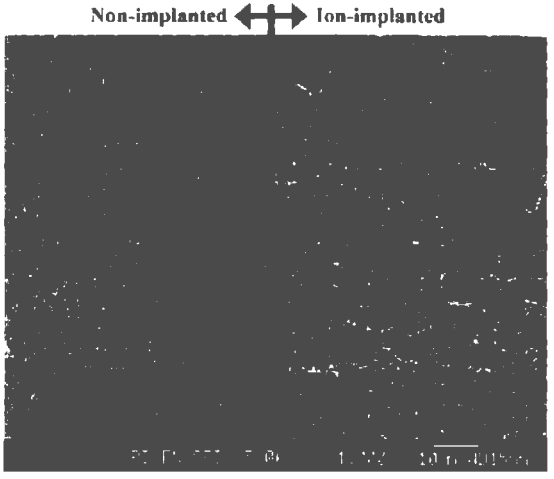

Figure 1.31. SEM images of nonimplanted ePTFE membrane and N^+-implanted with 5 × 1015 ions/cm^2. (Reprinted with permission from Okamura et al. 2007. Copyright 2007 Elsevier.)

which affects the membrane's conductivity. Nafion is a hygroscopic polymer, and changes in the water content cause the membrane to physically swell (Sondheimer et al. 1986). This swelling alters the size and shape of the membrane and thereby changes the rate of proton diffusion, and proton diffusion is the charge-carrier mechanism within the polymer. Therefore, a changeable, very dry, or very wet atmosphere provides a difficult working environment for Nafion-based H_2 sensors. Even Nafion in contact with a water phase to maintain the water content constant is sometimes not sufficient to remove the signal dependence on relative humidity, since local chemical and physical effects at the sample/electrode interface can dominate the response, and the rate of water exchange in the Nafion itself can change (Opekar and Svozil 1995).

New polymers that are fast proton-conducting membranes, based on a hybrid inorganic–organic phosphosilicate polymers prepared from othophosphoric acid, dichlorodimethylsilane, and tetraethoxysilane have been synthesized (Mika et al. 2007). The membranes are amorphous, translucent, and flexible. The proton conductivity increased with rising temperature following Arrhenius behavior with an activation energy 20 kJ/mol. In dry conditions at 120°C, the conductivity was 1.6 S/m. A potentiometric gas sensor with a TiH_x reference electrode and a Pt sensing electrode exhibited fast, stable, and reproducible response to dry H_2 and O_2 gases at temperatures above 100°C. Operation at high temperature might be at least one way to resolve the RH response of polymer H_2 sensors. However, at higher temperatures, any degradation mechanism will be enhanced, and this can cause drift. The new hybrid inorganic–polymer electrolyte sensors did exhibit drift, which resulted in a need for frequent calibration. The hybrid polymers appeared to be stable up to 400°C, but the membrane slowly degraded, as was revealed by thermal analysis (Mika et al. 2007).

Another polymer, H_3PO_4-doped polybenzimidazole (PBI), has sufficiently high proton conductivity in dry air for sensor applications. Experiments have confirmed operation in RH of only 10–30%, and this is about the same as the performance of the PVA/H_3PO_4 polymer electrolyte (Ramesh et al. 2003).

Pt/air electrodes designed with a PVC polymer composite have much better stability in comparison with electrodes made from Nafion/metal composites. Pt/air or Au/air electrodes are very often used as pseudo-reference electrodes in amperometric gas sensors (Stetter and Maclay 2004). These electrodes are not reversible electrodes, but their potential is reported to be sufficiently stable for use over long time in gas sensors (Bay et al. 1972). The Pt/air electrode potential is a mixed potential determined by oxygen reduction (Hoare 1968):

$$O_2 + 4H^+ + 4e^- \leftrightarrow 2H_2O \tag{1.26}$$

$$O_2 + 2H_2O + 4e^- \leftrightarrow 4OH^- \tag{1.27}$$

According to reactions (1.26) and (1.27), the electrode potential depends on the activity of water. In aqueous solutions, the effect of the water activity is not considered to change, as the water is actually at 55 M concentration and small changes produced by reactions have little or no effect on its activity. This does not hold for solid-state sensor systems with solid-state electrolytes. These systems contain no macroscopic water phase, and the concentration of water in the solid-state electrolyte is determined entirely by the relative humidity (water fugacity) of the surrounding gaseous environment and by the partition coefficient (equilibrium constant) for water between the gas phase and the solid-state electrolyte phase. Therefore, the electrode potential in such a sensor is influenced by a change in the relative humidity of the test gas. Measurements show that the potential changes with RH are less for the hydrophobic PVC composite reference electrode than for the hydrophilic Nafion composite reference electrode (Hrncirova and Opekar 2002). Quantitatively, over a 30–70% RH range, the potential of the Pt-PVC/air RE changes only a few millivolts, as opposed to tens of millivolts for the Pt-Nafion RE. For this reason, the Pt-PVC/air RE is preferable to the Pt-Nafion electrode for sensors that operate in environments with variable humidity.

8.3. HIGH-TEMPERATURE H_2 SENSORS

Specific advantages of high-temperature solid-state potentiometric hydrogen sensors include both accuracy and sensitivity, rugged construction, the possibility of miniaturization, and the wide concentration range that can be measured. The use of ceramic solid electrolytes in electrochemical gas sensors at elevated temperatures allows for the detection of H_2 under harsh conditions, where typical aqueous electrolytes, liquids, or polymeric materials cannot be used. The high operating temperature frequently reduces the RH influence that is bothersome in many sensing applications.

As we wrote earlier, typical solid electrolytes which can be used for fabricating high-temperature gas sensors include yttria-stabilized zirconia (YSZ) and perovskites. The best-known perovskites include $SrCeO_3$, $SrCeO_3$:Yb, $SrCeO_3$:In, $BaCeO_3$, $BaCeO_3$:Gd, $SrZrO_3$, $BaZrO_3$, and $CaZrO_3$, all of which have high thermal stability and exhibit appreciable proton conduction with low activation energy at elevated temperatures (>700°C) in steam and hydrogen atmospheres (Yajima et al. 1991; Iwahara et al. 1993; Zheng and Chen 1994; Nowick et al. 1999; Norby 2001; Wakamura 2005) and have been used for hydrogen sensors (Yajima et al. 1993). The conductivity of these ion-conducting materials is strongly dependent

on the temperature (Sundmacher et al. 2005); data on proton conductance for several perovskites are presented in Figure 1.32. As a rule, the embedding of the fourth element is used to control the conductivity, e.g., in the case of $SrCeO_3$:Yb, doping with 5% of Yb^{3+} achieved the maximum of ionic conductivity.

These proton conductors are ceramic materials and typically do not have high porosity but rather can reach 96–99% of the theoretical density (Jacobs et al. 1993). Because of the exceptional thermal and chemical stability of the materials, a hydrogen sensor for molten metals has been developed and widely used in process control in the metal-melting industry (Yajima et al. 1995; Nishimura et al. 1996; Fukatsu et al. 1998). In order to produce high-quality castings, it is necessary to reduce the hydrogen concentration in the molten metals during the casting process to an acceptable level, and a hydrogen sensor provides important process control data (Yajima et al. 1995).

One novel protonic conductor includes $BaZr_{0.4}Ce_{0.4}In_{0.2}O_3$ (BZCI), a material that has practical durability in the presence of steam and also relatively high conductivity (Taniguchi et al. 2005). This material was able to produce a very stable output H_2 sensor at 800 and 1000°C in a wet but pure hydrogen atmosphere. The crystal structure and the composition of all samples did not change during a test

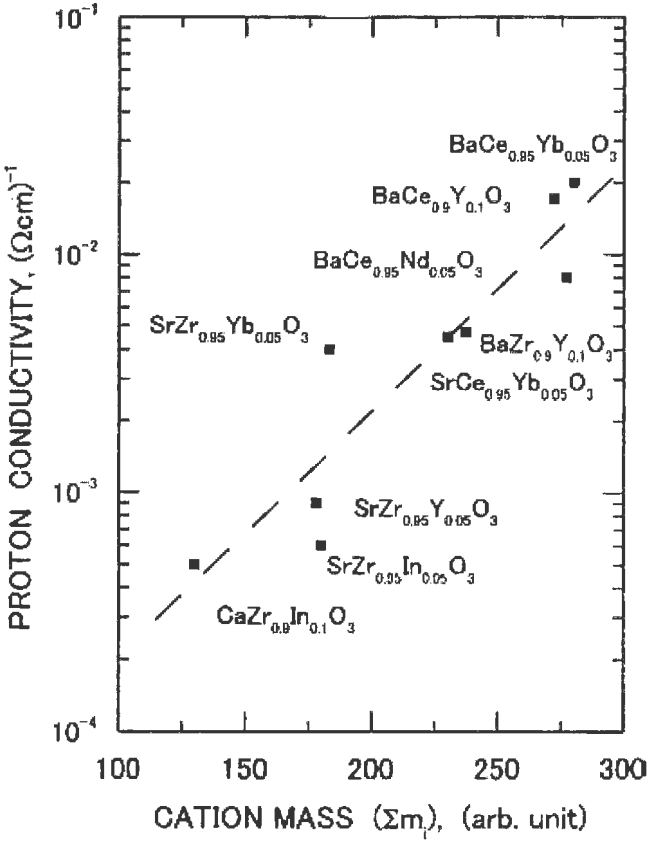

Figure 1.32. Total mass of constituent atoms in a unit cell versus the H^+ ion conductivity at 600°C for several perovskite-type proton conductors. A least-squares line is drawn through the data. (Reprinted with permission from Wakamura 2005. Copyright 2005 Elsevier.)

with hydrogen. The actual EMFs almost coincided with the theoretical values below 800°C but were lower than the theoretical values at 1000°C. Protonic conduction in BZCI was confirmed below 800°C and seems to decrease at higher temperature.

Many of the oxides discussed above ($SrCeO_3$, $BaCeO_3$) easily react with carbon dioxide to form carbonates of the alkaline earth elements and therefore are not good candidates for applications in sensors exposed to CO_2, including ambient atmosphere sensors (Tanner and Virkar 1996; Sakthivel and Weppner 2007). Barium cerate ceramics ($BaCe_{0.8}Gd_{0.2}O_3$, i.e., BCG) also were affected by steam or CO_2 and have had problems in practical use (Lander 1951; Colomban 1992; Scholten et al. 1993; Taniguchi et al. 1994). It was shown that $SrCeO_3$:Yb reacts with 10% CO_2 at temperatures below 800°C, and this reaction can take place already at 500°C (Wang and Virkar 2005). Research has demonstrated that cerates such as $BaCeO_3$ are thermodynamically unstable when a critical H_2O vapor pressure is exceeded (Tanner and Virkar 1996). It was established that $BaCeO_3$ in a H_2O vapor–containing environment (~430 torr H_2O) decomposed into CeO_2 and $Ba(OH)_2$ within relatively short periods of time at temperatures below 900°C. Also, doped $BaCeO_3$ decomposed at a faster rate than undoped $BaCeO_3$. It was assumed that the rapid decomposition of both powder and sintered samples was the result of the high solubility of H_2O in $BaCeO_3$, which accelerates the kinetics of decomposition.

The zirconates, such as $CaZrO_3$ $BaZrO_3$, are less reactive with CO_2 than cerates and more stable in H_2O- and CO_2-containing atmospheres (Yajima et al. 1990; Iwahara et al. 1993). The Y-doped $BaZrO_3$ has been reported to exhibit high proton conductivity and good chemical stability (Kreuer 1999, 2003). Furthermore, it has been demonstrated (Luyten et al. 1991) that strontium cerate is not stable in a simulated coal gasification atmosphere containing 0.0033 vol% H_2S at 800°C, since SrS and CeO_2 are formed. Considering all these stability issues causes the majority of H_2 sensors for application in real systems to be based on YSZ.

Recently, nonstoichiometric complex or mixed perovskite-type oxides of the formula $A_2B(1)_{1+x}B(2)_{1-x}O_{6-\delta}$ and $A_3B(1)_{1+x}B(2)_{2-x}O_{9-\delta}$ have been demonstrated to become proton conductors upon exposure to H_2O vapor (Liang and Nowick 1993; Liang et al. 1994). Among them, the $A_3B(1)_{1+x}B(2)_{2-x}O_{9-\delta}$ (A = Sr, Ba) compounds are particularly interesting because of their excellent protonic conductivity (Nazri et al. 1995). In addition, unlike Ce-based perovskites, these compounds have a wide band gap (Lecomte et al. 1984) and are superior insulators without producing detectable electronic conduction under either oxidizing or reducing gas influence up to 1000°C (Nazri et al. 1995).

Additional materials for high-temperature solid electrolytes suitable for use in H_2 sensors include $Sn_{0.9}In_{0.1}P_2O_7$ (Tomita et al. 2007). The EMF of sensors varied linearly with the logarithm of the H_2 concentration, and EMF was minimally affected by the water vapor concentration (Tomita et al. 2007). Results presented by Mukundan et al. (2000) also provoke interest. A $Pt/Ce_{0.8}Gd_{0.2}O_{1.9}/Au$ mixed-potential sensor allowed the possibility to detect H_2 in a gas mixture of H_2 and air. The sensor response was maximum for H_2 and negligible for methane; other gases followed the trend methane < propane < CO, propylene < hydrogen.

An example of a high-temperature solid-state mixed potential gas sensor designed for hydrogen detection and aimed at commercialization is shown in Figure 1.33. The H_2 sensors were fabricated using a half-open, yttria-stabilized zirconia tube (YSZ, 8 mol% Y_2O_3 doped, NKT) (Lu et al. 1996a, 1996b). The tube was 30 mm in length and 5 and 8 mm in inner and outer diameters, respectively. This design is essentially the same structure as that used for potentiometric YSZ oxygen sensors except that the sensing

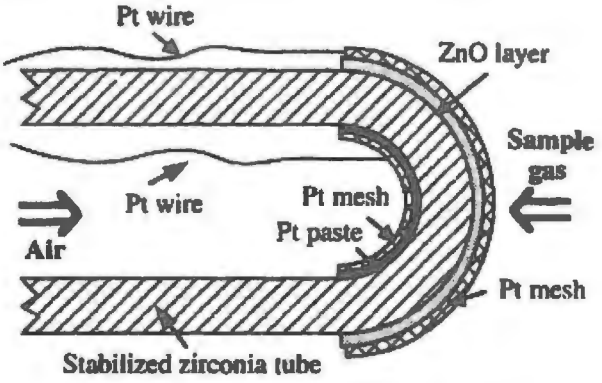

Figure 1.33. Mixed-potential-type H_2 sensor using YSZ- and ZnO-Pt electrode. Device structure with ZnO layer deposited around the YSZ tube. (Reprinted with permission from Lu et al. 1996. Copyright 1996 Elsevier.)

electrode on the outer surface is provided with a porous ZnO layer: The Pt mesh is designed to work as an electron collector. Pt black and Pt mesh were pressed on the inner surface of the YSZ tube at the closed end to form a reference electrode. This electrode was always exposed to static atmospheric air. Oxide powder was mixed with a-terpineol and beltlike ethylcellulose, and the resulting paste was applied on the outside of the tube, followed by calcining at 600–650°C for 2 h, to form the sensing oxide layer. The oxide layer thus formed was porous and about 30 μm thick. This device generated fairly large EMF response to H_2 in air at temperatures in the range 450–600°C, as shown in Figure 1.34.

The EMF response is seen to be linear to the logarithm of H_2 concentration, but the slopes are about −100 mV/decade, inconsistent with the behavior of an equilibrium-type device (Lu et al. 1996a) and more

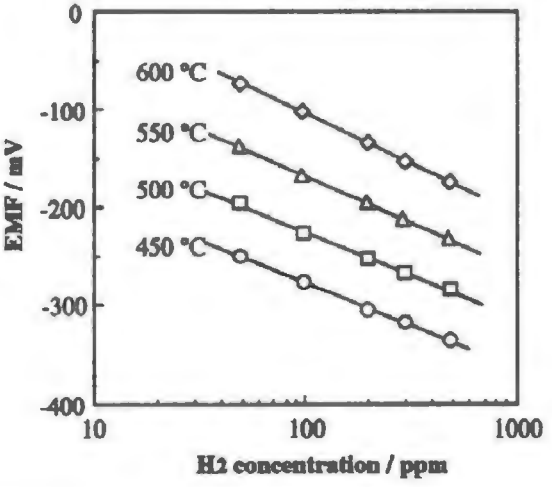

Figure 1.34. Mixed-potential H_2 sensor using YSZ and ZnO electrode. EMF as a function of concentration of H_2 in air. (Reprinted with permission from Lu et al. 1996. Copyright 1996 Elsevier.)

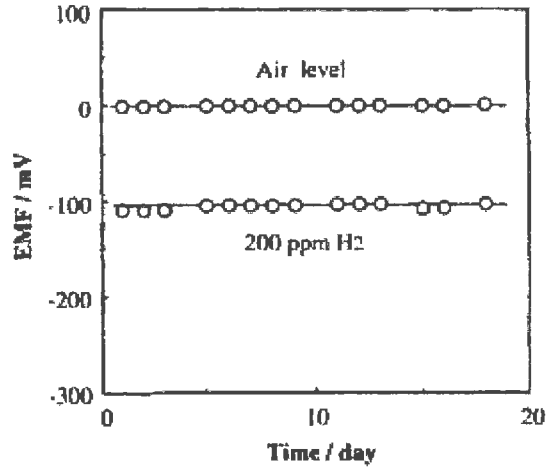

Figure 1.35. Long-term stability of the ZnO-attached YSZ-based device at 600°C. (Reprinted with permission from Lu et al. 1996a. Copyright 1996 Elsevier.)

typical of a mixed-potential device The EMF appears to decrease rapidly with a rise in temperature, and this seems to result from the enhancement of catalytic oxidation of H_2 on the sensing electrode with temperature. In this particular device with the ZnO electrode, the EMF response is still large at 600°C, being capable of detecting 50 ppm H_2 in air. The 90% response and recovery times to 200 ppm H_2 at 600°C for this device are 5 and 10 s, respectively. The stability of this sensor, see Figure 1.35, exemplified by both air and H_2 EMF, was demonstrated, and the device is one of the promising H_2 elevated-temperature sensors.

Other approaches to the design of high-temperature H_2 sensors have been reported, one of which is shown in Figure 1.36. The goal of these devices was to simplify and miniaturize the sensor structure.

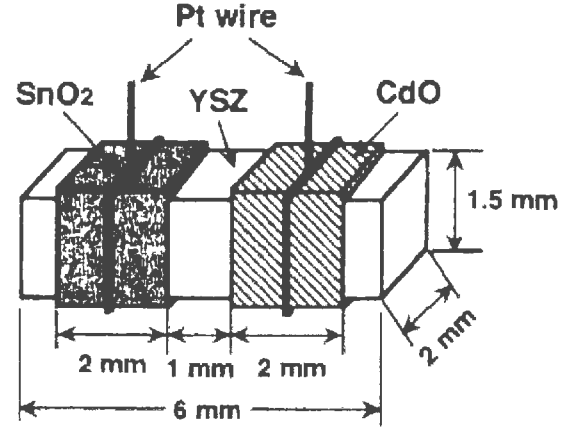

Figure 1.36. Chip-type YSZ-based device attached with CdO and SnO_2 electrodes: schematic view of device structure. (Reprinted with permission from Miura et al. 1998. Copyright 1998 Elsevier.)

The chip-type device was fabricated using a small bar of YSZ (8 YSZ, 6 × 2 × 1.5 mm), as shown in Figure 1.36, and applying two kinds of oxide pastes, one at each end of the zirconia bar, leaving about 1 mm space in between, followed by calcining at 650°C for 2 h, to form a couple of belt-shaped oxide electrodes (width about 2 mm; thickness about 30 mm). A Pt wire was wound around each oxide electrode as an electrical collector (Miura et al. 1008). The test of sensing characteristics has showed that the EMF values varied almost logarithmically with the concentrations of H_2 in the tested range of 20–200 ppm. Furthermore, the authors could operate this chip-type device at 600°C for approximately 400 h as a stability test. The EMF value was relatively stable during the test period. Due to its good sensing characteristics, the YSZ-based device has the potential to be used as a H_2 sensor that can operate in high-temperature combustion exhaust. In fact, this device does not require a reference gas for operation.

9. MEMS AND NANOTECHNOLOGY IN ELECTROCHEMICAL GAS SENSOR FABRICATION

Microelectromechanical systems (MEMS), especially micro working electrodes, with very small electrode surface area, have increasingly been employed in the fabrication of electrochemical sensors. Microfabrication of electrochemical devices has numerous advantages over standard fabrication processes. These advantages include precise reduced sensor size, reduced cost, smaller sample size, faster response time, higher concentration sensitivity, well-defined geometric features, and potential for mass production. These advantages can be obtained without degradation of the signal-to-noise ratio, as the sensor size is reduced using careful design.

Progress in the development of microamperometric sensors was slow compared to the production of micropotentiometric sensors. Microamperometric sensors of the early 1980s consisted only of microfabricated electrodes on a suitable substrate (Stetter et al. 1988). These electrodes were then coated with a liquid electrolyte solution that also carried the sample to the electrode area for analysis. An example of an early microamperometric sensor was presented by Sleszynski and Osteryoung in 1984. That sensor, which used very small electrodes constructed from nonconductive epoxy and reticulated vitreous carbon (RVC), was shown to yield desirable results compared to standard fabricated sensors.

However, the goal of constructing complete, practical, and commercially successful amperometric gas sensors using the microfabrication approach has still not been achieved. During the late 1980s, microfabrication technology for the construction of amperometric sensors was investigated with the introduction of novel sensor electrode designs. In 1988, Maclay and co-workers (Maclay et al. 1988; Buttner et al. 1990) introduced a series of Nafion-based microfabricated amperometric gas sensors using gold sensing electrodes in the shape of a square grid. The newly designed sensors were evaluated by comparing their analytical characteristics with those of conventional sensors. The response time of the miniaturized sensors was more than one order of magnitude faster than conventional sensors, although they had lower sensitivity. This work also elucidated the fact that the sensitivity of the device depended not only on the chemical nature of the electrode surface but also on the specific structure of the electrocatalytic surface and the interface created by gas/electrode/electrolyte.

In an effort to improve the sensitivity of microamperometric sensors, Buttner et al. (1990) constructed devices with an integrated design in which the working electrodes, counter electrodes, and

reference electrodes were photolithographically etched onto a gold-coated silicon oxide surface of a silicon wafer and spin-coated with a thin film of a solution of Nafion. The working electrode of the sensor was an ultrafine square grid with evenly spaced regions of gold and holes every 50 μm. The signal observed for the sensor following exposure to gases such as H_2S and NO greatly exceeded the response that would be expected on the basis of simple geometric considerations of microelectrodes (Buttner et al. 1990). More recently, gold microelectrodes are used with and without membranes in nonaqueous media for oxygen, carbon dioxide, and nitrous oxide detection simultaneously over a wide concentration range (Wadhawan et al. 2003; Floate and Hahn 2005).

Another approach to design of electrochemical microsensors was proposed by Li's group, who used nanostructures in making the microsensors. Various highly sensitive carbon nanotube-based sensors such as sensors using pristine carbon nanotubes (Li et al. 2003), carbon nanotubes loaded with metal clusters (Lu et al. 2004; Young et al. 2005), and carbon nanotubes coated with polymers (Li et al. 2006) were developed. An interdigitated electrode (IDE) was utilized as a transducer, with many of them on a chip that was fabricated on a silicon wafer (Li et al. 2005). This electrochemical sensor depended on the transfer of charge from one electrode to another electrode. The gases and vapors introduced to this sensor array were NO_2, HCN, HCl, Cl_2, acetone, and benzene in parts-per-million concentration levels in dry air. These are toxic gases and vapors that are of interest to both military and civilian personnel in defense applications, as well as in industry process and environmental monitoring. The detection limit of carbon nanotube sensors can achieve the parts-per-billion concentration level (Qi et al. 2003). Carbon nanotubes can be coated with metals to prepare hydrogen sensors (Stetter et al. 2003) or with Nafion to make humidity sensors (Star et al. 2004).

For many years, it was generally reported that potentiometric sensors were more easily microfabricated because the signal size did not depend at all on the electrode size, whereas amperometric sensor currents were directly proportional to electrode size. An ideal use of nanostructures to create large surface area in small-sized devices is found here. With the use of nanostructures, the electrode area of the amperometric sensor can be reduced by orders of magnitude while preserving the sensor signal magnitude, and this is a perfect example of the importance of nanostructures in the design and construction of amperometric gas sensors.

Several other designs for AGSs were also introduced during the 1990s. For example, Wallgren and Sotiropoulos reported (1999) the construction of an oxygen sensor based on a planar sensor design. The design consisted of both the working electrodes and the counter electrodes being vacuum-deposited as nonporous Au layers on the same face of a Nafion electrolyte and in contact with the gas sample. Potential advantages of this design include faster response times and higher sensitivities per useful electrode area, due to the high mass transport rates of the gas to the sensing electrode since no membrane or significant liquid film barrier is present. Also, smaller quantities of precious metal catalyst could be used for the working electrode, and the labor-intensive stacking steps required for the fabrication of conventional-type designs are avoided. As shown by the results of this research, oxygen reduction leads to an exponential current rise over a wide potential range, indicating very high mass transport rates and implying that the electroactive gas reacts at the line formed by the gas/solid electrolyte/metal layer interface (Wallgren and Sotiropoulos 1999). However, the practicality of the design may be questioned because, in practice, if the water content of the membrane changes, so do the dimensions, and this can lead to stresses that will fracture the electrodes and alter the response.

Berger and Edelman (2000) also described the production of a planar sensor used to detect the partial pressure of oxygen in blood samples. In this sensor, a semipermeable membrane, comprising an acrylonitrile butadiene copolymer or an acrylate-based copolymer, was provided to act as an impermeable barrier for ions and blood constituents other than oxygen. In 2004, Meyerhoff and co-workers reported a planar amperometric nitric oxide sensor based on platinized platinum anode (Lee et al. 2004). A microporous poly(tetrafluoroethylene) gas-permeable membrane was used. Platinization of the working platinum electrode surface dramatically improved the analytical performance of the sensor by providing ~10-fold higher sensitivity (0.8–1.3 pA/nM), ~10-fold lower detection limit (e1 nM), and extended (at least 3-fold) stability (>3 d) compared to sensors prepared with bare Pt electrodes. In this article, both experimental results and theory of NO measurements as a function of sensor diameter and distance from a point source were discussed in the context of an investigation of monitoring NO release from diazeniumdiolate-doped polymeric films. By modifying the above-discussed NO amperometric gas sensor with thin hydrophilic polyurethane films containing catalytic Cu(II)/(I) sites, the direct amperometric detection of *S*-nitrosothiol species (RSNOs) was realized (Cha et al. 2005). Catalytic Cu(II)/(I)-mediated decomposition of *S*-nitrosothiols generates NO(*g*) in the thin polymeric film at the distal tip of the NO sensor. A planar electrochemical sensor with solid electrolytes was also designed by Hohercakova and Opekar, (2004). The use of hydrogels or plasticized PVC membranes containing an electrolyte has been proposed for amperometric solid-state devices, and a schematic drawing of such a device is shown in Figure 1.37.

Another type of planar thick-film sensor with centro-symmetric diffusion geometry for detection of hydrocarbons in oxygen, nitrogen, and hydrocarbon gas mixtures has been developed for monitoring exhaust gases (Schmidt-Zhang and Guth 2004). In this work, propene (C_3H_6) was chosen for sensor

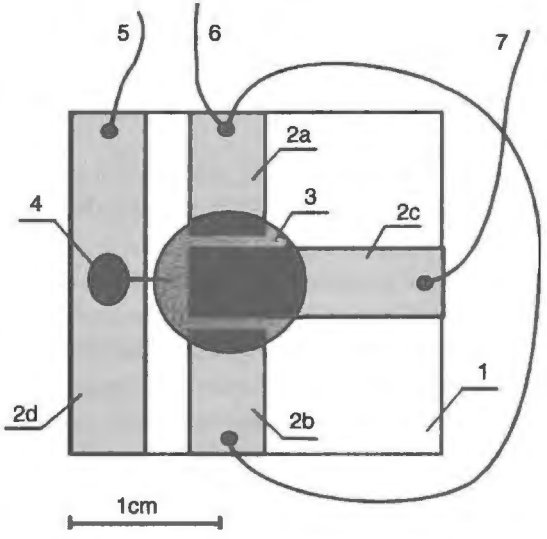

Figure 1.37. Schematic drawing of a planar solid-state device: 1, support; 2a and 2b, Pt-film reference electrodores; 2c, auxiliary electrode; 2d, contact to indicator electrode; 3, Au/PVC composite membrane indicator electrode; and 4–7, electrical contacts. (Reprinted with permission from Hohercakova and Opekar 2004. Copyright 2004 Elsevier.)

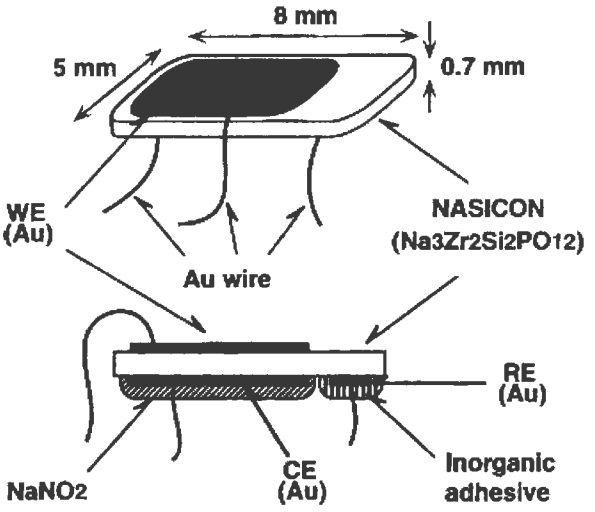

Figure 1.38. Schematic drawing of a solid-state device based on an inorganic salt. (Reprinted with permission from Miura et al. 1998. Copyright 1998 Elsevier.)

tests as a model hydrocarbon. The solid-state electrochemical cell based on YSZ operates in the amperometric mode. Oxygen is pumped out at the Au/YSZ electrode, and C_3H_6 is oxidized at the Pt/YSZ electrode. At a gas temperature of 600°C, the sensitivity is 2 nA/ppm C_3H_6 for this high-temperature amperometric gas sensor design.

Solid-state amperometric sensors based on cation-conducting inorganic materials have also been described (Miura et al. 1998). The sodium or lithium ions pumped through the membrane form salts with the reduced form of the analyte gas (NO_2 or CO_2). In Figure 1.38 the arrangement for such a sensor is shown.

10. ELECTROCHEMICAL SENSOR APPLICATIONS

The use of a variety of materials, unique geometries or structures, and different methods gives the electrochemical sensors their analytical properties and allows them to serve diverse applications. We can find electrochemical sensors in such areas as industrial safety, biochemistry, clinical chemistry, health and medicine, agriculture, food safety, environmental protection, automotive technology, space exploration, military threat detection, and process control. The most widely used electrochemical sensor is the oxygen sensor, which is used for automotive engine and boiler control. Oxygen sensors for automotive use were first introduced by Bosch in 1976 and have been standard on all passenger cars sold in the United States since 1980–1981 (Riegel et al. 2002).

Applications for electrochemical sensors continue to grow in many markets. Compared to spectrometric (FTIR, UV-visible), mass spectrometric (MS), and chromatographic techniques (GC, HPLC), electrochemical sensors are simple in their setup as well as in the electronic equipment necessary for operation and for data acquisition. The effort for maintenance and calibration is slight. Sensor signals

are obtained directly (*in situ*) and provide real-time information for process control. Therefore, they are preferred tools in industrial applications and for screening in field applications (Guth et al. 2009). With proper materials, electrochemical sensors can be applied in real matrices at temperatures from –30 up to 1600°C. The so-called conventional electrochemical sensors, which work with aqueous or liquid electrolytes, are usually used at low temperatures, whereas solid electrolyte–based sensors operate in the temperature range >500°C. In the low-temperature range, electrochemical sensors are used to measure pH-value, electrical conductivity (impedance), and the concentration (activity) of dissolved ions and/or gases. For measurements of different components at high temperatures in exhaust gases and molten metals, solid electrolyte sensors are commonly utilized. Sensors for determining free oxygen, equilibrium oxygen in reducing gases, and dissolved oxygen in metal melts that have been applied in various technical processes, e.g., in the steel, ceramic, cement, and glass-making industries, are commercially available (Guth et al. 2009). The challenges are common to all applications and include the following: inexpensive fabrication steps, sensor robustness, reliability, reproducibility, low power consumption, and easy system integration (Bryzek et al. 2006).

Electrochemical sensors are also suitable for security and defense applications because of their portability and low power consumption. They potentially can offer higher sensitivity, specificity, and lower power consumption for detection of toxic gass. Some examples include monitoring filter breakthrough (e.g., toluene concentration inside the mask), personnel badge detectors (e.g., toxins accumulation), embedded suit leak-detection sensors (e.g., soldiers' suits for upcoming warfare agents), and other applications. For example, Ni et al. (2008) recently described a sensor array that included electrochemical sensors for early warning of electrical fires. Additionally, a wireless capability with the sensor can be used for networked mobile and fixed-site detection and early warning systems for military bases, work facilities, and battlefield areas. Many other examples of electrochemical sensor applications can be elsewhere in this series and throughout trade and commerce worldwide. Due to success achieved in development of electrochemical sensors, they have become among of the most widely used gas-sensing devices.

11. PARAMETERS IN GAS SENSOR APPLICATION

The physical size, geometry, selection of various components, and construction of an electrochemical gas sensor usually depend on its intended use as well as on the manufacturer. However, the main characteristics of electrochemical gas sensors in application are essentially very similar independent of the manufacturer (Anderson and Hadden 1999; Chou, 1999; Elter et al. 1994). It is necessary to note that electrochemical sensors with liquid electrolytes are the most sensitive to environmental conditions. Therefore, we use this type of sensor to illustrate the effects of sensor operational conditions on the observed performances and lifetime.

11.1. TEMPERATURE

Electrochemical sensors are quite sensitive to temperature. In general, if the sensor is calibrated at 25°C, then, when the temperature is above 25°C, the sensor will read higher; when the temperature is below

25°C, it will read lower. The temperature effect is typically 0.5–1.0% per degree centigrade, depending on the manufacturer and the type of sensor. In general, the lowest temperature at which a sensor can be expected to function properly over long periods of time is 0°C. Therefore, sensors are typically internally temperature-compensated. For this purpose, electrochemical H_2 sensors should incorporate a sensitive temperature sensor which the electronics can use to compensate for temperature variations. However, it is better to keep the sample temperature as stable as possible. All chemical sensors depend on the kinetic and thermodynamics of a chemical reaction and therefore will have a temperature effect. This can sometimes be minimized by design in which diffusion to the sensor limits the signal, in which case the diffusion temperature coefficient is observed. In any case, temperature effects need to be minimized for any field use that will involve operation at different temperatures.

11.2. HUMIDITY

Unlike many solid-state or semiconductor devices, aqueous electrolyte electrochemical gas sensors are not affected directly by humidity. However, continuous operation below 15% RH or above 90% RH can change the water content of the electrolyte, thus affecting the operation of the cell. This process occurs very slowly and depends on the temperature, the electrolyte, and the vapor barrier. In high-humidity conditions, prolonged exposure can cause excessive water to build up and, if not planned for in the sensor design, can create leakage. In low-humidity conditions, the sensor can dry out. In dry conditions, the acid content of the electrolyte can rise, causing crystallization, or allow the acid to attack the sensor seals and materials of construction. In general, high-temperature and low-humidity conditions are most likely to result in large changes in electrolyte hydration.

11.3. PRESSURE

Amperometric electrochemical gas sensors are typically partial-pressure sensors and therefore directly proportional to pressure. Capillary-design sensors compensate for pressure changes by using Knudsen flow geometry. It is important to keep the entire sensor at the same pressure, since differential pressure within the sensor may cause sensor damage if a proper vent has not been designed. Solid-state electrochemical sensors do not have such susceptibility to pressure changes. A change in pressure can sometimes cause more gas to be forced into the sensor, producing a current transient. These transients rapidly decay to zero as the normal diffusion conditions are reestablished. However, some transients may trigger false alarms. The pressure coefficient should be determined experimentally for any given sensor design.

11.4. CALIBRATION

For electrochemical sensors, stable cylinders of calibration gases in the concentration range of interest as well as other, less convenient chemical-generation systems (e.g., permeation tubes) may be used for calibration. The frequency of calibration cannot be prescribed exactly, but there are sensors that require only

yearly or more calibration while others need more frequest calibration in order to maintain a given accuracy. One must determine the calibration cycle that will maintain the performance required for a given application. Manufacturer's instructions and/or user experience should dictate the frequency of calibration.

For maximum accuracy, the environmental conditions (temperature, relative humidity, barometric pressure) of the monitor at the time of calibration should be as near as possible to those that will be encountered during use. Of these three factors, temperature is most important because changes in temperature are most often encountered in the field and can cause bias in the readings obtained. Even with the temperature-compensating circuitry employed in most sensors, some time is required for equilibrium to be reached. If it is not possible to calibrate at the working temperature, the user must allow sufficient time for field equilibration of temperature. Small changes in barometric pressure are usually less significant than temperature changes and so are of less concern to the user.

11.5. SENSOR FAILURE MECHANISMS

11.5.1. Blocking Mechanisms

Blocking is a condition which causes the sensor to function poorly or not at all until the condition is removed. Normally the block does not damage the sensor permanently, as a poison would. Some of the most common blocking mechanisms for electrochemical cells are the following.

- *Freezing of the electrolyte.* As the temperature of the cell decreases, the chemical reaction which the user sees as a signal decreases. At some point, depending on the electrolyte, the cell current stops. Usually, upon returning to a normal temperature, the cell will often reactivate.
- *Filter or membrane clogging.* If the cell's diffusion barrier becomes clogged or coated, the normal supply of signal gas may be cut off. Sensors used in front of air inlets, exhaust fans, or in dusty areas are likely to become clogged. A dust filter should be used, and it should be cleaned regularly to prevent the cell's oxygen supply from being depleted.
- *Vapor condensation.* Condensation on the sensor diffusion barrier can also effectively cut off the signal gas. If the sensor temperature is lower than the atmosphere temperature, condensation can occur. To prevent this, the cell may need to be heated or the air sample being circulated to the cell may need to be dried.

11.5.2. Poisoning Mechanisms

A poison blocks and/or degrades the sensor's operation permanently. Prolonged exposure to a poison usually results in destroying the sensor. Most sensors are not poisoned directly by a gas or vapor, but they may be poisoned indirectly. The most common causes of poisoning are the following.

- *Solvent vapors.* High concentrations of solvent vapors may attack the plastic housing or filters. The most common solvents which can cause problems (depending on the construction of the

sensor) are alcohols, ketones, phenols, pyridine, amines, or chlorinated solvents. Sensors used in these atmospheres may have a shorter life.

- *High temperatures.* All sensors must be operated within their specified temperature range. Continuous operation at high temperatures can cause sensor failure by changing the chemistry or by degrading the mechanical properties of the device.

11.6. SENSOR LIFE

The life expectancy of an electrochemical gas sensor depends on several factors, including environmental conditions, such as temperature, pressure, and humidity. For a truly catalytic sensor, degradation of the catalyst can be very slow, and lifetimes in excess of 5 years have been observed for many sensors. However, some sensors use sacrificial reagents and therefore have a limited lifetime and one that is often dependent on the length of time of exposure to analyte (e.g., galvanic oxygen sensors). Therefore their normal life expectancy may be up to 5 years from the date of manufacture. Certain manufacturers recommend that electrochemical cells be stored with a shorting clip to extend the lifetime on the shelf. In general, however, each sensor may be designed differently, and its lifetime can be prolonged by following the manufacturer's recommendations. Some sensors have filters for added selectivity, and onboard filters also have a limited life. Prolonged exposure to gases being removed by the filter will shorten its effective life and the lifetime of the selectivity of the sensor.

12. MARKET FOR ELECTROCHEMICAL GAS SENSORS

Electrochemical gas sensors occupy a large market sector, and sensors for electroactive gases such as CO, NH_3, SO_2, NO, NO_2, and H_2 exist today. Typical electrochemical sensors are illustrated in Figures 1.39 and 1.40.

At present, many companies market electrochemical sensors. The practical capabilities of some present-day industrial electrochemical gas sensors are summarized in Table 1.9.

The first sensors were developed for the more common atmospheric pollutants, namely, CO, NO, NO_2, H_2S, and SO_2. Sensors have also been developed for some special cases such as the hydrazines,

Figure 1.39. Hydrogen sulfide sensor with reduced cross-sensitivity to methanol (7HH-LM) designed by City Technology Ltd. (www.citytech.com).

Figure 1.40. Carbon monoxide electrochemical gas sensors fabricated by Alphasense (www.alphasense.com).

Cl_2, CH_4, O_3, alcohol, and, of course, medical applications for the detection and measurement of N_2O, O_2, CO_2, and $CHClBrCF_3$ (Chang et al. 1993). Other candidates for analysis using electrochemical gas sensors (many of which have been performed) include electrochemically active compounds such as acetylene, alcohols, aldehydes (acetone), phosphine, arsine, and phosgene. These compounds are often encountered as interferences with present-day commercial instruments. More detailed information about these companies and their sensors can be found on the companies' websites.

Table 1.9. Example capabilities of electrochemical sensors

Gas/vapor measured	Detection range available	Resolution
O_2	0–25 %vol	0.1% vol
CO	0–500–20,000 ppm	0.5–1 ppm
H_2	0–100–2,000 ppm	1 ppm
NO	0–100–1,000 ppm	1 ppm
NO_2	0–20–500 ppm	10 ppb–0.1 ppm
H_2S	0–100–1,000 ppm	0.1–1 ppm
SO_2	0–20–5,000 ppm	0.1–1 ppm
Cl_2	0–20–200 ppm	0.1–1 ppm
O_3	0–5–20 ppm	5–50 ppb
HCl	0–200 ppm	1 ppm
PH_3	0–100 ppm	0.1 ppm
NH_3	0–50–1,000 ppm	1 ppm
MMH	0 – 500 ppm	0.1 ppm

13. OUTLOOK AND FUTURE TRENDS

The present discussion has revealed that electrochemical sensors are important members of the gas sensor technologies. Many research and development efforts have resulted in practical life-saving sensors for detection of CO, H_2S, NO_2, O_2, and other electrochemically active gases that are now routinely used in industrial hygiene and safety monitoring of people and workplaces. The practical performance of electrochemical gas sensors provides value to many markets.

Electrochemical sensor research and development is most interesting and exciting. New sensors will reach lower levels, higher selectivity, and enhanced stability. There are many creative and innovative solutions to gas monitoring in specific cases that have been provided by application of electrochemical sensor technology. Electrochemical sensors compete well with the myriad of optical, electronic, mechanical, and thermal sensing techniques and particularly when sensitivity must be combined with low cost and low power consumption. In general, electrochemical sensors can be much less expensive than optical, mechanical, or thermal sensors that include spectrometers or complex electronics, and electrochemical sensors can still be amenable to microfabrication batch processes (Maclay et al. 1988; Buttner et al. 1990). Unlike catalytic and semiconductor sensors, electrochemical sensors can often provide response at room temperature, where the power required is much lower. Electrochemical sensors can often operate in the absence of oxygen on the sensing side, whereas availability of oxygen is essential for pellistor and semiconductor sensors. In applications such as cover gas monitoring in "fast reactors," where there is no oxygen on the sensing side, the solid-electrolyte proton-conductor hydrogen sensor can be used. Thus one can state that electrochemical gas sensors have and will continue to have an important impact on the market for gas sensors.

As we have shown, every type of electrochemical gas sensor discussed in this chapter has either advantages or shortcomings in one or more applications. Potentiometric sensors have wide dynamic range but lack accuracy at higher concentrations because of their logarithmic response. Amperometric sensors are usually optimized for gas detection in a considerably more narrow concentration range but have a simple linear response. Ultimately, the choice of the specific sensor will be conditioned by the requirements the application makes of the measuring system.

Overall, there is a growing need for gas sensors for safety, security, process control, and medical diagnostics. The applications will dictate the challenges remaining and put pressure on sensor developers for improvements. The improvements will evolve through the application of human creativity and the basic knowledge of materials, structure, fabrication, and operation methods illustrated by the scientific and engineering reports cited in this review. The most difficult applications defy all types of senor technologies, including electrochemical sensors. The issues yet to be solved include sensor stability and durability when operating in severe environments, e.g., environments such as inside gasifiers and combustion processes. However, great progress has been made.

The many alternatives illustrated in this chapter show the possibilities but have not completely solved all the problems of gas sensors. New electrode materials with greater stability are possible. New electrolytes not yet utilized to any significant extent, such as the ionic liquids, need to make a contribution. The structure of the material has just begun to emerge as electrodes and electrolytes. The geometry of the sensor and control of each interface is critical, and new MEMS sensors need to emerge for gas sensing (Bryzek et al. 2006). MEMS and nanotechnology will also obviously contribute to the development of new electrochemical gas sensors.

The advancement of MEMS technology and the fast pace of nanotechnology will no doubt enable new electrochemical gas sensor designs and materials such that new applications are found for large gas molecules and weakly electroactive gas molecules in applications that will analyze for chemical threats, toxins, food flavors, and fragrances. Much of today's work focuses on new designs that incorporate microfabrication and nanofabrication to achieve smaller size, lower power, lower cost, and portable sensors and sensor arrays with intelligence (Guth et al. 2009). With its combination of desirable measurement characteristics and interface to modern electronics, electrochemical sensors can put sophisticated monitoring capability in the palm of your hand (see Figure 1.41).

New nanomaterials are being developed, and this will change the building blocks that are available for electrochemical sensors, offering well-organized nanostructures with high surface area, high chemical reactivity at lower temperature, good mechanical strength, and better thermal stability, and new catalysts for selectivity, new electrolytes for higher-temperature operation, multiple working electrodes for self-amplifying sensors, and combinations with bioanalytical approaches for biosensors and enzyme-based sensors. MEMS technology and nanotechnology combined with new computational power brighten the future of the electrochemical sensor and its use within analytical chemistry and especially in field analytical measurements.

Finally, many of the operating modes for these sensors have not been fully explored. Time-dependent signals and sensor arrays can solve many of the selectivity problems that are still present in today's sensors.

The results reviewed here illustrate the insight we have today and collect much of the fundamental knowledge needed to move forward. There are more practical opportunities for monitoring today than 10 years ago, and one can envision practical solutions that integrate new materials, structures, and technology over the next 10 years to produce ever-better electrochemical sensors and sensor systems. We now begin a new era of electrochemical sensor development using new materials, new time-resolved and spatially resolved sensor array approaches, and smaller sensor devices. It is clear that the utility of electrochemistry will continue and will preserve its place in gas sensor applications now and in the future (Yao and Stetter 2004; Yang and Dutta 2007) and will continue to serve for the betterment of human health, safety, and the environment.

Figure 1.41. KWJ pocket instrument with incorporated electrochemical sensor for either CO, H_2S, H_2, or ozone. The instrument continuously displays real-time concentration and can report dosimetry information including the 8-h time-weighted average concentration, the total exposure (ppm h), and the magnitude and time of occurrence of the maximum. (Reprinted with permission from Ebeling et al. 2009. Copyright 2009 Elsevier.)

REFERENCES

Achmann S., Hammerle M., and Moos R. (2008) Amperometric enzyme-based gas sensor for formaldehyde: Impact of possible interferences. *Sensors* **8**(3), 1351–1365.

Alber K.S., Cox J.A., and Kulesza P.J. (1997) Solid-state amperometric sensors for gas phase analytes: A review of recent advances. *Electroanalysis* **9**, 97–101.

Alberti G., Casicola M., and Palombari R. (1993) Amperometric sensor for carbon monoxide based on solid state protonic conduction. *Solid State Ionics* **61**, 241–244.

Alberti G. and Casciola M. (2001) Solid state protonic conductors, present main applications and future prospects. *Solid State Ionics* **145**, 3–16.

Albery W.J. (1982) Carbon dioxide measurement. U.S. Patent 4,377,446.

AlNashef I.M., Leonard M.L., Matthews M.A., and Weidner J.W. (2002) Superoxide electrochemistry in an ionic liquid. *Ind. Eng. Chem. Res.* **41**, 4475–4478.

Anantaraman A.V. and Gardner C.L. (1996) Studies on ion-exchange membranes. Part 1. Effect of humidity on the conductivity of Nafion. *J. Electroanal. Chem.* **414**, 115–120.

Anastas P.T. (2007) Introduction: Green chemistry. *Chem. Rev.* **107**, 2167–2168.

Anderson G. and Hadden D. (1999) *The Gas Monitoring Handbook.* Avocet Press, New York.

Ando M. Recent advances in optochemical sensors for the detection of H_2, O_2, O_3, CO, CO_2 and H_2O in air. *Trends Anal. Chem.* **25**, 937–948.

Aroutiounian V. (2007) Metal oxide hydrogen, oxygen, and carbon monoxide sensors for hydrogen setups and cells. *Int. J. Hydrogen Energy* **32**, 1145–1158.

Baker G.A., Baker S.N., Pandey S., and Bright F.V. (2005) An analytical view of ionic liquids. *Analyst* **130**, 800–808.

Bakker E., Buhlmann P., and Pretsch E. (1997) Carrier-based ion-selective electrodes and bulk optodes. 1. General characteristics. *Chem. Rev.* **97**, 3083–3132.

Bakker E. and Pretsch E. (2005) Potentiometric sensors for trace-level analysis. *Trends Anal. Chem.* **24**, 199–207.

Baltruschat H., Kamphausen I., Oelgeklaus R., Rose J., and Wahlkamp M. (1997) Detection of volatile organic solvents using potentiodynamic gas sensors. *Anal. Chem.* **69**, 743–748.

Bard A.J. (ed.) (1978) *Encyclopedia of Electrochemistry of the Elements*, Vol. 4. Marcel Dekker, New York.

Barisci J.N., Wallace G.G., MacFarlane D.R., and Baughman R.H. (2004) Investigation of ionic liquids as electrolytes for carbon nanotube electrodes. *Electrochem. Commun.* **6**, 22–27.

Barrosse-Antle L.E., Silvester D.S., Aldous L., Hardacre C., and Compton R.G. (2008) Electroreduction of sulfur dioxide in some room-temperature ionic liquids. *J. Phys. Chem. C* **112**, 3398–3404.

Barrosse-Antlle L.E., Hardacre C., and Compton R.G. (2009) SO_2 saturation of the room temperature ionic liquid [C(2)mim][NTf2] much reduces the activation energy for diffusion. *J. Phys. Chem. B* **113**, 1007–1011.

Barsan N., Stetter J.R. ,Findlay M., and Göpel W. (1999) High-performance gas sensing of CO: Comparative tests for semiconducting (SnO_2-based) and for amperometric gas sensors. *Anal. Chem.* **71**, 2512–2517.

Bay H.W., Blurton K.F., Lieb H.C., and Oswin H.G. (1972) Electrochemical measurement of carbon monoxide. *Am. Lab.* **4**, 57–58 and 60–61.

Berger J. and Edelman P. (2000) Extended use planar sensors. U.S. Patent 6,068,748.

Biswas S.K., Gnanasekaran T., Ghorai T.K., and Pramanik P. (2008) Sensing properties of chemically synthesized pristine and Pt-impregnated nanosized $FeNbO_4$ in hydrogen, ammonia, and LPG. *J. Electrochem. Soc.* **155**, J26–J31.

Blurton K.F. and Sedlak J.M. (1974) The electro-oxidation of carbon monoxide on platinum. *J. Electrochem. Soc.* **121**, 1315–1317.

Blurton K.F. and Stetter J.R. (1977) The gas phase and electrochemical oxidation of carbon monoxide on platinum, palladium, and ruthenium catalysts: A comparative study. *J. Catal.* **46**, 230–233.

Blurton K.F. and Stetter J.R. (1978) Sensitive electrochemical detector for gas chromatography. *J. Chromatogr.* **155**, 35–45.

Bobacka J. (2006) Conducting polymer-based solid-state ion-selective electrodes. *Electroanalysis* **18**, 7–18.

Bobacka J., Ivaska A., and Lewenstam A. (2008) Potentiometric ion sensors. *Chem. Rev.* **108**, 329–351.

Bonanos N. (2001) Oxide-based protonic conductors: Point defects and transport properties. *Solid State Ionics* **145**, 265–274.

Bontempelli G., Comisso N., Toniolo R., and Schiavon G. (1997) Electroanalytical sensors for nonconducting media based on electrodes supported on perfluorinated ion-exchange membranes. *Electroanalysis* **9**, 433–443.

Bouchet R. and Siebert E. (1999) Proton conduction in acid doped polybenzimidazole. *Solid State Ionics* **118**, 287–299.

Bouchet R., Siebert E., and Vitter G. (2000a) Polybenzimidazole-based hydrogen sensors. I. Mechanism of response with an E-TEK gas diffusion electrode. *J. Electrochem. Soc.* **147**, 3125–3130.

Bouchet R., Siebert E., and Vitter G. (2000b) Polybenzimidazole-based hydrogen sensors. II. Effect of the electrode preparation. *J. Electrochem. Soc.* **147**, 3548–2551.

Bouchet R., Rosini S., Vitter G., and Siebert E. (2001) Solid-state hydrogen sensor based on acid-doped polybenzimidazole. *Sens. Actuators B* **76**, 610–616.

Bouchet R., Rosini S., Vitter G., and Siebert E.A (2002) Solid-state potentiometric sensor based on polybenzimidazole for hydrogen determination in air. *J. Electrochem. Soc.* **149**, H119–H122.

Brajnikov V.V. (1992) *Detectors for chromatography*. Mashinostroenie, Moscow (in Russian).

Brett C.M.A. (2001) Electrochemical sensors for environmental monitoring. Strategy and examples. *Pure Appl. Chem.* **73**, 1969–1977.

Broder T.L., Silvester D.S., Aldous L., Hardacre C., and Compton R.G. (2007) Electrochemical oxidation of nitrite and the oxidation and reduction of NO_2 in the room temperature ionic liquid [C2mim][NTf2]. *J. Phys. Chem. B* **111**, 7778–7785.

Bryzek J.S., Roundy S., Bircumshaw B., Chung C., Castellano K., Vestel M., and Stetter J.R. (2006) Marvelous MEMS. *IEEE Circ. Dev.* **22**(2), 8–28.

Buhlmann P., Pretsch E., and Bakker E. (1998) Carrier-based ion-selective electrodes and bulk optodes. 2. Ionophores for potentiometric and optical sensors. *Chem. Rev.* **98**, 1593–1688.

Bui P.A., Vlachos D.C., and Westmoreland P.R. (1997) Modeling ignition of catalytic reactors with detailed surface kinetics and transport: Oxidation of H_2/air mixtures over platinum surfaces. *Ind. Eng. Chem. Res.* **36**, 2558–2567.

Buttner W.J., Stetter J.R., and Maclay G.J. (1990) Microfabricated amperometric gas sensors with and integrated design. *Sensors Mater.* **2**, 99–106.

Buzzeo M.C., Evans R.G., and Compton R.G. (2004a) Non-haloaluminate room-temperature ionic liquids in electrochemistry—A review. *ChemPhysChem.* **5**, 1106–1120.

Buzzeo M.C., Giovanelli D., Lawrence N.S., Hardacre C., Seddon K.R., and Compton R.G. (2004b) Elucidation of the electrochemical oxidation pathway of ammonia in dimethylformamide and the room temperature ionic liquid, 1-ethyl-3-methylimidazolium bis(trifluoromethylsulfonyl)imide. *Electroanalysis* **16**, 888–896.

Campbell D.N., Davis R.C., and Schmidt J.C. (1986) Amperometric gas sensor containing a solid electrolyte. U.S. Patent 4,744,954.

Cao Z. and Stetter J.R. (1991) Amperometric gas sensors. In: Madou M. and Joseph J.P. (eds.), *Opportunities for Innovation: Chemical and Biological Sensors*. NIST Publication GCR 91-593-1, U.S. Department of Commerce.

Cao Z., Buttner W.J., and Stetter J.R. (1992) The properties and applications of amperometric gas sensors. *Electroanalysis* **4**, 253–266.

Cha W., Lee Y., Oh B.K., and Meyerhoff M.E. (2005) Direct detection of *S*-nitrosothiols using planar amperometric nitric oxide sensor modified with polymeric films containing catalytic copper species. *Anal. Chem.* **77**, 3516–3524.

Chang S.C., Stetter J.R., and Cha C.S. (1993) Amperometric gas sensors. *Talanta* **40**, 461–477.

Chao Y., Buttner W.J., Yao S., and Stetter J.R. (2005) Amperometric sensor for selective and stable hydrogen measurement. *Sens. Actuators B* **106**, 784–790.

Chou J. (1999) *Hazardous Gas Monitors: A Practical Guide to Selection, Operation, and Applications.* McGraw-Hill Professional, New York.

Christofides C. and Mandelis A. (1990) Solid-state sensors for trace hydrogen gas detection. *J. Appl. Phys.* **68**, R1–R30.

Colomban Ph. (ed.) (1992) *Proton Conductors.* Cambridge University Press, Cambridge, UK.

Colomban Ph. (1999) Latest developments in proton conductors. *Ann. Chim. Sci. Mater.* **24**, 1–18.

Criddle W.J., Hansen N.R.S., and Jones D. (1995) Fuel cell detector for gas chromatography. *Analyst* **120**, 1639–1642.

Dabill D.W., Gentry S.J., Holland H.B., and Jones A. (1978) The oxidation of hydrogen and carbon monoxide mixtures over platinum. *J. Catal.* **53**, 164–167.

Damgaard L.R., Revsbech N.P., and Reichardt W. (1998) Use of an oxygen-insensitive microscale biosensor for methane to measure methane concentration profiles in a rice paddy. *Appl. Environ. Microbiol.* **64**, 864–870.

De Vos R.M. and Verweij H. (1998) High-selectivity, high-flux silica membranes for gas separation. *Science* **279**, 1710–1711.

Dubbe A. and Moos R. (2006) Solid electrolyte hydrocarbon gas sensor using zeolite as the sensitive phase. *Electrochem. Solid-State Lett.* **9**(5), H31–H34.

Ebeling D., Patel V., Findlay M., and Stetter J. (2009) Electrochemical ozone sensor and instrument with characterization of the electrode and gas flow effects. *Sens. Actuators B* **137**, 129–133.

Elter P.M. and Cassinelli M.E. (eds.) (1994) *NIOSH Manual of Analytical Methods*, 4th ed. U.S. Department of Health and Human Services, Cincinnati, OH.

Fergus J.W. (2007) Perovskite oxides for semiconductor-based gas sensors. *Sens. Actuators B* **123**, 1169–1179.

Floate S. and Hahn C.E.W. (2005) The development of new microelectrode gas sensors: An odyssey: Part V. Simultaneous electrochemical determination of oxygen, carbon dioxide and nitrous oxide gas mixtures in a non-aqueous solvent using membrane shielded gold microelectrodes. *J. Electroanal. Chem.* **583**, 203–211.

Garzon F.H., Mukundan R., and Brosha E.L. (2000) Solid-stale mixed potential gas sensors: Theory, experiments and challenges. *Solid State Ionics* **136**, 633–638.

Guth U., Vonau W., and Zosel J. (2009) Recent developments in electrochemical sensor application and technology—A review. *Meas. Sci. Technol.* **20**, 042002.

Hartel G., Rompf F., and Puschel T. (1996) Separation of a CO_2/H_2 gas mixture under high pressure with polyethylene terephthalate membranes. *J. Membrane Sci.* **113**, 115–120.

Hartel G. and Puschel T. (1999) Permselectivity of a PA6 membrane for the separation of a compressed CO_2/H_2 gas mixture at elevated pressures. *J. Membrane Sci.* **162**, 1–8.

Hashimoto A., Hibino T., Mori K., and Sano M. (2001) High-temperature hydrocarbon sensors based on a stabilized zirconia electrolyte and proton conductor-containing platinum electrode. *Sens. Actuators B* **81**, 55–63.

Hitchman M.L. (1978) *Measurements of Dissolved Oxygen.* John Wiley, New York.

Ho K.D. and Hung W.T. (2001) An amperometric NO_2 gas sensor based on Pt/Nafion® Electrode. *Sens. Actuators B* **79**, 11–16.

Hoare J.P. (1968) *The Electrochemistry of Oxygen.* John Wiley, New York.

Hodgson A.W. E., Jacquinot P., Jordan L.R., and Hauser P.C. (1999a) Amperometric gas sensors of high sensitivity. *Electroanalysis* **11**, 782–787.

Hodgson A.W.E., Jacquinot P., and Hauser P.C. (1999b) Electrochemical sensor for the detection of SO_2 in the low-ppb range. *Anal. Chem.* **71**, 2831–2837.

Holzinger M., Maier J., and Sitte W. (1997) Potentiometric detection of complex gases: Application to CO_2. *Solid State Ionics* **94**, 217–225.

Hohercakova Z. and Opekar F. (2004) Au/PVC composite—A new material for solid-state gas sensors: Detection of nitrogen dioxide in the air. *Sens. Actuators B* **97**, 379–386.

Hrncirova P. and Opekar F. (2002) Effect of gas humidity on the potential of pseudoreference Pt/air electrode in amperometric solid-state gas sensors. *Sens. Actuators B* **81**, 329–333.

Huang X.-J., Silvester D.S., Streeter I., Aldous L., Hardacre C., and Compton R.G. (2008) Electroreduction of chlorine gas at platinum electrodes in several room temperature ionic liquids: Evidence of strong adsorption on the electrode surface revealed by unusual voltammetry in which currents decrease with increasing voltage scan rates. *J. Phys. Chem. C* **112**, 19477–19483.

Imaya H., Ishiji T., and Takahashi K. (2005) Detection properties of electrochemical acidic gas sensors using halide–halate electrolytic solutions. *Sens. Actuators B* **108**, 803–807.

Inaba T., Saji K., and Takahashi H. (1999) Limiting current-type gas sensor using a high temperature-type proton conductor thin film. *Electrochemisty* **67**, 458–462.

Ishihara T. and Matsubara S. (1998) Capacitive type gas sensors. *J. Electroceram.* **2**, 215–228.

Ishihara T., Fukuyama M., Dutta A., Kabemura K., Nishiguchi H., and Takita Y. (2003) Solid state amperometric hydrocarbon sensor for monitoring exhaust gas using oxygen pumping current. *J. Electrochem. Soc.* **150**, H241–H245.

Ives D.J.G. and Janz G.J. (eds.) (1961) *Reference Electrodes: Theory and Practice.* Academic Press, New York.

Iwahara H., Uchida H., Ogaki K., and Nagato H. (1991) Nernstian hydrogen sensor using $BaCeO_3$-based, proton-conducting ceramics operative at 200°–900°C. *J. Electrochem. Soc.* **138**, 295–299.

Iwahara H., Yajima T., Hibino T., and Ozaki K. (1993) Protonic conduction in calcium, strontium and barium zirconates. *Solid State Ionics* **61**, 65–69.

Iwahara H. (1995) Technological challenges in the application of proton conducting ceramics. *Solid State Ionics* **77**, 289–298.

Jacquinot P., Muller B., Wehrli B., and Hauser P.C. (2001) Determination of methane and other small hydrocarbons with a platinum–Nafion electrode by stripping voltammetry. *Anal. Chim. Acta* **432**, 1–10.

Jacobs A. ,Vangrunderbeek J., Beckers H., De Schumr F., Luyten J., Van Landschoot R., Fukatsu N., Kurita N., Koide K., and Ohashi T. (1998) Hydrogen sensor for molten metals usable up to 1500 K. *Solid State Ionics* **113–115**, 219–224.

Janata J. (1989) *Principles of Chemical Sensors.* Plenum Press, New York.

Janata J., Josowicz M., Vanysek P., and DeVaney D.M. (1998) Chemical sensors. *Anal. Chem.* **70**, R179–R208.

Jiang Y.Y., Zhou Z., Jiao Z., Li L., Wu Y.T., and Zhang Z.B. (2007) SO_2 gas separation using supported ionic liquid membranes. *J. Phys. Chem. B* **111**, 5058–5061.

Jin X., Yu L., Garcia D., Ren R. X., and Zeng X. (2006) Ionic liquid high temperature gas sensor array. *Anal. Chem.* **78**, 6980–6989.

Jin X., Yu L., and Zeng X. (2008) Enhancing the sensitivity of ionic liquid sensors for methane detection with polyaniline template. *Sens. Actuators B* **133**, 526–532.

Jordan L.R. and Hauser P.C. (1997) Electrochemical sensor for acetylene. *Anal. Chem.* **69**, 2669–2672.

Jordan L.R., Hauser P.C., and Dawson G.A. (1997) Portable trap–sensor system for monitoring low levels of ethylene. *Analyst* **122**, 811–814.

Josowicz M. (1995) Applications of conducting polymers in potentiometric sensors. *Analyst* **120**, 1019–1024.

Knake R. and Hauser P.C. (2003) Portable instrument for electrochemical gas sensing. *Anal. Chim. Acta* **500**, 145–153.

Knake R., Jacquinot P., Hodgson A.W.E., and Hauser P.C. (2005) Amperometric sensing in the gas-phase. *Anal. Chim. Acta* **549**, 1–9.

Kordesch K. and Simader G. (1996) *Fuel Cells and Their Applications*. VCH, New York.

Korotcenkov G., Han S.D., and Stetter J.R. (2009) Review of electrochemical hydrogen sensors, *Chem. Rev.* **109**(3), 1402–1433.

Kosacki I. and Anderson H.U. (1998) Nanostructured oxide thin films for gas sensors. *Sens. Actuators B* **48**, 263–269.

Kou Y., Xiong W., Tao G., Liu H., and Wang T. (2006) Absorption and capture of methane into ionic liquid. *J. Natural Gas Chem.* **15**, 282–286.

Kreuer K.D. (1999) Aspects of the formation and mobility of protonic charge carriers and the stability of perovskite-type oxides. *Solid State Ionics* **125**, 285–291.

Kreuer, K. D. (2003) Proton-conducting oxides. *Annu. Rev. Mater. Res.* **33**, 333–359.

Kulesza P.J. and Cox J.A. (1998) Solid-state voltammetry—Analytical prospects. *Electroanalysis* **10**, 73–80.

Kuver A., Vielstich W., and Kitzelmann D. (1993) On the quantitative determination of carbon dioxide in air. A new sensor technique using anodic adsorbate stripping. *J. Electroanal. Chem.* **353**, 255–263

La Conti A.B. and Maget H.J.R. (1971) Electrochemical detection of H_2, CO, and hydrocarbons in inert or oxygen atmospheres. *J. Electrochem. Soc.* **118**, 506–510.

La Conti A.B. (1977) Electrically biased two electrode, electrochemical gas sensor with a H_2. U.S. Patent 4025412. *Chem. Abstr.* (1977) **87**, 86843h.

Lander J.J. (1951) Experimental heat contents of SrO, BaO, CaO, $BaCO_3$ and $SrCO_3$ at high temperatures. Dissociation pressures of $BaCO_3$ and $SrCO_3$. *J. Am. Chem. Soc.* **73**, 5794–5797.

Lecomte J., Loup J.P., Bosser G., Hervieu M., and Raveau B. (1984) Defect structure and electrical conductivity of niobates with related perovskite-type structures. *Solid State Ionics* **12**, 113–118.

Lee Y., Oh B.K. and Meyerhoff M.E. (2004) Improved planar amperometric nitric oxide sensor based on platinized platinum anode. 1. Experimental results and theory when applied for monitoring NO release from diazeniumdiolate-doped polymeric films. *Anal. Chem.* **76**, 536–544.

Li J., Lu Y., Ye Q., Cinke M., Han J., and Meyyappan M. (2003) Carbon nanotube sensors for gas and organic vapor detection. *Nanoletters* **3**(7), 929–933.

Li J., Lu Y., Ye Q., Delzeit L., and Meyyappan,M. (2005) A gas sensor array using carbon nanotubes and microfabrication technology. *Electrochem. Solid State Lett.* **8**(11), H100–H102.

Li J., Lu Y., and Meyyappan M. (2006) Nano chemical sensors with polymer-coated carbon nanotubes. *IEEE Sens. J.* **6**(5), 1047–1051.

Liang K.C. and Nowick A.S. (1993) High-temperature protonic conduction in mixed perovskite ceramics. *Solid State Ionics* **61**, 77–81.

Liang K.C., Du Y., and Nowick A.S. (1994) Fast high-temperature proton transport in nonstoichiometric mixed perovskites. *Solid State Ionics* **69**, 117–120.

Limoges B., Degrand C., and Brossier P. (1996) Redox cationic or procationic labeled drugs detected at a perfluorosulfonated ionomer film-coated electrode. *J. Electroanal. Chem.* **402**, 175–187.

Liu J. and Weppner W. (1992) Limiting-current chlorine gas sensor based on β″-alumina solid electrolyte. *Sens. Actuators B* **6**, 270–273.

Liu Y.C., Hwang B.J., and Tzeng I.J. (2002) Solid-state amperometric hydrogen sensor using Pt/C/Nafion composite electrodes prepared by a hot-pressed method. *J. Electrochem. Soc.* **149**, H173–H178.

Lu G., Miura N., and Yamazoe N. (1996a) High-temperature hydrogen sensor based on stabilized zirconia and a metal oxide electrode. *Sens. Actuators B* **35–36**, 130–135.

Lu G., Miura N., and Yamazoe N. (1996b) Mixed potential hydrogen sensor combining oxide ion conductor with oxide electrode. *J. Electrochem. Soc.* **143**, L154–L155.

Lu Y.J., Li J., Han J., Ng H.T., Binder C., Partridge C., and Meyyappan M. (2004) Room temperature methane detection using palladium loaded single-walled carbon nanotube sensors. *Chem. Phys. Lett.* **391**, 344–348.

Lu X., Wu S., Wang L., and Su Z. (2005) Solid-state amperometric hydrogen sensor based on polymer electrolyte membrane fuel cell. *Sens. Actuators B* **107**, 812–817.

Lucisano J.Y., Armour J.C., and Gough D.A. (1987) In vitro stability of an oxygen sensor. *Anal. Chem.* **59**, 736–739.

Lukow S.R. and Kounaves S.P. (2005) Analysis of simulated Martian regolith using an array of ion selective electrodes. *Electroanalysis* **17**, 1441–1449.

Lundstrom I., Sundgren H., Winquist F., Eriksson M., Krantz-Rulcker C., and Lloyd-Spetz A. (2007) Twenty-five years of field effect gas sensor research in Linköping. *Sens. Actuators B* **121**, 247–262.

Luyten J., De Schutter F., Schram J., and Schoonman J. (1991) Chemical and electrical properties of Yb-doped strontium cerates in coal combustion atmospheres. *Solid State Ionics* **46**, 117–120.

Maclay G.J., Buttner W.J., and Stetter J.R. (1988) Microfabricated amperometric gas sensors. *IEEE Trans. Electron. Dev.* **35**, 793–799.

Madou M. and Joseph J.P. (eds.) (1991) *Opportunities for Innovation: Chemical and Biological Sensors.* NTIS GCR 91593I, U.S. Department of Commerce, Springfield,VA.

Maffei N. and Kuriakose A.K. (1999) A hydrogen sensor based on a hydrogen ion conducting solid electrolyte. *Sens. Actuators B* **56**, 243–246.

Maffei N. and Kuriakose A.K. (2004) Solid-state potentiometric sensor for hydrogen detection in air. *Sens. Actuators B* **98**, 73–76.

Maksymiuk K. (2006) Chemical reactivity of polypyrrole and its relevance to polypyrrole based electrochemical sensors. *Electroanalysis* **18**, 1537–1551.

Mari C.M., Terzaghi G. Bertolini M., and Barbi G.B. (1992) A chlorine gas potentiometric sensor. *Sens. Actuators B* **8**, 41–45.

McCandless F.P. (1972) Separation of binary mixtures of CO and H_2 by permeation through polymeric films. *Ind. Eng. Process Des. Develop.* **11**, 470–478.

Mika M., Paidar M., Klapste B., Masinova M., Bouzek K., and Vondrak J. (2007) Hybrid inorganic–organic proton conducting membranes for fuel cells and gas sensors. *J. Phys. Chem. Solids* ***68***, 775–779.

Mitsubayashi K., Nishio G., Sawai M., Saito T., Kudo H., Saito H., Otsuka K., Noguer T., and Marty J.L. (2008) A bio-sniffer stick with FALDH (formaldehyde dehydrogenase) for convenient analysis of gaseous formaldehyde. *Sens. Actuators B* **130**, 32–37.

Michalska A. (2006) Optimizing the analytical performance and construction of ion-selective electrodes with conducting polymer-based ion-to-electron transducers. *Anal. Bioanal. Chem.* **384**, 391–406.

Millet P., Durand R., Dartyge E., Tourillon G., and Fontaine A. (1993) Precipitation of metallic platinum into Nafion ionomer membranes. *J. Electrochem. Soc.* **140**, 1373–1380.

Miura N., Ono M., Shimanzoe K., and Yamazoe N. (1998) A compact solid-state amperometric sensor for detection of NO_2 in ppb range. *Sens. Actuators B* **49**, 101–109.

Miura N., Raisen T., Lu G., and Yamazoe N. (1998) Highly selective CO sensor using stabilized zirconia and a couple of oxide electrodes. *Sens. Actuators B* **47**, 84–91.

Mohammad F. (1998) Compensation behaviour of electrically conductive polythiophene and polypyrrole. *J. Phys. D: Appl. Phys.* **31**, 951–959.

Mosley P.T., Norris J., and Williams D.E. (eds.) (1991) *Techniques and Mechanisms in Gas Sensing*. Adam Hilger, New York.

Mukundan R., Brosha E.L., Brown D.R., and Garzon F.G. (2000) A mixed-potential sensor based on a $Ce_{0.8}Gd_{0.2}O_{1.9}$ electrolyte and platinum and gold electrodes. *J. Electrochem. Soc.* **147**, 1583–1588.

Nazri G.-A., Tarascon J.-M., and Schreiber M. (eds.) *Solid State Ionics IV*, MRS Symposium Proceedings, 1995, Vol. 369, 289.

Ni M., Stetter J.R., and Buttner W.J. (2008) Orthogonal gas sensor arrays with intelligent algorithms for early warning of electrical fires. *Sens. Actuators B* **130**, 889–899.

Niedrach L.W. and Alford H.R. (1965a) Novel fuel cell structure. U.S. Patent 3905832. *Chem. Abstr.* 1965a, **62**, 11416c.

Niedrach L.W. and Alford H.R. (1965b) A new high-performance fuel cell employing conducting-porous-teflon electrodes and liquid electrolytes. *J. Electrochem. Soc.* **112**, 117–124.

Nikolova V., Nikolov I., Andreev P., Najdenov V., and Vitanov T. (2000) Tungsten carbide-based electrochemical sensors for hydrogen determination in gas mixtures. *J. Appl. Electrochem.* **30**, 705–710.

Nishimura R., Toba K., and Yamakawa K. (1996) The development of a ceramic sensor for the prediction of hydrogen attack. *Corrosion Sci.* **38**, 611–621.

Norby T. (2001) The promise of protonics. *Nature* **410**, 877–878.

Nowick A.S., Du Y., and Liang K.C. (1999) Some factors that determine proton conductivity in nonstoichiometric complex perovskites. *Solid State Ionics* **125**, 303–311.

Ogumi Z., Inatomi K., Hinatsu J.T., and Takehara Z.I. (1992) Application of the SPE method to organic electrochemistry—XIII. Oxidation of geraniol on Mn,Pt-Nafion. *Electrochim. Acta* **37**, 1295–-1299.

Okamura K., Ishiji T., Iwaki M., Suzuki Y., and Takahashi K. (2007) Electrochemical gas sensor using a novel gas permeable electrode modified by ion implantation. *Surf. Coat. Technol.* **201**, 8116–8119.

Ollison W.M., Penrose W.M., and Stetter J.R. (1995) Sensitive measurement of ozone using amperometric gas sensors. *Anal. Chim. Acta* **313**, 209–219.

O'Mahony A.M., Silvester D.S., Aldous L., Hardacre C., and Compton R.G. (2008) The electrochemical reduction of hydrogen sulfide on platinum in several room temperature ionic liquids. *J. Phys. Chem. C* **112**, 7725–7730.

Opekar F. (1992) An amperometric solid-state sensor for nitrogen dioxide based on a solid polymer electrolyte. *Electroanalysis* **4**, 133–138.

Opekar F., Langmaier J., and Samec Z. (1994) Indicator and reference platinum | solid polymer electrolyte electrodes for a simple solid-state amperometric hydrogen sensor. *J. Electroanal. Chem.* **379**, 301–306.

Opekar F. and Svozil D. (1995) Electric resistance in a Nafion® membrane exposed to air after a step change in the relative humidity. *J. Electroanal. Chem.* **385**, 269–271.

Opekar F. and Stulık K. Electrochemical sensors with solid polymer electrolytes. *Anal. Chim. Acta* **385**, 151–162.

Opekar F. and Stulık K. (2002) Amperometric solid-state gas sensors: Materials for their active components. *Crit. Rev. Anal. Chem.* **32**, 253–259.

Orme C.J., Stone M.L., Benson M.T., and Peterson E.S. (2003) Testing of polymer membranes for the selective permeability of hydrogen. *Sep. Sci. Technol.* **38**, 3225–3238.

Otagawa T., Zaromb S., and Stetter J.R. (1985) Electrochemical oxidation of methane in nonaqueous electrolytes at room temperature: Application to gas sensors. *J. Electrochem. Soc.* **132**, 2951–2957.

Paganin V.A., Ticianelli E.A., and Gonzalez E.R. (1996) Development and electrochemical studies of gas diffusion electrodes for polymer electrolyte fuel cells. *J. Appl. Electrochem.* **26**, 297–-304.

Pages X., Rouessac V., Cot D., Nabias G., and Durand J. (2001) Gas permeation of PECVD membranes inside alumina substrate tubes. *Sep. Purif. Technol.* **25**, 399–406.

Park Y.K., Aghalayam P., and Vlachos D.G. (1999) A generalized approach for predicting coverage-dependent reaction parameters of complex surface reactions: Application to H_2 oxidation over platinum. *J. Phys. Chem. A* **103**, 8101–8107.

Park C.O., Akbar S.A., and Weppner W. (2003) Ceramic electrolytes and electrochemical sensors. *J. Mater. Sci.* **38**, 4639–4660.

Pasierb P. and Rekas M. (2009) Solid-state potentiometric gas sensors-current status and future trends. *J. Solid State Electrochem.* **13**, 3–25.

Post M.L., Tunney J.J., Yang D., Du X., and Singleton D.L. (1999) Material chemistry of perovskite compounds as chemical sensors. *Sens. Actuators B* **59**, 190–194.

Potje-Kamloth K. (2008) Semiconductor junction gas sensors. *Chem. Rev.* **108**, 367–399.

Pretsch E. (2007) The new wave of ion-selective electrodes. *Trends Anal. Chem.* **26**, 46–51.

Qi P., Vermesh O., Grecu M., Javey A., Wang Q., Dai H., Peng S., and Cho K.J. (2003) Toward large arrays of multiplex functionalized carbon nanotube sensors for highly sensitive and selective molecular detection. *Nano Lett.* **3**, 347–351.

Ramesh C., Velayutham G., Murugesan N., Ganesan V., Dhathathreyan K.S., and Periaswami G. (2003) An improved polymer electrolyte-based amperometric hydrogen sensor. *J. Solid State Electrochem.* **8**, 511–516.

Ramesh C., Velayutham G., Murugesan N., Ganesan V., Manivannan V., and Periaswami G. (2004) Studies on modified anode polymer hydrogen sensor. *Ionics* **10**, 50–55.

Ramesh C., Murugesan N., Krishnaiah M.V., Ganesan V., and Periaswami G. (2008) Improved Nafion-based amperometric sensor for hydrogen in argon. *J. Solid State Electrochem.* **12**, 1109–1116.

Reinhardt G., Mayer R., and Rosch M. (2002) Sensing small molecules with amperometric sensors. *Solid State Ionics* **150**, 79–92.

Ren X., Wilson M.S., and Gottesfeld S. (1996) High performance direct methanol polymer electrolyte fuel cells. *J. Electrochem. Soc.* **143**, L12–L15.

Rieger P.H. (1987) *Electrochemistry.* Prentice Hall, Englewood Cliffs, NJ.

Riegel J., Neumann H., and Wiedenmann H.M. (2002) Exhaust gas sensors for automotive emission control. *Solid State Ionics* **152–153**, 783–800.

Roh S. and Stetter J.R. (2003) Gold film amperometric sensors for NO and NO_2. *J. Electrochem. Soc.* **150**, H272–H278.

Rosini S. and Siebert E. (2005) Electrochemical sensors for detection of hydrogen in air: Model of the non-Nernstian potentiometric response of platinum gas diffusion electrodes. *Electrochim. Acta* **50**, 2943–2953.

Sakthivel M. and Weppner W. (2006a) Response behaviour of a hydrogen sensor based on ionic conducting polymer-metal interfaces prepared by the chemical reduction method. Sensors **6**, 284–297.

Sakthivel M. and Weppner W. (2006b) Development of a hydrogen sensor based on solid polymer electrolyte membranes. *Sens Actuators B* **113**, 998–104.

Sakthivel M. and Weppner W. (2007a) Electrode kinetics of amperometric hydrogen sensors for hydrogen detection at low parts per million level. *J. Solid State Electrochem.* **11**, 561–570.

Sakthivel M. and Weppner W. (2007b) Application of layered perovskite type proton conducting $KCa_2Nb_3O_{10}$ in H_2 sensors: Pt particle size and temperature dependence. *Sens. Actuators B* **125**, 435–440.

Sakthivel M. and Weppner W. (2008) A portable limiting current solid-state electrochemical diffusion hole type hydrogen sensor device for biomass fuel reactors: Engineering aspect. *Int. J. Hydrog. Energ.* **33**, 905–911.

Samec Z., Opekar F., and Gjef C. (1995) Solid-state hydrogen sensor based on a solid-polymer electrolyte. *Electroanalysis* **7**, 1054–1058.

Satyanarayana L., Noh W.S., Jin G.H., Lee W.Y., and Park J.S. (2008) A potentiometric CO_2 sensor combined with composite metal oxide and DOP plasticizer operative at low temperature. *IEEE Sensors J.* **8**, 1565–1570.

Scheider A.A. (1978) Electrochemical cell for the detection of chlorine. U.S. Patent 4,184,937.

Schmidt J.C., Campbell D.N., and Clay S.B. (1985) Electrochemical gas sensor. U.S. Patent 4,595,486.

Schmidt-Zhang P. and Guth U. (2004) A planar thick film sensor for hydrocarbon monitoring in exhaust gases. *Sens. Actuators B* **99**, 258–263.

Schober T. (2003) Applications of oxidic high-temperature proton conductors. *Solid State Ionics* **162–163**, 277–281.

Scholten M.J., Schoonman J., Van Miltenburg J.C., and Oonk H.A.J. (1993) Synthesis of strontium and barium cerate and their reaction with carbon dioxide. *Solid State Ionics* **61**, 83–91.

Schoonman J. (1993) Hydrogen measuring probe for coal gasification processes. *Fuel Process. Technol.* **36**, 251–258.

Sedlak J.M. and Blurton K.F. (1976a) Electrochemical determination of hydrogen sulphide in air. *Talanta* **23**, 445–448.

Sedlak J.M. and Blurton K.F. (1976b) The electrochemical reactions of carbon monoxide, nitric oxide, and nitrogen dioxide at gold electrodes. *J. Electrochem. Soc.* **123**, 1476–1478.

Shi M. and Anson F.C. (1996) Effects of hydration on the resistances and electrochemical responses of nafion-coatings on electrodes. *J. Electroanal. Chem.* **415**, 41–46.

Schiavon G., Zotti G., Toniolo R., and Bontempelli G. (1995) Electrochemical detection of trace hydrogen sulfide in gaseous samples by porous silver electrodes supported on ion-exchange membranes (solid polymer electrolytes). *Anal. Chem.* **67**, 318–323.

Silvester D.S., Ward K.R., Aldous L., Hardacre C., and Compton R.G. (2008) The electrochemical oxidation of hydrogen at activated platinum electrodes in room temperature ionic liquids as solvents. *J. Electroanal. Chem.* **618**, 53–60.

Skoog D.A., West D.M., and Holler F.J. (1988) *Fundamentals of Analytical Chemistry*. Saunders, Philadelphia, 147.

Sleszynski N. Osteryoung J., and Carter M. (1984) Arrays of very small voltammetric electrodes based on reticulated vitreous carbon. *J. Anal. Chem.* **56**, 130–135.

Sondheimer S.J., Bunce N.J., and Fyfe C.A. (1986) Structure and chemistry of Nafion-H: A fluorinated sulfonic acid polymer. *J. Macromol. Sci. Rev. Macromol. Chem. Phys. C* **26**, 353–413.

Star A., Han T.R., Joshi V., and Stetter J.R. (2004) Sensing with Nafion coated carbon nanotube field-effect transistors. *Electroanalysis* **16**, 108–112.

Stetter J.R. (1978) A surface chemical view of gas detection. *J. Colloid Interface Sci.* **65**, 432–443.

Stetter J.R. (1984) Instrumentation to monitor chemical exposure in the synfuel industry. *ACGIH Transactions—Annals of the American Conference of Governmental Industrial Hygienists*, **11**, 225–269.

Stetter J.R. and Blurton K.F. (1976) Portable high-temperature catalytic reactor: Application to air pollution monitoring instrumentation. *Rev. Sci. Instrum.* **47**, 691–694.

Stetter J.R. and Blurton K.F. (1977) Selective oxidation of hydrogen in carbon monoxide/air streams: Applications to environmental monitoring, industrial and engineering chemistry. *Product Research Dev.* **16**, 22–25.

Stetter J.R., Zaromb S., and Findlay Jr. M.W. (1985) Monitoring of electrochemically inactive compounds by amperometric gas sensors. *Sens. Actuators* **6**, 269–288.

Stetter J.R., Maclay G.J., and Buttner W.J. (1988) Microfabricated amperometric gas sensor. *IEEE Trans. Electron. Devices* **35**(6), 793–799.

Stetter J.R. and Maclay G.J. (2004) Carbon nanotubes and sensors: A review. In: Baltes H., Brand O., Fedder G.K., Hierold C., Korvink J., and Tabata O. (eds.), *Advanced Micro and Nano Systems*, Vol. I, Wiley-VCH, Weinheim, Germany, 357–382.

Stetter J.R. and Li J. (2008) Amperometric gas sensors—A review. *Chem. Rev.* **108**, 352–366.

Stetter J.R., Blurton K.F., Valentine A.M., and Tellefsen K.A. (1978) The electrochemical oxidation of hydrazine and methylhydrazine on gold: Application to gas monitoring. *J. Electrochem. Soc.* **125**, 1804–1807.

Stetter J.R., Tellefsen K.A., Saunders R.A., and DeCorpo J.J. (1979) Electrochemical determination of hydrazine and methyl- and 1,1-dimethylhydrazine in air. *Talanta* **26**, 799–804.

Stetter J.R., Sedlak L.M., and Blurton K.F. (1977) Electrochemical gas chromatographic detection of hydrogen sulfide at ppm and ppb levels. *J. Chromatogr. Sci.* **15**, 125–128.

Stetter J.R., Bradley K., Cumings J., Gabriel J.-C.P., Gruner G., and Star A. (2003) Nano-electronic sensors: Practical device designs for sensors. *Nanotechnology* **3**, 313–316.

Stetter J.R., Penrose W.R., and Yao S. (2003b) Sensors, chemical sensors, electrochemical sensors, and ECS. *J. Electrochem. Soc.* **150**, S11–S16.

Sundmacher K., Rihko-Struckmann L.K., and Galvita V. (2005) Solid electrolyte membrane reactors: Status and trends. *Catal. Today* **104**, 185–199.

Tan C.K. and Blackwood D.J. (2000) Interactions between polyaniline and methanol vapour. *Sens. Actuators B* **71**, 184–191.

Taniguchi N. and Gamo T. (1994) Structure changes of $BaCe_{0.8}Gd_{0.2}O_{3-\delta}$ electrolyte for fuel cell at high temperatures in air and CO_2 atmosphere, *Denki Kagaku oyobi Kogyo Butsuri Kagaku* **62**, 326–331 (in Japanese).

Taniguchi N., Kuroha T., Nishimura C., and Iijima K. (2005) Characteristics of novel $BaZr_{0.4}Ce_{0.4}In_{0.2}O_3$ proton conducting ceramics and their application to hydrogen sensors. *Solid State Ionics* **176**, 2979–2982.

Tanner C.W. and Virker A.V. (1996) Instability of $BaCeO_3$ in H_2O-containing atmospheres. *J. Electrochem. Soc.* **143**, 1386–1389.

Tejuca L.J. and Fierro J.L.G. (eds.) (1993) *Properties and Applications of Perovskite-Type Oxides.* Marcel Dekker, New York.

Tomita A., Namekata Y., Nagao M., and Hibino T. (2007) Room-temperature hydrogen sensors based on an In^{3+}-doped SnP_2O_7 proton conductor. *J. Electrochem. Soc.* **154**, J172–J176.

Vaihinger S., Goepel W., and Stetter J.R. (1991) Detection of halogenated and other hydrocarbons in air: Response functions of catalyst/electrochemical sensor systems. *Sens. Actuators B* **4**, 337–343.

Venkatasetty H.V. (1985) Electrochemical sensing of carbon monoxide. U.S. Patent 4,522,690.

Vielstich W. Lamm A. Gasteiger H.A. (eds.) (2003) *Handbook of Fuel Cells—Fundamentals, Technology and Applications*, Vol. 2, Part 3. John Wiley, Chichester, UK.

Virji S., Huang J., Kaner R.B., and Weiller B.H. (2004) Polyaniline nanofiber gas sensors: Examination of response mechanisms. *Nano Lett.* **4**, 491–496.

Vork F.T.A., Janssen L.J.J., and Barendrecht E. (1986) Oxidation of hydrogen at platinum-polypyrrole electrodes. *Electrochim. Acta* **31**, 1569–1575.

Wakamura K. (2005) Empirical relationships for ion conduction based on vibration amplitude in perovskite-type proton and superionic conductors. *J. Phys. Chem. Solids* **66**, 133–142.

Wadhawan J.D., Welford P.J., McPeak H.B., Hahn C.E.W., and Compton R.G. (2003) The simultaneous voltammetric determination and detection of oxygen and carbon dioxide: A study of the kinetics of the reaction between superoxide and carbon dioxide in non-aqueous media using membrane-free gold disc microelectrodes. *Sens. Actuators B* **88**, 40–52.

Wallgren K. and Sotiropoulos S. (1999) Oxygen sensors based on a new design concept for amperometric solid state devices. *Sens. Actuators B* **60**, 174–183.

Wang P., Zakeeruddin S.M., Moser J.E., and Gratzel M. (2003) A new ionic liquid electrolyte enhances the conversion efficiency of dye-sensitized solar cells. *J. Phys. Chem. B* **107**, 13280–13285.

Wang R., Okajima T., Kitamura F., and Ohsaka T. (2004a) A novel amperometric O_2 gas sensor based on supported room-temperature ionic liquid porous polyethylene membrane-coated electrodes. *Electroanalysis* **16**, 66–72.

Wang R., Hoyano S., and Ohsaka T. (2004b) O_2 gas sensor using supported hydrophobic room-temperature ionic liquid membrane-coated electrode. *Chem. Lett.* **33**, 6–7.

Wang W. and Virkar A.V. (2005) Ionic and electron–hole conduction in $BaZr_{0.93}Y_{0.07}O_{3-\delta}$ by 4-probe dc measurements. *J. Power Sources* **142**, 1–9.

Watcharaphalakorn S., Ruangchuay L., Chotpattahanont D., Sirivat A., and Schwank J. (2005) Polyaniline/polyimide blends as gas sensors and electrical conductivity response to CO-N_2 mixtures. *Polymer Int.* **54**, 1126–1133.

Wei D. and Ivaska A. (2008) Applications of ionic liquids in electrochemical sensors. *Anal. Chim. Acta* **607**, 126–135.

Welton T. (1999) Room-temperature ionic liquids. Solvents for synthesis and catalysis. *Chem. Rev.* **99**, 2071–2084.

Weppner W. (1987) Solid-state electrochemical gas sensors. *Sens. Actuators* **12**, 107–119.

Wesselingh J.A. and Krishna R. (2000) Gas permeation. In: *Mass Transfer in Multicomponent Mixtures.* Delft University Press, Delft, The Netherlands, 233–241.

Wilson D.M., Hoyt S., Janata J., Booksh K., and Obando L. (2001) Chemical sensors for portable, handheld field instruments. *IEEE Sensors J.* **1**, 256–274.

Wroblewski W., Dybko A., Malinowska E., and Brzozka Z. (2004) Towards advanced chemical microsensors—An overview. *Talanta* **63**, 33–39.

Wu E.L., Landolt G.R., and Chester A.W. (1986) Hydrocarbon adsorption characterization of some high silica zeolites. *Stud. Surf. Sci. Catal.* **28**, 547–554.

Xie D., Jiang Y., Pan W., Li D., Wu Z., and Li Y. (2002) Fabrication and characterization of polyaniline-based gas sensor by ultra-thin film technology. *Sens. Actuators B* **81**, 158–164.

Yajima T., Iwahara H., Uchida H., and Koide K. (1990) Relation between proton conduction and concentration of oxide ion vacancy in $SrCeO_3$ based sintered oxides. *Solid State Ionics* **40/41**, 914–917.

Yajima T., Iwahara H., Koide K., and Yamamoto K. (1991) $CaZrO_3$-type hydrogen and steam sensors: Trial fabrication and their characteristics. *Sens. Actuator B* **5**, 145–147.

Yajima T., Koide K., Fukatsu N., Ohashi T., and Iwahara H. (1993) A new hydrogen sensor for molten aluminum. *Sens. Actuators B* **13–14**, 697–699.

Yajima T., Koide K., Takai H., Fukatu N., and Iwahara H. (1995) Application of hydrogen sensor using proton conductive ceramics as a solid electrolyte to aluminum casting industries. *Solid State Ionics* **79**, 333–337.

Yamazoe N. and Miura N. (1998) Potentiometric gas sensors for oxidic gases. *J. Electroceram.* **2**, 243–255.

Yan H. and Liu C. (1993) Humidity effects on the stability of a solid polymer electrolyte oxygen sensor. *Sens. Actuators B* **10**, 133–136.

Yang J.C. and Dutta P.K. (2007) High temperature amperometric total NO_x sensors with platinum-loaded zeolite Y electrodes. *Sens. Actuators B* **123**, 929–936.

Yao S. and Wang M. (2002) Electrochemical sensor for dissolved carbon dioxide measurement. *J. Electrochem. Soc.* **149**, H28–H32.

Yao S. and Stetter J.R. (2004) Modification of NASICON solid electrolyte for NO_x measurements. *J. Electrochem. Soc.* **151**, H75–H80.

Yasuda A., Doi K., Yamaga N., Fujioka T., and Kusanagi S. (1992) Mechanism of the sensitivity of the planar CO sensor and its dependency on humidity. *J. Electrochem. Soc.* **139**, 3224–3229.

Young P., Lu Y., Terrill R., and Li J. (2005) High-sensitivity NO_2 detection with carbon nanotube–gold nanoparticle composite films. *J. Nanosci. Nanotechnol.* **5**, 1509–1513.

Yu L., Diego G., Ren X.R., and Zeng X. (2005) Ionic liquid high temperature gas sensors, *Chem. Commun.* 2277–2279.

Yu L., Jin X., and Zeng X. (2008) Methane interactions with polyaniline / butylmethylimidazolium camphorsulfonate ionic liquid composite. *Langmuir* **24**, 11631–11636.

Yu L., Huang Y., Jin X., Mason A., and Zeng X. (2009) Ionic liquid thin layer EQCM explosives sensor. *Sens. Actuators B* **140**, 363–370.

Zaromb S., Stetter J.R., and Attard G.J. (1983) The potential-dependence of the electro-oxidation of nitric oxide on gold in acid solution. *J. Electroanal. Interfacial Electrochem.* **148**, 289–291.

Zawodzinski T.A., Springer T.E., Uribe F., and Gottesfeld S. (1993) Characterization of polymer electrolytes for fuel cell applications. *Solid State Ionics* **60**, 199–211.

Zheng M. and Chen X. (1994) Preparation and electrochemical characterization of $SrCeO_3$-based proton conductor. *Solid State Ionics* **70**, 595–600.

Zeng Z.M., Wang K., Zhang Z.X., Chen J.J., and Zhou W.L. (2009) The detection of H_2S at room temperature by using individual indium oxide nanowire transistors. *Nanotechnology* **20**, 045503.

CHEMICAL SENSORS

COMPREHENSIVE SENSORS TECHNOLOGIES

VOLUME 5: ELECTROCHEMICAL AND OPTICAL SENSORS

EDITED BY

GHENADII KOROTCENKOV

GWANGJU INSTITUTE OF SCIENCE AND TECHNOLOGY
GWANGJU, REPUBLIC OF KOREA

MOMENTUM PRESS

MOMENTUM PRESS, LLC, NEW YORK

Chemical Sensors: Comprehensive Sensors Technologies. Volume 5: Electrochemical and Optical Sensors

First published in 2011 by
Momentum Press®, LLC
222 East 46th Street, New York, NY 10017
www.momentumpress.net

ISBN-13: 978-1-60650-236-5 (hard back, case bound)
ISBN-10: 1-60650-236-0 (hard back, case bound)
ISBN-13: 978-1-60650-238-9 (e-book)
ISBN-10: 1-60650-238-7 (e-book)
DOI forthcoming

Cover design by Jonathan Pennell
Interior design by Derryfield Publishing, LLC

First Edition: July 2011

10 9 8 7 6 5 4 3 2 1

Printed in Taiwan